

MEMBERS OF THE JURY

Prof. dr. I. Lambrichts, Universiteit Hasselt, Diepenbeek, Belgium, *Chairman*

Prof. dr. J.-M. Rigo, Universiteit Hasselt, Diepenbeek, Belgium, *Promotor*

Dr. G. Hoogland, Universiteit Maastricht, Maastricht, the Netherlands, *Copromotor*

Prof. dr. M. Ameloot, Universiteit Hasselt, Diepenbeek, Belgium

Prof. dr. R. Raedt, Universiteit Gent, Gent, Belgium

Prof. dr. L. Ris, Université Mons, Bergen, Belgium

Prof. dr. H. Steinbusch, Universiteit Maastricht, Maastricht, the Netherlands

Prof. dr. E. Van Kerkhove, Universiteit Hasselt, Diepenbeek, Belgium

TABLE OF CONTENTS

| | |
|--|-------------|
| List of Figures | v |
| List of Tables | vii |
| List of Abbreviations | viii |
| 1 Introduction and aims | 1 |
| 1.1 FEBRILE SEIZURES | 2 |
| 1.1.1 How does fever generate seizures in the developing brain? | 2 |
| 1.1.1.1 The developing brain: a state of hyperexcitability | 2 |
| 1.1.1.2 Generation of seizures in response to fever: the involved mechanisms | 5 |
| 1.1.2 Febrile seizures and epilepsy: Is there a causal relationship? | 6 |
| 1.1.2.1 Evidence from epidemiological studies | 6 |
| 1.1.2.2 Evidence from experimental febrile seizures | 7 |
| 1.2 TEMPORAL LOBE EPILEPTOGENESIS: DIFFERENT HYPOTHESES | 10 |
| 1.2.1 The 'neurogenesis hypothesis' | 10 |
| 1.2.1.1 Neurogenesis in the adult hippocampal dentate gyrus | 10 |
| 1.2.1.2 Role of seizure-induced newborn neurons in the process of epileptogenesis | 13 |
| 1.2.2 The 'ion channel hypothesis' | 15 |
| 1.2.2.1 Ion channels: general aspects | 15 |
| 1.2.2.2 Involvement of ion channels in the process of epileptogenesis | 16 |
| 1.3 AIMS OF THE STUDY | 20 |
| 2 Validation of reference genes for quantitative real time PCR studies in the dentate gyrus after experimental febrile seizures | 23 |
| 2.1 ABSTRACT | 24 |
| 2.2 INTRODUCTION | 25 |
| 2.3 MATERIALS AND METHODS | 27 |
| 2.3.1 Induction of febrile seizures and tissue sampling | 27 |
| 2.3.2 RNA isolation and cDNA synthesis | 28 |
| 2.3.3 Quantitative real time PCR | 28 |
| 2.3.4 Data analysis | 29 |
| 2.4 RESULTS | 31 |
| 2.4.1 Expression levels of candidate reference genes | 31 |

| | | |
|-------|---|----|
| 2.4.2 | Validating candidate reference genes | 32 |
| 2.4.3 | Influence of different normalization approaches on the expression profile of a gene of interest | 36 |
| 2.5 | DISCUSSION | 38 |

3 Functional characterization of hippocampal dentate granule GABA_A receptors after experimental early-life febrile seizures

41

| | | |
|-------|---|----|
| 3.1 | ABSTRACT | 42 |
| 3.2 | INTRODUCTION | 43 |
| 3.3 | MATERIALS AND METHODS | 45 |
| 3.3.1 | Induction of hyperthermic seizures | 45 |
| 3.3.2 | Preparation of hippocampal slices | 45 |
| 3.3.3 | Whole-cell patch-clamp recordings | 46 |
| 3.3.4 | Analysis of electrophysiological data | 47 |
| 3.3.5 | Quantitative real time PCR | 48 |
| 3.3.6 | Statistical analysis | 49 |
| 3.4 | RESULTS | 51 |
| 3.4.1 | Properties of sIPSCs in dentate granule cells are changed after hyperthermic seizures | 51 |
| 3.4.2 | GABA-evoked currents in dentate granule neurons are altered after HT treatment | 55 |
| 3.4.3 | HT-associated alterations in GABA _A R subunit composition | 59 |
| 3.5 | DISCUSSION | 61 |

4 Phenotypical characterization of ligand-gated ion channels in dentate gyrus cells born after experimental early-life febrile seizures

67

| | | |
|-------|--------------------------------------|----|
| 4.1 | ABSTRACT | 68 |
| 4.2 | INTRODUCTION | 69 |
| 4.3 | MATERIAL AND METHODS | 71 |
| 4.3.1 | Induction of febrile seizures | 71 |
| 4.3.2 | BrdU labeling and tissue preparation | 71 |
| 4.3.3 | Antibodies | 72 |

| | | |
|-------|--|----|
| 4.3.4 | Immunofluorescent labeling | 72 |
| 4.3.5 | Confocal microscopy and quantification | 74 |
| 4.3.6 | Statistical analysis | 74 |
| 4.4 | RESULTS | 75 |
| 4.4.1 | Febrile seizures increase neurogenesis in the DG granule cell layer, but do not change the number newborn cells in the DG hilar region | 75 |
| 4.4.2 | Cells born after FS express more often GABA _A Rs and equally express GlyRs | 77 |
| 4.4.3 | Febrile seizures do not alter the number of newborn DG cells expressing NMDARs | 79 |
| 4.5 | DISCUSSION | 82 |

5 Towards assessment of functional neurogenesis after experimental febrile seizures

87

| | | |
|-------|--|----|
| 5.1 | ABSTRACT | 88 |
| 5.2 | INTRODUCTION | 89 |
| 5.3 | MATERIAL AND METHODS | 91 |
| 5.3.1 | Stereotactic surgery | 91 |
| 5.3.2 | Production of eGFP-expressing retroviral vectors | 91 |
| 5.3.3 | Detection of replication competent retroviruses | 92 |
| 5.4 | RESULTS | 94 |
| 5.4.1 | Stereotactic coordinates of the dentate gyrus in P11 Sprague-Dawley rats | 94 |
| 5.4.2 | Detection of replication competent retroviral particles | 95 |
| 5.5 | DISCUSSION | 97 |

6 Summary and general discussion

99

7 Nederlandse samenvatting

109

Reference list

115

Curriculum Vitae

129

Dankwoord

133

LIST OF FIGURES

| | | |
|-------------------|---|----|
| Figure 1.1 | Excitatory actions of GABA and the switch in chloride homeostasis during brain development | 3 |
| Figure 1.2 | Age-dependency of seizure threshold | 4 |
| Figure 1.3 | Schematic representation of the hippocampal formation and the process of adult hippocampal neurogenesis | 11 |
| Figure 1.4 | Schematic overview of altered neurogenesis in the dentate gyrus after seizures | 14 |
| Figure 1.5 | Schematic representation of the three structural categories of ligand-gated ion channels | 17 |
| Figure 2.1 | Cycle threshold (Cq) levels of candidate reference genes in each experimental group | 32 |
| Figure 2.2 | Evaluation of candidate reference genes using geNorm analysis software | 33 |
| Figure 2.3 | Evaluation of candidate reference genes using Normfinder analysis software | 35 |
| Figure 2.4 | Influence of reference genes selected for normalization on the expression profile of Cnr1 one week after FS induction | 36 |
| Figure 3.1 | Comparison of sIPSCs in DG granule cells of normothermia (NT) and hyperthermia rats with (HT+FS) and without (HT-FS) seizures | 53 |
| Figure 3.2 | Physiological characterization of GABA-elicited currents in DG granule cells from normothermia (NT) and hyperthermia rats with (HT+FS) and without (HT-FS) seizures | 56 |
| Figure 3.3 | Desensitization kinetics of GABA-elicited currents in DG granule cells from normothermia (NT) and hyperthermia rats with (HT+FS) and without (HT-FS) seizures | 58 |
| Figure 3.4 | Relative GABA _A R subunit mRNA expression in the dentate gyrus of normothermia and hyperthermia rats | 59 |
| Figure 4.1 | Hyperthermia-induced seizures increase the number of newborn DG granule cells | 76 |
| Figure 4.2 | Hyperthermia-induced seizures significantly increased the number of BrdU/GABA _A R β _{2,3} colocalizing DG granule cells | 78 |

| | | |
|-------------------|--|-----|
| Figure 4.3 | Alpha2-containing GlyRs were predominantly detected in the hilus and were hardly expressed by newborn cells | 79 |
| Figure 4.4 | The number of BrdU/NMDAR NR2A/B colocalizing cells was similar in all experimental groups | 80 |
| Figure 4.5 | AMPA GluR2/3 subunits were predominantly expressed in the hilar region | 81 |
| Figure 5.1 | Stereotactic coordinates of the dentate gyrus in P11 Sprague-Dawley rats | 94 |
| Figure 5.2 | Fluorescent detection of eGFP positive NIH 3T3 cells | 95 |
| Figure 5.3 | Analysis of VSVG expression in the supernatant of NIH 3T3 cells infected with eGFP-expressing retroviral vectors | 96 |
| Figure 6.1 | Schematic representation of febrile seizure-induced long-term changes in DG cells described in this thesis | 102 |

LIST OF TABLES

| | | |
|------------------|---|----|
| Table 2.1 | Selected reference genes for analysis of expression stability | 30 |
| Table 2.2 | Cycle threshold (C _q) values of candidate reference genes | 31 |
| Table 2.3 | Ranking of reference genes based on the expression stability evaluated by geNorm and Normfinder candidate reference genes | 34 |
| Table 3.1 | SYBR® green-based qPCR primer assays for quantitative real time PCR | 50 |
| Table 3.2 | Membrane properties of DG granule cells of normothermia (NT) animals and hyperthermia animals with (HT+FS) and without (HT-FS) seizures | 51 |

LIST OF ABBREVIATIONS

| | |
|-------------------------------------|---|
| 18S rRNA | 18 (Svedberg units) ribosomal RNA |
| ActB | Beta actin |
| AMPA | α -amino-3-hydroxy-5-methylisoxazole-4-propionic acid |
| AMPAR | α -amino-3-hydroxy-5-methylisoxazole-4-propionic acid receptor |
| Arbp | Acidic ribosomal phosphoprotein P0 |
| BrdU | 5-bromo-2'-deoxyuridine |
| CA | cornu ammonis |
| CB1 | cannabinoid type 1 |
| CNQX | 6-cyano-7-nitroquinoxaline-2,3-dione |
| CSF | cerebrospinal fluid |
| CycA | CyclophylinA |
| DG | dentate gyrus |
| DL-APV | DL-2-amino-5-phosphonopentanoic acid |
| DMEM | Dulbecco's modified Eagle's medium |
| E_{GABA} | equilibrium potential for GABA |
| FCS | fetal calf serum |
| FS | febrile seizure |
| GABA | γ -aminobutyric acid |
| GABA_AR | γ -aminobutyric acid type A receptor |
| GFP | green fluorescent protein |
| GluR | glutamate receptor |
| GusB | beta-glucuronidase |
| HCN | hyperpolarization-activated cyclic nucleotide-gated |
| HKG | housekeeping gene |
| HT | hyperthermia |
| I_h | hyperpolarization-activated current |
| IL-1β | interleukin-1 β |
| KCC2 | K ⁺ -Cl ⁻ cotransporter |
| LGIC | ligand-gated ion channel |
| LPS | lipopolysaccharide |
| NDS | normal donkey serum |
| NMDA | <i>N</i> -methyl-D-aspartate |
| NMDAR | <i>N</i> -methyl-D-aspartate receptor |
| NRS | normal rabbit serum |
| NKCC1 | Na ⁺ -K ⁺ -2Cl ⁻ cotransporter |
| NT | normothermia |
| PBS | Phosphate buffered saline |
| PI | Propidium iodide |

| | |
|---------------|--|
| qPCR | quantitative real time polymerase chain reaction |
| RCR | Replication competent retrovirus |
| Rpl13A | Ribosomal protein L13A |
| SGZ | subgranular zone |
| sIPSC | spontaneous inhibitory postsynaptic current |
| SVZ | subventricular zone |
| Tbp | TATA box binding protein |
| TLE | temporal lobe epilepsy |
| TM | transmembrane |
| TRPV4 | transient receptor potential vanilloid 4 |
| VSVG | Vesicular stomatitis virus glycoprotein |

1

Introduction and aims

This chapter is partly based on:

Potential role for ligand-gated ion channels after seizure-induced neurogenesis

Ann Swijssen¹, Govert Hoogland² and Jean-Michel Rigo¹

Biochem Soc Trans. 2009 Dec;37(Pt 6):1419-22. Review

¹ BIOMED Research Institute, Hasselt University and transnationale Universiteit Limburg, Diepenbeek, Belgium

² Department of Neurosurgery, school of Mental Health and Neurosciences, University Medical Center Maastricht, The Netherlands

1.1 FEBRILE SEIZURES

Febrile seizures (FS) are a common neurological disorder in childhood. They are defined by the National Institutes of Health as a fever-associated event in infancy without evidence of intracranial infection or other defined cause [1] and are the most frequent seizure type in childhood affecting 2-3% of the children between the age of 3 months and 5 years [191]. FS are, like any other type of cerebral seizures, due to a sudden, excessive or abnormal, synchronous and rhythmic firing of populations of neurons. FS can be categorized in two types of seizures: simple and complex. Simple seizures last less than 10-15 minutes and are not linked to adverse long-term effects on the developing brain and hence supposed to be benign. In contrast, the consequences of complex FS that are defined as focal, prolonged (>10 min) or repetitive seizures are controversial. Retrospective studies have associated a history of prolonged FS in childhood with temporal lobe epilepsy (TLE) later in life. However, prospective studies did not implicate FS as a strong risk factor for the development of TLE [56, 158, 163, 176].

This section will first focus on the mechanisms by which fever may lead to seizures during a critical time window of brain development. Additionally, current knowledge from epidemiological and animal studies concerning the relationship between FS and epilepsy will be discussed.

1.1.1 How does fever generate seizures in the developing brain?

1.1.1.1 The developing brain: a state of hyperexcitability

Although seizures can occur at any age, children are at much higher risk than adults to suffer from seizures with the highest incidence of seizure disorders in the first year of life [78]. The age-dependent occurrence of FS suggests that characteristics of specific stages of brain development contribute to seizure generation. Results from clinical and animal studies provide evidence that the immature brain is more susceptible to seizures than the mature brain. Several mechanisms inherent to normal brain development are responsible for the state of hyperexcitability in the developing brain [12].

Immature neurons show a high tendency to oscillate as a result of their large input resistance facilitating the generation of action potentials and enhancing excitability. Also, the prevalence of gap junctions during early development could amplify small changes in neuronal activity into large-scale synchronization [16, 83]. In addition, inhibitory and excitatory circuits do not develop simultaneously. GABAergic synapses mature first and are active at a stage when glutamatergic synapses, which initially constitute of exclusively *N*-methyl-D-aspartate receptors (NMDARs) and lack functional α -amino-3-hydroxy-5-methylisoxazole-4-propionic acid receptors (AMPA), are still silent [17]. Interestingly, γ -aminobutyric acid (GABA), which is the main inhibitory neurotransmitter in the adult brain, exerts excitatory effects during this early postnatal period. Because immature neurons have higher intracellular Cl^- concentrations compared with mature neurons, γ -aminobutyric acid type A receptor (GABA_AR) activation results in a Cl^- efflux instead of a Cl^- influx [15] (Figure 1.1).

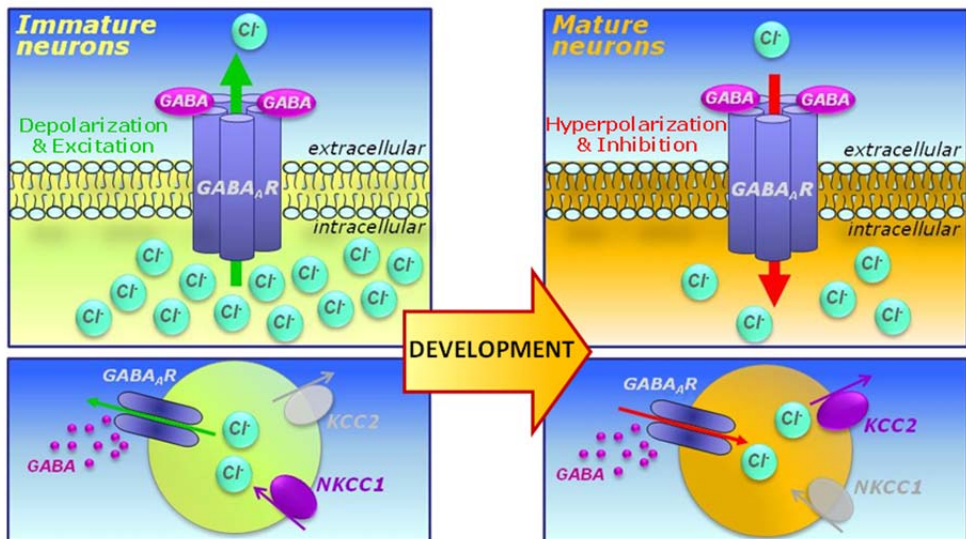


Figure 1.1: Excitatory actions of GABA and the switch in chloride homeostasis during brain development. The equilibrium potential for GABA (E_{GABA}) is depolarizing in the developing brain as a consequence of the higher intracellular Cl^- concentration in immature compared with mature neurons. As a result, GABA_AR activation leads to a Cl^- efflux and depolarization in immature neurons. On the contrary, GABA_AR activation in mature neurons results in a Cl^- influx and hyperpolarization. E_{GABA} becomes hyperpolarizing during postnatal brain development, due to an upregulation of the Cl^- extruding K^+-Cl^- cotransporter (KCC2) synergistically with a down-regulation of the Cl^- importing $\text{Na}^+-\text{K}^+-2\text{Cl}^-$ cotransporter (NKCC1).

The resulting depolarization reaches the threshold for Na^+ action potential generation, activates voltage-dependent Ca^{2+} channels and removes the Mg^{2+} block from NMDA channels leading to a Ca^{2+} influx [17]. In rats, GABA has a depolarizing effect until postnatal day 14 [97]. The action of GABA reverses during postnatal brain development as a result of an upregulation of the Cl^- extruding K^+-Cl^- cotransporter (KCC2) synergistically with a down-regulation of the Cl^- importing $\text{Na}^+-\text{K}^+-2\text{Cl}^-$ cotransporter (NKCC1) installing the adult Cl^- concentrations [15] (Figure 1.1). Additionally, maturation of the postsynaptic G protein mediated GABA_B -mediated inhibition that involves activation of K^+ and inhibition of Ca^{2+} currents, is also delayed [69]. Taken together, late maturation of an efficient inhibitory GABAergic system and early excitatory effects of GABA will contribute to neuronal hyperexcitability in the immature brain and may facilitate synchronized activity [59]. The action of excitatory GABA synapses along with excitatory NMDAR-mediated postsynaptic currents, which are prolonged in immature compared with mature neurons, generate giant depolarizing potentials in the hippocampal network. This synchronous network-driven activity is characterized by recurrent bursts with large, polysynaptic currents. The importance of giant depolarizing potentials declines when GABA is becoming inhibitory and the glutamate-mediated excitatory drive is increasing [12, 13]. Rodents exhibit the lowest seizure threshold during the second postnatal week. At this time point, the action of GABA is gradually shifting from depolarizing to hyperpolarizing but is not yet fully inhibitory; however the

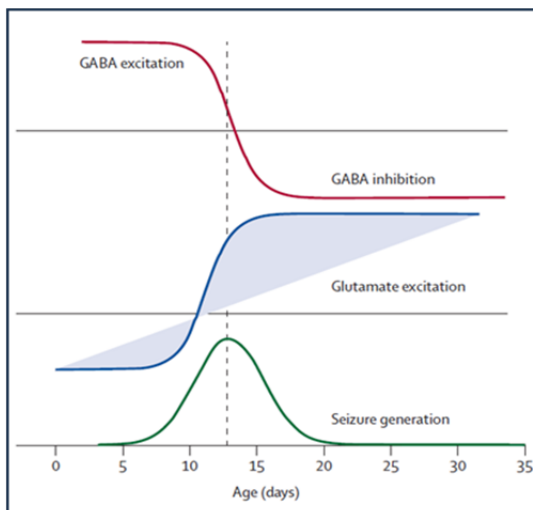


Figure 1.2: Age-dependency of seizure threshold. The threshold for seizure generation peaks in the second postnatal week. This coincides with the shift of GABA from excitatory to inhibitory, but the action of GABA is not completely inhibitory yet. Importantly, at this moment glutamatergic synapses have almost reached their adult density. Consequently, propagation of seizures is facilitated [16].

density of glutamatergic synapses has reached approximately their adult level facilitating propagation of seizures [16] (Figure 1.2).

1.1.1.2 Generation of seizures in response to fever: the involved mechanisms

Even small changes in brain temperature (2-3°C) are known to influence brain function. Elevations in brain temperature have been associated with enlarged excitatory field potentials in the dentate gyrus (DG) [128]; and recently, TRPV4 (transient receptor potential vanilloid 4), one of the thermosensitive TRP channels, has been identified as a key regulator for hippocampal neural excitability [175]. In addition, hyperthermia suppresses GABA_AR-mediated synaptic inhibition in the hippocampus more than it suppresses excitatory synaptic transmission and may shift the excitation/inhibition balance towards excitation [154]. These *ex vivo* findings suggest that a rise in brain temperature increases neuronal firing and hence the probability of generating seizures. Clinical data also indicate that a hot water bath may elicit seizures in young children implying that an increase in brain temperature may be sufficient to provoke seizures [68].

Fever is not only associated with an increased brain temperature, but involves also an inflammatory response including secretion of cytokines in the periphery as well as in the brain [3, 35]. In the context of FS, interleukin-1 β (IL-1 β), a pro-inflammatory pyrogenic cytokine, has received much attention. IL-1 β may enhance neuronal excitability by enhancing NMDAR function through activation of tyrosine kinases and subsequent NMDAR phosphorylation [194], by inhibiting astrocytic glutamate reuptake [85], by increasing the glutamate release [93] and by inhibiting of GABA_AR-mediated inhibition [197]. Also, *in vivo* studies point to a role of IL-1 β signaling in fever-induced hyperexcitability underlying FS. Intraventricular infusion of IL-1 β decreases the seizure threshold in 14-day old rats treated with lipopolysaccharide (LPS) [80] and in 14-day old mice exposed to hyperthermia [55]. The threshold temperature for developing seizures is higher in mice lacking the receptor for IL-1 β [55]. In addition, clinical studies suggest that an enhanced IL-1 β response may play a role in the pathogenesis of FS in children. Indeed, children with a FS history display an increased frequency of IL-1 β (-511) allele, which is associated with enhanced IL-1 β production, [193] and their peripheral mononuclear cells produce abnormally

high IL-1 β levels in response to stimulation with LPS [81] or viral RNA [124]. However, data from clinical studies determining IL-1 β levels in the cerebrospinal fluid (CSF) from children with FS are controversial: some studies point to increased CSF levels of IL-1 β [77], while others report no changes [105].

It still remains an unresolved issue why some children with a febrile illness develop seizures and others not. Epidemiological studies indicate that a family history of FS increases the risk of developing seizures in response to fever. This familial factor suggests also that genetic background may contribute to seizure generation. Indeed, mutations in GABA_AR γ 2 subunit [27, 75, 94] and voltage-gated sodium (Na⁺)-channel type 1 alpha and beta subunit (SCN1A and SCN1B) [63, 196] genes have been associated with FS and generalized human epilepsy. Additionally, single nucleotide polymorphisms in the Camk2d gene, encoding the delta chain of calcium/calmodulin dependent kinase II, are correlated with the individual variability in FS susceptibility in rats [159].

Recently, Schuchmann *et al* proposed the principle of hyperthermia-induced respiratory alkalosis as mechanism underlying FS generation. They have shown that hyperthermia-induction in young rat pups increases the breathing rate, which enhances the elimination of CO₂ leading to brain alkalosis. Neurons in the hippocampus and cortex are hyperexcited by the increase in pH resulting in seizure generation [169, 185]. The relevance of this mechanism in humans is still unresolved [56].

1.1.2 Febrile seizures and epilepsy: Is there a causal relationship?

1.1.2.1 Evidence from epidemiological studies

The outcome of simple FS is considered to be benign. Most studies indicate that the risk of developing epilepsy after simple seizures is only slightly different from the general population. However, whether complex FS cause TLE is still a controversial issue in epilepsy research.

Epilepsy is a chronic brain disorder characterized by spontaneous, recurrent seizures. It has a prevalence ranging from 0.4% to 0.8%. Epilepsy cannot be considered as one specific disease but rather as a diverse family of disorders reflecting underlying brain dysfunction that may arise from many different causes. The common feature of these different 'epilepsies' is a persistent increase of neuronal excitability that is occasionally and unpredictably expressed

as a seizure. The behavioral manifestation of such an epileptic seizure is dependent on the functions of the region of the cortex in which neurons fire abnormally. In general, epileptic seizures are divided in two groups, namely generalized and partial seizures, according to their site of origin. Partial seizures have a local onset arising in a part of one hemisphere and possibly spreading to other parts of the brain during the seizure. Generalized seizures involve both hemispheres from the beginning of the seizure. Partial seizures can be further subdivided in simple seizures, which are usually short and are associated with preservation of consciousness, and complex seizures, which last longer and are associated with alterations or loss of consciousness [65, 152]. Approximately 80% of the patients with complex partial seizures display seizures originating in the temporal lobe most often from structures of the mesial temporal lobe such as the hippocampus and amygdala. Patients with TLE exhibit seizures that most often start with motor arrest typically followed by oro-alimentary automatisms, postictal confusion and amnesia [152]. Retrospective studies clearly associated a history of complex FS, particularly prolonged FS and febrile status epilepticus, with a considerably higher risk of developing TLE in adulthood. On the other hand, prospective population-based studies provided only minor evidence for a role of FS in epileptogenesis [56, 158, 163, 176]. Importantly, these prospective studies of the epileptogenicity of FS in humans are limited by confounding factors which may arise during the extensive latency period (average 7.5 years) between the occurrence of FS and the development of identifiable TLE. Moreover, it still remains a point of debate whether preexisting abnormalities make the brain more prone to the development of seizures and seizure-induced injury or if FS themselves cause an injury that further develops into TLE [66, 121]. These issues stress the importance of using appropriate-aged animal models of FS to explore the relationship between early-life FS and TLE in adulthood.

1.1.2.2 Evidence from experimental febrile seizures

Animal models of FS are based on the principle of mimicking fever by increasing body temperature. In the past, several heat sources such as infrared light [130], microwave [34], warm water [90] or warm air [11] have been used to induce hyperthermia in rats that vary in age from 2 to 30 days. Based on hippocampal

maturational characteristics, several studies have tried to correlate the timing of rodent and human brain development (reviewed in [10]). These studies suggest that the first week of life in rats corresponds to the third trimester of gestation in humans and the second week of life in rats are comparable to the first year of human life, *i.e.* the period wherein children are most susceptible to seizures and hence the most relevant period to induce hyperthermia when studying the epileptogenicity of FS. To approximate the human condition as close as possible, it is important to elicit FS at a relevant temperature threshold for seizures, *i.e.* ~40-42.5°C which is comparable to the body temperature resulting in FS in children.

A frequently applied animal model of FS is the model developed by Baram and colleagues in 1997 [11], which is also used for all experiments described in this thesis. In this model, FS are elicited by exposing 10-day old Sprague-Dawley rat pups to a regulated stream of mildly heated air in order to maintain a core temperature of 41-42.5°C. The resulting stereotyped behavioral seizures are lasting ~20 min, equivalent to prolonged childhood FS, and are associated with rhythmic epileptic discharges in the amygdala and hippocampus [11, 53]. This model is advantageous to other FS models because of the rats' appropriate developmental age, the physiological relevant temperature threshold for seizures and the low mortality and morbidity allowing long-term studies [11]. FS in the model of Baram *et al* have been shown to cause a long-lasting enhancement of hippocampal excitability resulting in an increased susceptibility to develop limbic seizures during adulthood [53]. Later-onset TLE was observed in 35% of the adult rats and interictal epileptiform EEG abnormalities were shown by 88% of the animals [54]. This animal model has been used extensively to study the relationship between FS and human TLE. Abnormal mossy fibre innervation of the granule cell and molecular layer, as seen in hippocampal biopsies from TLE patients, is evident at 3 months after experimental FS. In addition, an increased number of newborn dentate granule cells has been found after experimental early-life FS [110, 111]. These persistent structural changes are not accompanied with cell loss in the amygdala or the hippocampal region at 4 weeks after FS, though transient injury of neurons in the central nucleus of the amygdala and the hippocampal CA1 and CA3 pyramidal cell layer was evident within 24hr of FS [18, 186]. Hence, the

epileptogenic process initiated by FS might be dependent on changed neuronal function, rather than neuronal loss. Prolonged FS have been shown to induce alterations in the expression of ion channels governing hyperpolarization-activated (I_h) currents, *i.e.* the hyperpolarization-activated cyclic nucleotide-gated (HCN) cation channels [28, 29], resulting in a depolarization shift of the activation of HCN channels and a slowing of the kinetics of the I_h current in CA1 neurons [38]. Prolonged FS also increase the number of hippocampal presynaptic interneuronal cannabinoid type 1 (CB1) receptors which basically enhances depolarization-dependent retrograde inhibition in GABA release [40, 41]. Both phenomena, *i.e.* changes in I_h and endocannabinoid signaling, promote hyperexcitability and contribute to the decreased seizure threshold following long experimental early-life FS. It is proposed that also other persistent alterations in gene expression that associate with a change in neuronal function might be responsible for the hippocampal hyperexcitability following experimental FS.

1.2 TEMPORAL LOBE EPILEPTOGENESIS: DIFFERENT HYPOTHESES

TLE is one of the most common seizure disorders. The main morphopathological change present in hippocampi resected from TLE patients is hippocampal sclerosis. The sclerotic hippocampus is characterized by mossy fibre sprouting, astrogliosis, granule cell dispersion and neuronal degeneration in CA1, CA3 and CA4 region [153]. These structural alterations are supposed to underlie the imbalance between excitation and inhibition in the hippocampal neuronal network, which is characteristic for the process of epileptogenesis. However, other mechanisms may also be involved.

The next section will focus on the putative role of neurogenesis and ion channels in the development of TLE. In this context, results from rodent models of seizures as well as surgical tissue from epilepsy patients will be discussed.

1.2.1 The 'neurogenesis hypothesis'

1.2.1.1 Neurogenesis in the adult hippocampal dentate gyrus

Neurogenesis, defined as a complex process starting with the division of a precursor cell leading to the integration of a new functioning neuron [95], has long been believed to be restricted to the prenatal period. In the 1960s, Altman and Das [4] described for the first time the generation of new neurons in the adult mammalian brain. Studies of the last few decades have provided evidence that neurogenesis persists in adulthood in two selected forebrain regions, namely (i) the subventricular zone (SVZ) which give rise to new interneurons in the olfactory bulb [5], and (ii) the subgranular zone (SGZ) of the hippocampal DG [103]. Adult hippocampal neurogenesis has been extensively studied by means of BrdU (5-bromo-2'-deoxyuridine), a thymidine analogue which integrates into the newly synthesized DNA during the S-phase of mitosis. By making use of this method, Kuhn et al. [103] demonstrated in rats that new neurons are generated from a population of precursor cells being located in the SGZ of the DG. Continuous generation of neurons in the adult DG has been detected in a similar way in other species such as mice [188], monkeys [102] and, finally, also humans [62]. Newborn hippocampal cells migrate from the SGZ to the granule cell layer, where they differentiate into

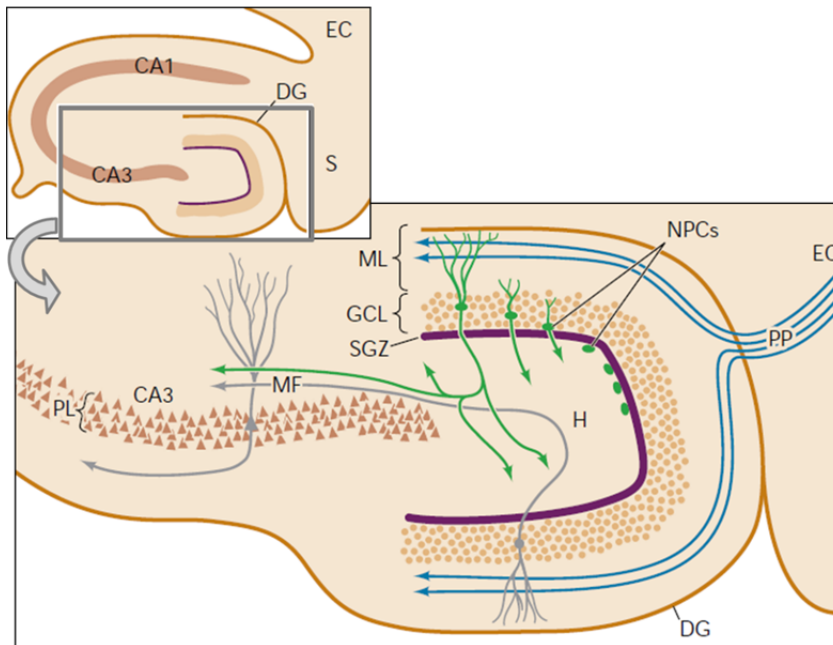


Figure 1.3: Schematic representation of the hippocampal formation and the process of adult hippocampal neurogenesis. *Top:* A transverse section of the rodent hippocampal formation illustrating the major cytoarchitectonic regions. DG, dentate gyrus; EC, entorhinal cortex; S, subiculum; CA, cornu ammonis. *Bottom:* Neural progenitor cells (NPCs) are located along the subgranular zone (SGZ), the border zone between the hilus (H) and the granule cell layer (GCL). The SGZ constitutes the neurogenic region in the DG. Neurogenesis progresses from division of radial glia-like stem cells over rapid division of intermediate progenitor cells to production of postmitotic cells which migrate superficially through the granule cell layer toward the molecular layer (ML) and differentiate into granule cells. Cell bodies stay in the GCL, dendrites project toward the ML and axons project toward the hilus and CA3 area. New granule cells (green) receive glutamatergic input from the perforant path (PP). Mature neurons born during development are shown in gray. PL, pyramidal layer; MF, mossy fibres [167].

neurons, form dendritic arbours reaching the molecular layer and project axons into the CA3 region in rats [103, 119] and mice [204] (Figure 1.3). Electrophysiological measurements, after *in vivo* labeling of the newly generated dentate granule cells with a GFP (green fluorescent protein)-expressing retroviral vector, show that newborn cells in the adult mouse hippocampus become functional neurons [189]. In young adult rats, each day, approx. 9000 new cells are generated, which is approx. 0.1% of the granule cell population [33]. The rate of neurogenesis in the adult primate hippocampus is estimated to


be lower in comparison with rodents [62, 102], *i.e.*, in the macaque monkey, approx. 0.004% of the total granule cell population is renewed per day [102]. Several physiological and pathological factors are known to change the rate of adult SGZ neurogenesis. For instance, stress [74] and aging [103] decrease the rate of neurogenesis, whereas neurogenesis is stimulated by environmental enrichment [96], exercise [188], stroke [115] and seizures. Bengzon et al. [20] reported that even single brief seizures are sufficient to increase neuronal cell proliferation in the adult rat DG. Similar increases have been demonstrated in other rodent models of seizures, such as those induced by amygdala kindling [140] and by electroconvulsive shock [171]. Status epilepticus elicited in rats by administration of chemoconvulsants such as pilocarpine, kainic acid or pentylenetetrazole also increases neurogenesis [47, 91]. A recent study shows that hippocampal neurogenesis is also stimulated after early-life FS induced by exposing young rat pups to a hyperthermia treatment [110, 111]. The demonstration of increased hippocampal neurogenesis after seizures in different animal models has led to the hypothesis that newborn DG neurons may contribute to the increased seizure susceptibility characterizing TLE, one of the most frequent seizure disorders. However, it remains controversial whether seizures increase hippocampal neurogenesis in epileptic patients. An increase of neuronal precursor cells in the hilus and the SGZ of the DG is found in resected hippocampal tissue of TLE patients who were less than 2 years old [21]. On the other hand, Mathern et al. [120] reported a decreased neurogenesis in the DG of older patients with seizure onset during childhood [120]. However, a more recent study on surgical hippocampal specimen from adult TLE patients demonstrated large numbers of neuronal progenitor cells in the SGZ [48]. Technical limitations might contribute to the observed conflicting results. Interpretation of the extent of proliferation may also vary according to the marker used to label immature neurons. Indeed, different markers of immature neuronal cells display diversity in the duration of expression [195]. Furthermore, study of the human epileptic hippocampus is only possible after surgical removal of the epileptogenic zone in pharmacoresistant TLE patients who may represent only a subset of the TLE patient population. The individuals studied so far may reflect a diverse population. In those studies, hippocampi obtained during autopsies or tumor resection from patients without epilepsy or other neurological

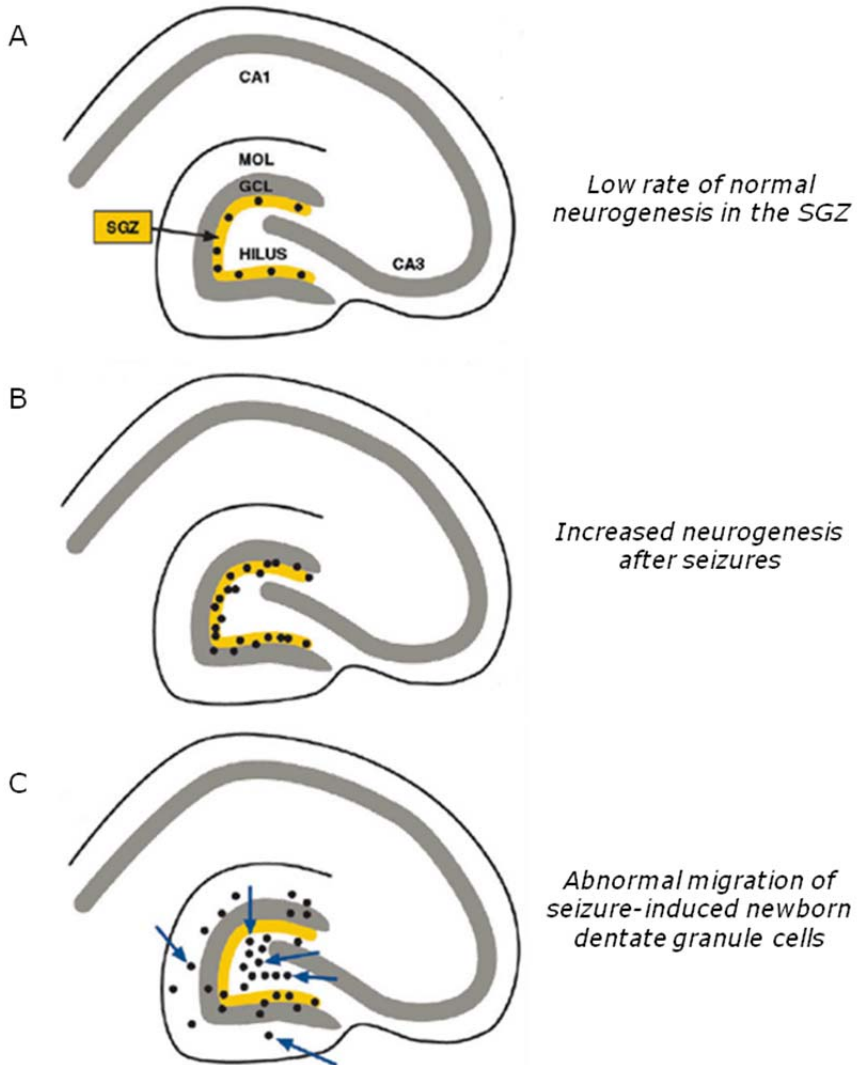
disorders were used as controls. Moreover, seizure-related neurogenesis could be influenced by the age of the patient at the onset of TLE, the individual genetic background as well as the seizure severity. Nevertheless, recent research by Parent et al. [139] points to the importance of increased neurogenesis at some point during the process of epileptogenesis.

1.2.1.2 Role of seizure-induced newborn neurons in the process of epileptogenesis

Hippocampi of both TLE patients and experimental rodent models of TLE exhibit characteristic morphopathological changes. A frequently observed morphological feature is neuronal cell loss due to seizure-related neuronal death. Neuronal degeneration is predominantly seen in the pyramidal cells of the CA1, CA3 and CA4 regions of the Ammon's horn, whereas the CA2 pyramidal cells and the granule cells of the DG are preserved in most cases. Initially, it was thought that newborn neurons could be beneficial by compensating for the neuronal cell loss. However, it has been suggested that seizure-induced newborn neurons may display a pro-epileptogenic role rather than a repair function. Indeed, it has been already demonstrated that suppression of seizure-induced neurogenesis attenuates later development of spontaneous recurrent seizures [92]. Approx. 20% of the newborn cells induced by experimental seizures survive [110]. The majority of these newborn cells differentiate into neurons in the dentate granule cell layer [111, 142] and extend axons to the CA3 region [142]. Seizures accelerate the integration of newborn dentate granule cells, but the biological significance of this phenomenon has not yet been elucidated [135]. Following seizures, mossy fibre axons project abnormally to the supragranular inner molecular layer of the DG and the stratum oriens of the CA3 region. But this reorganization of mossy fibres, described as mossy fibre sprouting, does not depend on newborn dentate granule cells [141]. However, adult born dentate granule cells show other abnormalities, including the formation of hilar basal dendrites. The generation of these dendrites, mainly originating from the granule cell somata at the hilar side and extending into the hilus, suggests that they may be postsynaptic targets of the mossy fibre collaterals [181]. Furthermore, Scharfman et al. [165] reported that some newborn granule-like neurons migrate aberrantly to the hilus and the molecular layer after

pilocarpine-induced seizures in rats. Suc ectopic cells could be relevant to TLE, since they are detected in the hilus and in the dentate molecular layer in surgically removed hippocampi of epileptic patients [139]. The ectopic granule-like neurons develop membrane properties, a firing behavior, morphological properties and an immunocytochemical profile similar to granule cells of the granule cell layer. However, in contrast with the normal granule cells, ectopic granule cells show, in addition, spontaneous bursts of action potentials which are synchronized with CA3 pyramidal cell discharges [165]. These findings support the 'neurogenesis hypothesis of epileptogenesis' which states that seizure-induced newborn hippocampal neurons may incorporate abnormally into the existing hippocampal network in such a way that they promote hippocampal hyperexcitability [104, 142, 165] (Figure 1.4).


Figure 1.4: Schematic overview of altered neurogenesis in the dentate gyrus after seizures. The rate of neurogenesis is low under physiological conditions. Newborn dentate granule cells are predominantly located in the subgranular zone (SGZ) of the dentate granule cell layer (A). Seizures increase the rate of neurogenesis (B) and some of these seizure-induced newborn dentate granule cells migrate aberrantly to the molecular layer (MOL) and the hilus (C) (adapted from Scharfman [164]).



1.2.2 The 'ion channel hypothesis'

1.2.2.1 Ion channels: general aspects

Ion channels are pore-forming transmembrane (TM) proteins that allow the flow of ions down their electrochemical gradient. Depending on their characteristics, ion channels permeate anions or cations in or outside of cells, leading to membrane depolarization or hyperpolarization. Hence, ion channels are involved in excitatory or inhibitory neurotransmission. This thesis focuses on ligand-gated

ion channels (LGICs), a class of ion channels that is opened upon ligand binding. The LGICs can be divided into three families: the Cys-loop superfamily, the glutamate receptor family and the P2X receptor family. In mammals the Cys-loop superfamily consists of nicotinic, GABA_A, glycine and serotonin (5HT₃) receptors (Figure 1.5) [44]. These ion channels are pentameric structures forming a central ion pore, with each subunit being composed of a large extracellular N-terminus, 4 TM domains and a short extracellular C-terminus. The ionotropic glutamate receptors are subdivided in NMDA, AMPA and kainate receptor subfamilies. These receptors are tetrameric structures, with each subunit being composed of 3 TM domains (with a re-entrant helical loop between the first and the second TM domain, which can be considered as a fourth TM domain). The P2X receptors, which are ATP-gated channels, are trimeric structures consisting only of two TM domains.

1.2.2.2 Involvement of ion channels in the process of epileptogenesis

Electrophysiological measurements in several animal models of TLE demonstrate that seizures lead to long-term changes in neuronal excitability. The resulting hyperexcitable neuronal network is likely to be caused by alterations in neuronal excitation and/or inhibition in the hippocampus, from which the seizures originate. Ion channels are known to be key players in the control of neuronal excitability. Hence, a change in the expression and/or properties of ion channels is suggested as a pathophysiological mechanism underlying epileptogenesis.

The NMDAR and the AMPAR are LGICs that belong to the family of ionotropic glutamate receptors that are responsible for fast excitatory neurotransmission. In the kindling model of epilepsy, the synaptic transmission in the DG is characterized by an increased contribution of NMDARs [126]. Furthermore, analyses of single NMDAR channels and whole-cell NMDA-gated currents in isolated dentate granule cells obtained from kindled animals show specific long-term alterations in the biophysical properties of NMDARs [100]. These reported functional changes may be related to an altered expression or modification in subunit composition of ionotropic receptors. Recent studies provide evidence that experimentally induced seizures can modify the hippocampal expression of NMDAR [9, 22] and AMPAR subunits [150, 202].

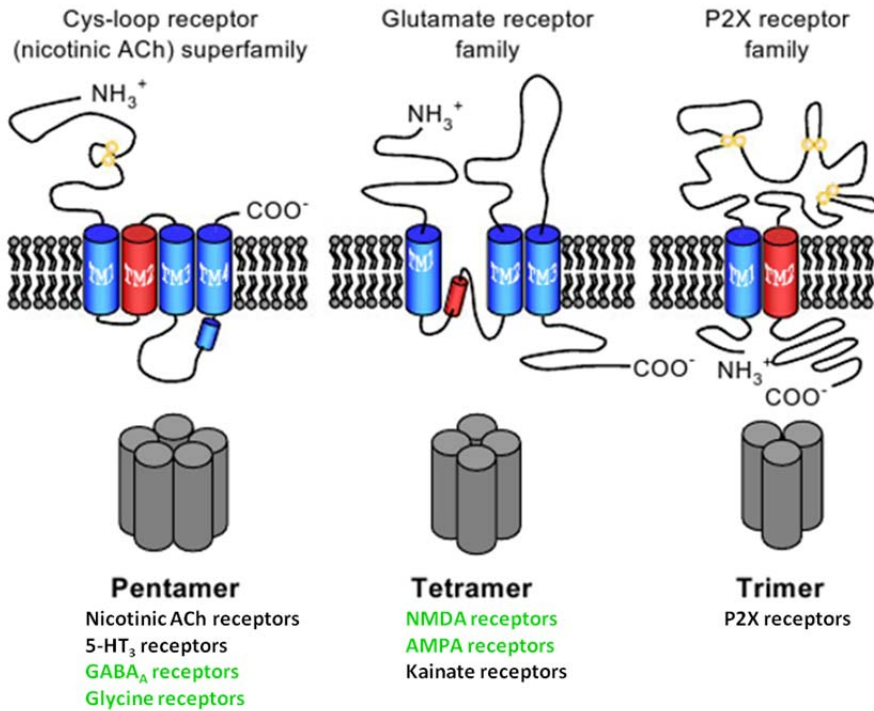


Figure 1.5: Schematic representation of the three structural categories of ligand-gated ion channels. See text for explanation. This thesis focuses on GABA_A, glycine, NMDA and AMPA receptors (indicated in green) (adapted from Collingridge [44]).

Additionally, human studies show greater NMDAR and AMPAR mRNA levels per neuron in hippocampi from TLE patients compared with autopsies without cerebral pathology. Specifically, in dentate granule cells, NMDAR2 and AMPA GluR1 (glutamate receptor 1) mRNA levels display the strongest increase relative to the other subunits [122]. These changes in mRNA are paralleled by changes in protein levels [123]. Recent work focused also on the contribution of I_h -conducting HCN channels to neuronal excitability. Chen et al. [38] reported a depolarization shift of the HCN channel activation and a slowing of the kinetics, thus a change in the I_h current which is associated with long-term hippocampal hyperexcitability in a rat model of FS. These functional changes are accompanied by an isoform-selective change in HCN1 expression in surviving DG granule cells of human and experimental chronic epileptic hippocampus [19].

Next to changes in excitatory systems, alterations in inhibitory circuits may prove to be equally important in the development of a hyperexcitable network. In this context, the ionotropic GABA_AR, known for its participation in mediating fast inhibitory neurotransmission, has received much attention. Altered functional properties of GABA_ARs in hippocampal neurons are observed after the development of TLE. Gibbs et al. [71] demonstrated in the pilocarpine model that the whole-cell dentate granule GABA_AR maximal current response was increased, whereas the whole-cell CA1 GABA_AR maximal current response was decreased. These changes in GABA_AR function are associated with alterations in subunit expression and, hence, receptor composition [26, 157, 170]. Consistent with findings in several animal models of TLE, Loup et al. [117] found an altered GABA_AR subunit expression profile in hippocampal tissue of TLE patients. These changes are most pronounced in surviving dentate granule cells, which display an up-regulation of the $\alpha 1$, $\alpha 2$, $\beta 2/3$ and $\gamma 2$ subunits. It has been suggested that this increased expression of GABA_ARs represents a compensatory response to the hippocampal hyperexcitability and recurrent seizures. The enhanced GABA_AR expression is accompanied by a polarized staining pattern with an increased staining on the soma membrane and apical dendrites and a significant reduction in staining in the basal dendrites of the granule cell. This redistribution of GABA_ARs on dentate granule cells is supposed to be compensatory in response to the recurrent excitatory circuits resulting from mossy fibre sprouting [117]. Next to their role in inhibitory neurotransmission, GABA_ARs can also have excitatory effects. As stated earlier in this introduction, the equilibrium potential for GABA (E_{GABA}) is depolarizing in the developing brain as a consequence of the higher intracellular Cl^- concentration in immature compared with mature neurons. Depolarizing GABAergic responses have also been observed in human and experimental epileptic hippocampi. A recent study in the pilocarpine model demonstrated a depolarizing shift in dentate granule cell E_{GABA} , resulting in an altered synaptic integration and an increased dentate granule cell excitability [143]. This switch in Cl^- homeostasis is probably due to a down-regulation of the Cl^- extruding K^+-Cl^- cotransporter (KCC2) synergistically with an up-regulation of the Cl^- -importing $\text{Na}^+-\text{K}^+-2\text{Cl}^-$ cotransporter (NKCC1) [50, 143]. The expression of these two main neuronal Cl^- co-transporters is likely to be influenced by brain-derived neurotrophic factor [50].

Taken together, the above-mentioned results describe altered inhibitory and excitatory neuronal hippocampal circuits following seizures. These alterations occur concurrently with an increased hippocampal neurogenesis induced by seizures. Until now, most of the studies reported a net change in excitatory and inhibitory receptor subunit expression, without addressing whether these changes can be attributed to old cells changing their expression profile or to new cells that were generated after a seizure. Porter et al. [38] showed a differential alteration of AMPAR subunit expression in dentate granule cells that had been generated before and after seizures. This suggests different contributions of these two cell populations to the process of epileptogenesis. The findings also suggest that seizure-induced neurogenesis may be a source of long-lasting alterations in LGIC expression, and thereby of hippocampal hyperexcitability. Future research should demonstrate whether these neuroplastic changes can be a target for new anti-epileptic therapies.

1.3 AIMS OF THE STUDY

Temporal lobe epileptogenesis is characterized by an imbalance between excitation and inhibition, leading to hippocampal hyperexcitability. In normal physiological conditions, the hippocampal dentate gyrus (DG) controls the amount of excitation passing through the hippocampal formation. The DG is a simple cortical region being an integral part of the hippocampal formation. Three layers can be distinguished in the DG (see also Figure 1.3): the granule cell layer, the molecular layer and the hilus (or polymorphic layer). The granule cell layer is largely composed of densely packed granule cells. The molecular layer is predominantly occupied by the dendrites of the dentate granule cells, but also receives fibres from the perforant pathway. The hilus consists mainly of axons of granule cells (mossy fibres), excitatory mossy cells and inhibitory interneurons. The DG receives its major input from cells located in layer II of the entorhinal cortex where the perforant pathway arises. Entorhinal terminals form synapses onto dendrites of granule cells in the outer two-thirds of the molecular layer. The only output from the rat hippocampal DG is the CA3 field of the hippocampus. The mossy fibre axons of granule cells provide synaptic input to neurons in the CA3 pyramidal cell layer. Hence, the DG being located between the entorhinal cortex and CA3 area is anatomically well situated but also physiologically predisposed to limit propagation of synchronous excitatory activity from the entorhinal cortex to downstream hippocampal structures. Intrinsic properties of normal adult DG granule cells (*i.e.* rare action potential generation due to limited direct connectivity between DG granule cells, high resting membrane potential and strong GABA_AR-mediated inhibition) contribute to the low excitability level of the DG circuit allowing it to function as a filter at the entrance of the hippocampal formation [6, 84]. It has been proposed that seizure-induced changes may compromise this DG filter function and contribute to enhanced neuronal excitability in the hippocampus [46]. In this thesis, we focused on the DG structure and we aimed at further elucidating the mechanisms by which early-life FS may lead to enhanced neuronal excitability. For all experiments, the appropriate-aged animal model of FS developed by Baram and colleagues was used [11].

Characterization of hippocampal dentate granule GABA_ARs after experimental early-life febrile seizures

It has already been shown that experimental early-life FS induce alterations in functional properties of hippocampal HCN channels, which are associated with isoform-selective changes in HCN expression. Based on these results, we hypothesized that early-life FS may also alter function and/or expression of other ion channels that are responsible for the control of hippocampal excitability. In that respect, the GABA_AR is an interesting candidate to study because of its developmental switch from excitatory to inhibitory signaling and because it has been demonstrated that the normal physiological function of the DG filter depends on adequate GABA_AR-mediated neurotransmission. Therefore, we investigated in **chapter 3** whether GABA_AR-mediated neurotransmission is influenced by early-life FS. To this end, we analyzed spontaneous inhibitory postsynaptic currents (sIPSCs) and whole-cell GABA-elicited responses using whole-cell patch-clamp recordings from dentate granule neurons in hippocampal slices obtained from rats with early-life FS. To elucidate if functional GABA_AR properties reflect GABA_AR subunit composition, we performed quantitative real time PCR (qPCR) analysis and determined GABA_AR subunit gene expression levels. The reliability of qPCR gene expression data depends on the used normalization strategy. Internal reference genes are most frequently used to normalize qPCR data. However, the expression of reference genes may differ under different experimental conditions. Therefore, we determined in **chapter 2** the gene expression stability of seven frequently used reference genes in the hippocampal DG of rats that had experienced early-life FS. The aim was to determine the most stably expressed reference genes to use for normalization of GABA_AR subunit gene expression levels.

Characterization of ligand-gated ion channels in newborn dentate gyrus cells after experimental early-life febrile seizures

The number of newborn DG granule cells is persistently increased after experimental early-life FS. It has been reported that these newborn DG granule cells develop a mature neuronal phenotype at 8 weeks after experimental FS. Yet, little is known of how these FS-induced newborn hippocampal neurons blend in the existing neuronal network and what the functional consequences

are. Further phenotyping may provide information about their possible role in the neuronal network. Therefore, we analyzed in **chapter 4** whether FS may be a source of long-lasting alterations in ligand-gated ion channel (LGIC) expression in newborn DG cells. To this end, dividing cells were labeled immediately after early-life FS with 5-bromo-2'deoxyuridine (BrdU). BrdU-labeled cells in the DG were evaluated in adulthood for the expression of inhibitory (GABA_AR and GlyR) and excitatory (NMDAR and AMPAR) LGICs to explore possible candidates underlying the hippocampal hyperexcitability observed after FS. However, functional characterization is necessary to further elucidate their physiological relevance in hippocampal hyperexcitability. Visualization of BrdU-labeled cells always requires tissue fixation, and hence does not allow functional characterization of newly generated cells in hippocampal slices. This limitation can be overcome by intrahippocampal injection of a retroviral vector expressing green fluorescent protein (GFP), which labels dividing cells only. In **chapter 5**, our purpose was to adapt the currently used animal model of FS to a model in which FS-induced DG cells are labeled with GFP making functional characterization possible in the future.

2

Validation of reference genes for quantitative real time PCR studies in the dentate gyrus after experimental febrile seizures

This chapter is based on:

Validation of reference genes for quantitative real time PCR studies in the dentate gyrus after experimental febrile seizures

[Ann Swijssen](#), Katherine Nelissen, Daniel Janssen, Jean-Michel Rigo* and Govert Hoogland*.

* Both authors contributed equally to this work

Submitted

2.1 ABSTRACT

Quantitative real time PCR (qPCR) is a commonly used technique to quantify gene expression levels. Validated normalization is essential to obtain reliable qPCR data. In that context, normalizing to multiple reference genes has become the most popular method. However, expression of reference genes may vary per tissue type, developmental stage and in response to experimental treatment. It is therefore imperative to determine stable reference genes for a specific sample set and experimental model.

The present study was designed to validate potential reference genes in hippocampal tissue from rats that had experienced early-life febrile seizures (FS). To this end, we applied an established model in which FS were evoked by exposing 10-day old rat pups to heated air. One week later, we determined the expression stability of seven frequently used reference genes (18S rRNA, ActB, GusB, Arbp, Tbp, CycA and Rpl13A) in the hippocampal dentate gyrus (DG) using geNorm and Normfinder software. Our results demonstrated that the geometric averaging of at least CycA, Rpl13A and Tbp allowed reliable interpretation of gene expression data in this experimental set-up. The data also showed that ActB and 18S rRNA were not suited as reference genes in this model.

2.2 INTRODUCTION

Febrile seizures (FS) are convulsions associated with fever and occur in 4% of children between the age of 3 months and 5 years [36, 191]. Retrospective studies demonstrate that adult patients with hippocampal sclerosis-associated temporal lobe epilepsy (TLE) have a 40% incidence of FS, suggesting a causal relationship [36]. Also, experimental FS have a long-lasting effect on hippocampal excitability, resulting in enhanced seizure susceptibility [39, 53, 54]. At a cellular level, an altered seizure threshold may come from a change in the expression of proteins that are known to control neuronal excitability (for review see [57]). Hence, quantification of the post-FS expression of genes that encode receptors, ion channels, etc. might help elucidating FS-induced epileptogenesis.

Nowadays, quantitative real time PCR (qPCR) is a commonly used tool to quantify gene expression. An advantage of this highly specific and sensitive technique is that it allows analysis on small amounts of starting material [31, 79]. However, measured gene expression levels may be confounded by several variables during the multistep procedure of isolating and processing RNA *e.g.* the amount and quality of starting material, enzymatic efficiency and variability between tissues or cells in overall transcriptional activity [182, 190, 192]. Internal reference genes are most frequently used to normalize methodology-induced variations in qPCR studies [87, 190]. Until recently, 'housekeeping genes' (HKGs) such as glyceraldehyde-3-phosphate dehydrogenase (GAPDH), 18S subunit ribosomal RNA (18S rRNA) or beta-actin (ActB) were commonly used as reference genes, also in neurobiological studies. HKGs are continually read and encode for products that are necessary for the metabolism and existence of a cell. They are supposed to be invariably expressed under different experimental conditions. However, the expression of these classical reference genes may vary per tissue type and developmental stage, and may even vary in response to experimental treatment [51, 52, 125, 155, 168]. Hence, validation of suitable reference genes for a specific sample set and experimental model is imperative to obtain consistent gene expression data. In addition, it has been shown that the accuracy of qPCR data further improves when at least three reference genes are used for normalization [190].

Although recent studies have validated reference genes for rat brain tissue in different experimental conditions [25, 76, 106, 147], to our knowledge there is thus far no report of validated reference genes in hippocampal tissue from rats that have been exposed to experimental FS. Therefore, we used an established model where FS are evoked by exposing 10-day old rat pups to heated air [89]. One week later, we evaluated the expression stability of seven frequently used reference genes in the hippocampal dentate gyrus (DG). To this end, we used two different mathematical algorithms (geNorm [190] and Normfinder [7] VBA applets for Microsoft Excel) for normalization.

2.3 MATERIALS AND METHODS

2.3.1 Induction of febrile seizures and tissue sampling

Litters of 5-10 male Sprague-Dawley rat pups (Harlan, Horst, The Netherlands) were housed with a dam under temperature controlled conditions and 12h dark-light cycle with water and food *ad libitum*. At postnatal day 10, FS were evoked by hyperthermia as described before [11, 110, 111]. Briefly, pups were injected subcutaneously with 0.2 ml 0.9% NaCl to prevent dehydration, placed in a perspex cylinder and exposed to a regulated stream of heated air. Rectal temperatures were monitored every 2.5 min. A core temperature $>39.5^{\circ}\text{C}$ (usually reached within 5 min) indicated the start of a 30 min hyperthermia phase in which the heated air stream was adjusted to maintain a core temperature of $41\text{-}42.5^{\circ}\text{C}$. Behavioral seizures occurring during treatment (HT+FS), were monitored by two observers. These seizures were stereotyped and previously shown to correlate with rhythmic epileptic discharges in the hippocampus [11]. Some rats did not display seizure behavior during the hyperthermia phase (HT-FS). The hyperthermia phase was terminated by dipping the pup in room temperature water, until the pre-treatment body temperature was reached and then returned to the dam. Control rats (NT) underwent the same treatment, except that the stream of air was adjusted to maintain the body temperature that was measured at the start of the experiment ($\sim 35^{\circ}\text{C}$). Six to nine days after FS induction, rats were decapitated, brains were rapidly removed from the skull and placed in ice-cold oxygenated ($95\%\text{O}_2/5\%\text{CO}_2$) sucrose-based artificial cerebrospinal fluid (sucrose-aCSF) containing (in mM): 210 sucrose, 2.5 KCl, 26 NaHCO_3 , 1.25 NaH_2PO_4 , 25 glucose, 1 CaCl_2 , and 7 MgSO_4 (pH 7.4, ~ 340 mOsm). Next, $350\text{-}\mu\text{m}$ -thick coronal slices were cut in ice-cold oxygenated sucrose-aCSF using a vibratome (Microm/Thermo Fisher Scientific, Walldorf, Germany) and DG regions were microdissected from each acute brain slice. DG samples were then quickly frozen in liquid nitrogen and stored at -80°C until RNA isolation. All experiments were approved by the Hasselt University ethics committee for animals.

2.3.2 RNA isolation and cDNA synthesis

Total RNA was isolated from DG samples using the RNAqueous-Micro kit (Ambion, Lennik, Belgium), according to the manufacturer's protocol. Trace amounts of genomic DNA were removed by DNase I provided with the kit. RNA purity and concentration were checked by optical density, using a NanoDrop ND-1000 spectrophotometer (Thermo Fisher Scientific, Waltham, USA). For cDNA synthesis, total RNA (220 ng) was first incubated for 10 min at 70°C in order to prevent secondary structures, and then reverse transcribed using the Reverse Transcription System (Promega, Leiden, The Netherlands) in a 20 µl reaction volume containing 5 mM MgCl₂, 1x Reverse Transcription buffer, 1mM dNTP mixture, 0.25 µg Oligo(dT)₁₅ primers, 0.25 µg hexamer oligonucleotides, 20 U RNase inhibitor and 12.5 U AMV reverse transcriptase, that was first incubated for 60 min at 42°C, then for 5 min at 95°C and then at 4°C. All cDNA samples were stored at -20°C until qPCR analysis.

2.3.3 Quantitative real time PCR

qPCR was performed in optical 96-well plates with an ABI PRISM 7500 Fast sequence detection system (Applied Biosystems, Carlsbad, California), and carried out in a 10 µl reaction volume containing 5 µl RT SYBR green qPCR master mix (SABiosciences/Qiagen, Venlo, The Netherlands), 0.4 µM forward and reverse primer (Table 2.1), and 11 ng cDNA dissolved in nuclease-free water. A no-template control containing nuclease-free water instead of cDNA was included to test for possible contamination of assay reagents. Samples were run in duplicate. PCR conditions comprised a 10 min preincubation at 95°C, followed by 40 cycles of 15s at 95°C and 60s at 60°C. Fluorescence was measured at 522 nm wavelength during each annealing step. Each PCR program was followed by a general dissociation curve protocol to check product specificity. PCR efficiency of the reference genes was determined by a standard curve of cDNA samples according to the MIQE guidelines [32].

2.3.4 Data analysis

RNA copy numbers were quantified using the comparative $\Delta\Delta C_t$ method as follows. Raw expression levels were first expressed relative to the sample with the highest expression before geNorm [190] or Normfinder [7] input. The geNorm algorithm provides a measure of gene expression stability (M value) and determines the optimal number of reference genes using pairwise variation (V) analysis. In contrast to geNorm, Normfinder estimates not only the overall expression variation of the candidate reference gene, but also the variation between sample subgroups. The output of Normfinder consists of a stability value based on both intra- and intergroup expression variation. The Accumulated Standard Deviation (Acc.SD), as indicator for the optimal number of reference genes, was determined using GenEx software.

Data are presented as mean \pm standard error of the mean (SEM). Statistical analysis was performed using Graphpad Prism5 software. Differences between means were tested using the Mann-Whitney test. A value of $P < 0.05$ was considered as statistically significant.

Table 2.1: Selected reference genes for analysis of expression stability

| Gene symbol | Gene function | Primer sequence (5'→3')^a or SABiosciences qPCR assay ID^b | Amplicon length (bp) |
|--------------------|---|---|-----------------------------|
| <i>ActB</i> | Cytoskeletal structural protein | F: TGT CAC CAA CTG GGA CGA TA R: GGG GTG TTG AAG GTC TCA AA | 165 |
| <i>CycA</i> | Serine-threonine phosphatase inhibitor | F: TAT CTG CAC TGC CAA GAC TGA GTG R: CTT CTT GCT GGT CTT GCC ATT CC | 126 |
| <i>18S rRNA</i> | Ribosomal subunit | F: ACG GAC CAG AGC GAA AGC AT R: TGT CAA TCC TGT CCG TGT CC | 310 |
| <i>Rpl13A</i> | Structural component of 60S ribosomal subunit | F: GGA TCC CTC CAC CCT ATG ACA R: CTG GTA CTT CCA CCC GAC CTC | 132 |
| <i>Tbp</i> | General transcription factor | F: TGG GAT TGT ACC ACA GCT CCA R: CTC ATG ATG ACT GCA GCA AAC C | 131 |
| <i>GusB</i> | Exoglycosidase in lysosomes | PPR43194B ^b | 137 |
| <i>Arbp</i> | Catalysis of protein synthesis | PPR42394Ab | 92 |
| <i>Cnr1</i> | Endocannabinoid signalling | PPR52793Ab | 156 |

ActB, beta-actin; *CycA*, CyclophilinA; *18S rRNA*, 18S subunit ribosomal RNA; *Rpl13A*, Ribosomal protein L13A; *Tbp*, TATA box binding protein; *GusB*, beta-glucuronidase; *Arbp*, Acidic ribosomal phosphoprotein P0; *Cnr1*, Cannabinoid Type 1 (CB1) receptor. F, forward primer; R, reverse primer.

^a primer sequences are based on literature [132]. ^b ID, identification.

2.4 RESULTS

Seven reference genes (ActB, CycA, 18S rRNA, Rpl13A, Tbp, GusB and Arbp) were chosen from literature [132, 147] and evaluated for gene expression stability in DG samples from 9 NT, 6 HT-FS and 7 HT+FS rats. To avoid coregulation, reference genes were selected from different functional classes. PCR efficiency of the reference genes was situated between 99.96% and 113.89% (Table 2.1).

2.4.1 Expression levels of candidate reference genes

When all samples were taken together, the reference genes showed expression levels varying from a cycle threshold (Cq) value of 15.40 for Arbp to 31.22 for Tbp (Table 2.2). With a $Cq \leq 22.23$, Arbp, ActB, CycA and Rpl13 were more expressed than GusB and Tbp that had a $Cq \geq 24.42$. 18S rRNA displayed the highest Cq variability, ranging from 17.91 to 29.75. A similar expression pattern was observed when Cq values were calculated per experimental group (Figure 2.1). Cq standard deviations provide a first idea about the variability in expression, ranking from most to least variably expressed as 18SrRNA>Actb>Arbp>GusB>Tbp> Rpl13>CycA.

Table 2.2: Cycle threshold (Cq) values of candidate reference genes

| | Arbp | ActB | CycA | Rpl13 | 18S rRNA | GusB | Tbp |
|-------------|-------------|-------------|-------------|--------------|---------------------|-------------|------------|
| Min | 15.40 | 15.71 | 17.75 | 18.33 | 17.91 | 24.42 | 26.79 |
| Max | 20.70 | 22.41 | 21.12 | 22.23 | 29.75 | 29.65 | 31.22 |
| Mean | 16.99 | 17.75 | 18.81 | 19.44 | 25.09 | 26.97 | 28.22 |
| SD | 1.41 | 1.66 | 0.94 | 1.11 | 2.95 | 1.28 | 1.22 |

Minimal (min), maximal (max), mean, standard deviation (SD) of the Cq of each evaluated reference gene in the total sample set (n=22).

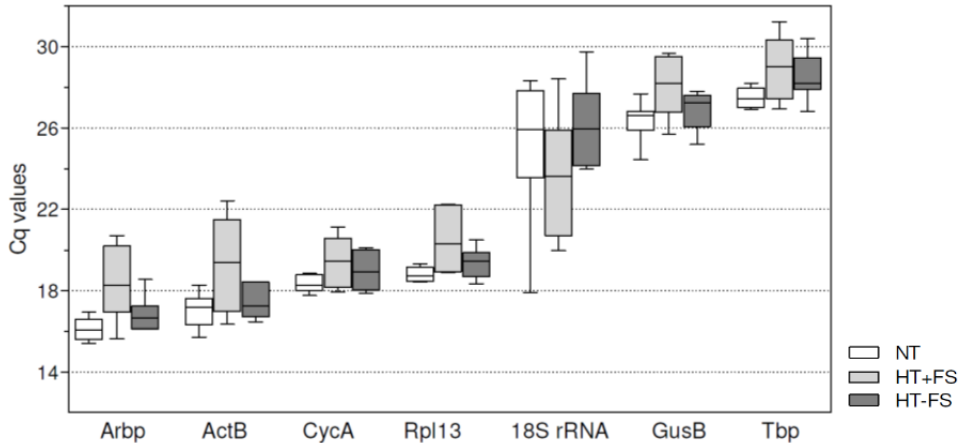


Figure 2.1: Cycle threshold (Cq) levels of candidate reference genes in each experimental group. Boxes represent lower and upper quartiles with medians, whiskers represent the outer 10%. NT, normothermia controls (n=9); HT-FS, hyperthermia without seizures (n=6); HT+FS, hyperthermia with seizures (n=7).

2.4.2 Validating candidate reference genes

geNorm is used to determine the average expression stability (M value), based on the average pairwise variation between a particular gene and all other reference genes in the study. With the exception of 18S rRNA, all genes did show high expression stability, indicated by M values below the default limit of 1.5 suggested by the geNorm software (Figure 2.2A). Based on the M values, CycA and Rpl13 were the most stably expressed genes. It is commonly known that normalization to multiple reference genes is advisable, as the use of a single gene may introduce normalization errors. In that respect, geometric averaging of multiple reference genes is a proven method to calculate an accurate normalization factor [190]. The optimal number of reference genes to be used for normalization can be determined by pairwise variation between two sequential normalization factors (NF_n and NF_{n+1}), starting with genes with the lowest M value. This analysis learned that for this dataset, the use of five reference genes is optimal when a variation value ($V_{n/n+1}$) < 0.15 is considered as not significantly improving the accuracy (Figure 2.2B). However, inclusion of the fourth ($V_{3/4} = 0.176$) and fifth ($V_{4/5} = 0.153$) most stable gene causes only slight differences in the pairwise variation value (Figure 2.2B).

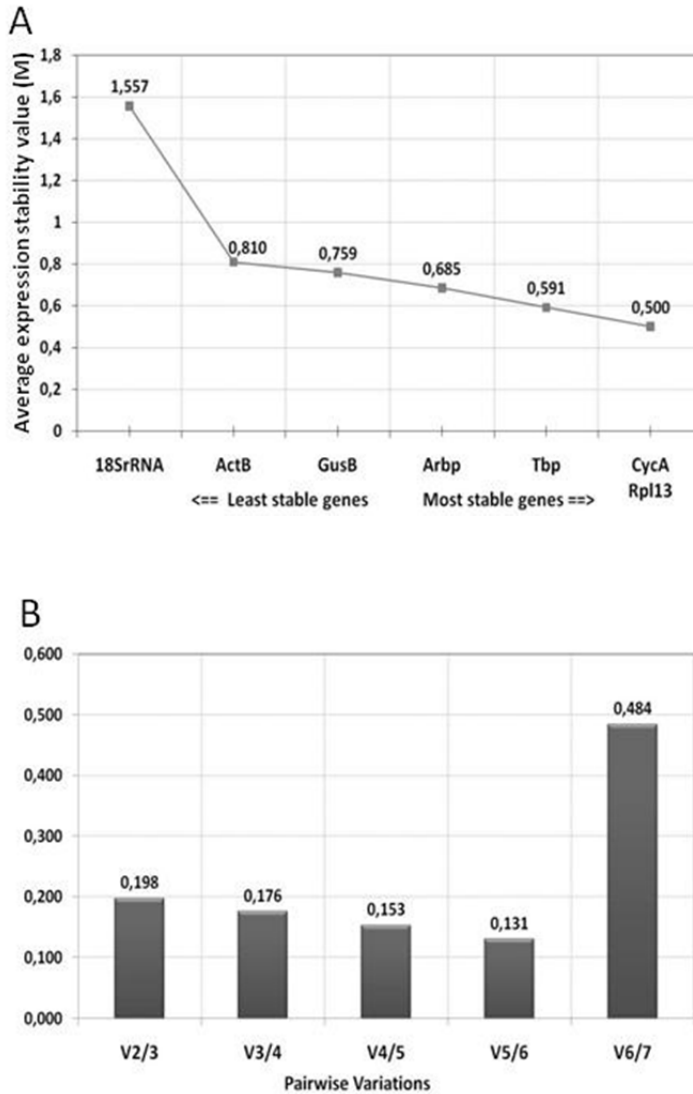


Figure 2.2: Evaluation of candidate reference genes using geNorm analysis software. A: Average expression stability measure (M) of reference genes in the total sample set (n=22), analyzed by stepwise exclusion of the least stable reference gene. B: Determination of the optimal number of reference genes for normalization by means of pair-wise variation ($V_{n/n+1}$) analysis. Every bar represents the variation in normalization accuracy when stepwise adding reference genes according to the ranking in A.

The stability ranking of the candidate reference genes determined by geNorm was compared with the Microsoft Excel-based applet termed Normfinder. This algorithm provides a stability value for each candidate reference gene and ranks the genes according to their expression stability in a given sample set and experimental design. Normfinder also identified Rpl13 as one of the most stably expressed genes, and 18SrRNA as the least stable gene (Figure 2.3A). Yet, Tbp was identified as the most stably expressed gene. This algorithm enables to calculate an Acc.SD, which is an indicator of the optimal number of reference genes necessary to obtain an accurate normalization factor. By this approach, we found that an Acc.SD of 0.119 using one gene could be lowered to 0.054 when six genes were included (Figure 2.3B). Most of this decrease in Acc.SD was attributable to the first three genes (Acc.SD = 0.072).

The ranking order of reference genes proposed by geNorm was not identical to that suggested by Normfinder. However, both algorithms indicated CycA, Rpl13 and Tbp as the most stable genes, whereas 18S rRNA and ActB were found to be the least stably expressed genes (Table 2.3).

Table 2.3: Ranking of reference genes based on the expression stability evaluated by geNorm and Normfinder candidate reference genes

| Ranking order | geNorm | Normfinder |
|---------------|--------------|------------|
| 1 | CycA – Rpl13 | Tbp |
| 2 | Tbp | Rpl13 |
| 3 | Arbp | CycA |
| 4 | GusB | GusB |
| 5 | ActB | Arbp |
| 6 | 18S rRNA | ActB |
| 7 | | 18S rRNA |

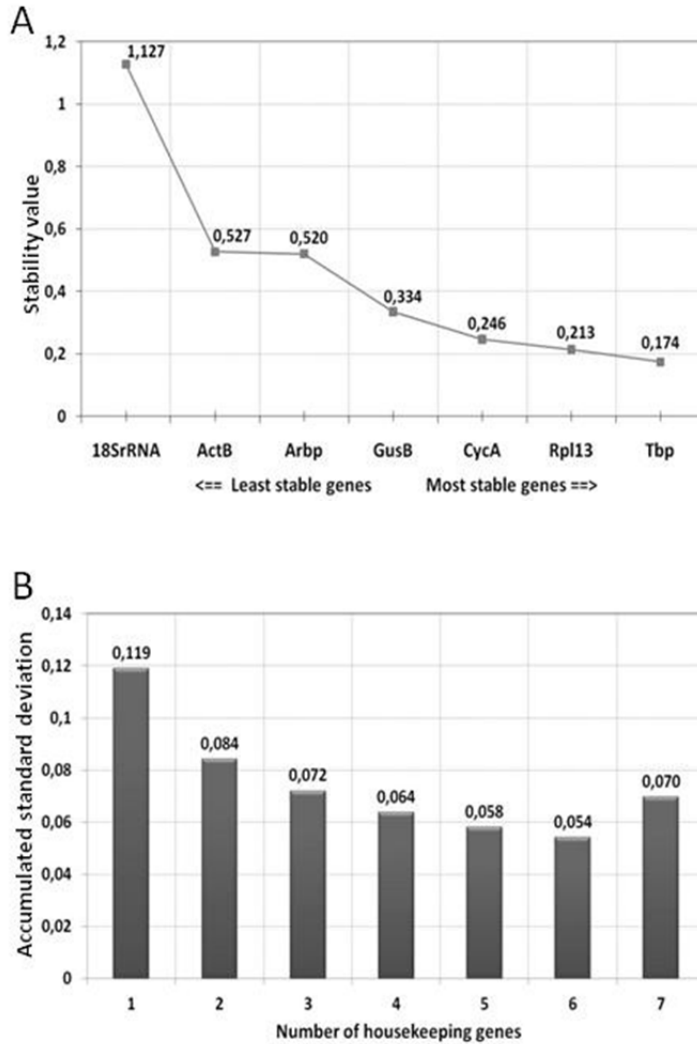

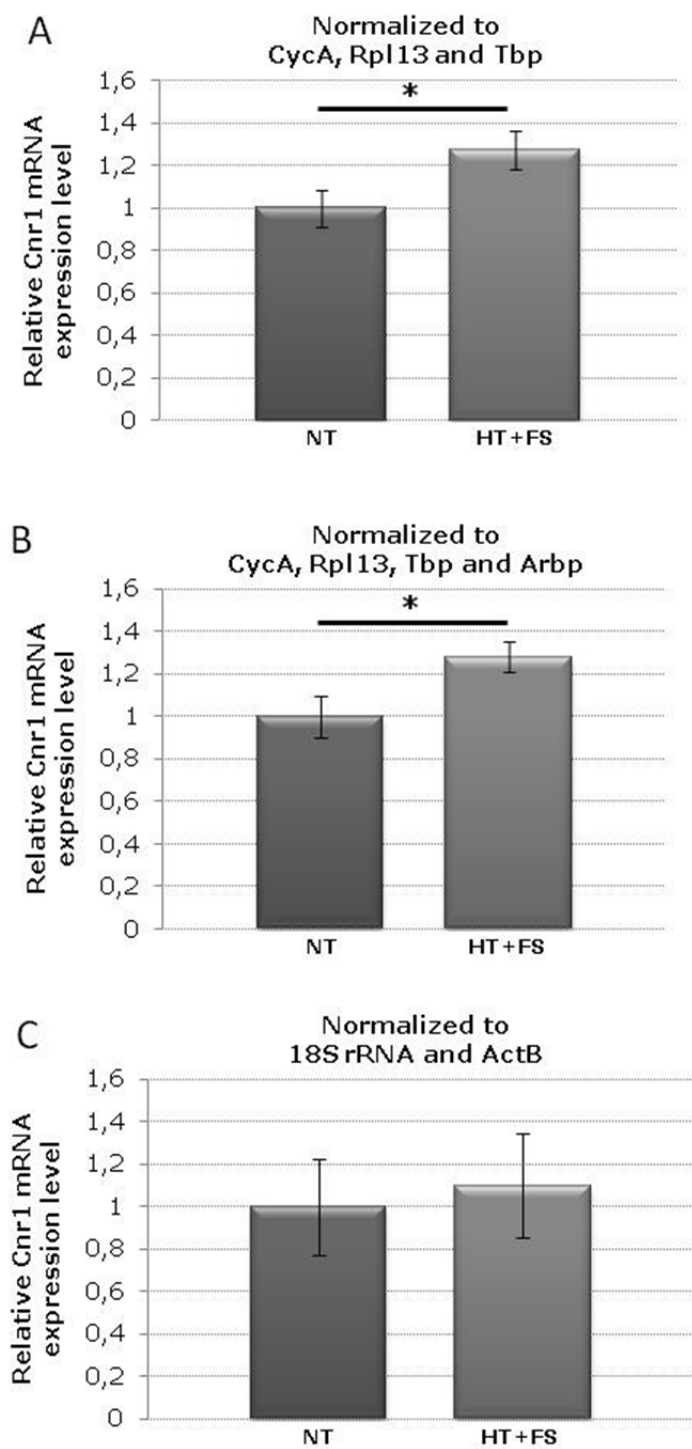


Figure 2.3: Evaluation of candidate reference genes using Normfinder analysis software. A: Stability values of each reference gene in the total sample set (n=22). B: Determination of the optimal number of reference genes for normalization using the accumulated standard deviation (Acc. SD).

2.4.3 Influence of different normalization approaches on the expression profile of a gene of interest

To demonstrate the importance of choosing sufficient and stably expressed reference genes, we normalized the expression of the cannabinoid type 1 receptor gene *Cnr1* to different normalization factors. This gene of interest was chosen because it was previously shown that hippocampal protein levels of this receptor are significantly increased one week after experimental FS [41]. Here, we first normalized *Cnr1* to the geometric average of the three reference genes (*CycA*, *Rpl13* and *Tbp*) that were indicated as most stably expressed by *geNorm* and *Normfinder* analysis. This resulted in a significant upregulation of *Cnr1* in HT+FS rats, compared to NT rats (Figure 2.4A). Inclusion of the fourth most stable gene suggested by *geNorm*, *Arbp*, in the normalization factor did not change the estimated value of the relative *Cnr1* expression levels (Figure 2.4B). However, the significance of *Cnr1* upregulation disappeared when the signal was normalized to the two commonly used reference genes 18S rRNA and *ActB*, which were identified as the most unstable genes by both algorithms (Figure 2.4C). This normalization strategy also caused a strong increase in the standard error.

 **Figure 2.4: Influence of reference genes selected for normalization on the expression profile of *Cnr1* one week after FS induction.** *Cnr1* expression levels were normalized by geometric averaging of three (A) or four (B) stably expressed genes as identified by *geNorm* and *Normfinder*. 18S rRNA and *ActB*, indicated by *geNorm* and *Normfinder* as the least stable genes, are used for normalization of *Cnr1* expression data (C). Data are presented as mean \pm SEM. *, $P < 0.05$; analyzed using a Mann-Whitney test.



2.5 DISCUSSION

Validated normalization is crucial to obtain reproducible qPCR data of genes of interest. In this context, normalizing to internal reference genes has become the most popular method to control for experimental errors introduced by the multitude of steps in this analysis. Several studies point out that the expression of reference genes may vary under different experimental conditions. This implies the necessity of validating these genes in each new experimental setup. To our knowledge, this is the first study that describes the stability of 18S rRNA, ActB, GusB, Arbp, Tbp, CycA and Rpl13A in the DG of rats one week after FS. Both, geNorm and Normfinder were used to rank the analyzed reference genes by their expression stability. This rank order differed slightly between both methods, probably because both tools are based on different mathematical models. Other studies have also described similar ranking discrepancies between geNorm and Normfinder [132, 147]. Interestingly though, both programs agreed on the three most stably expressed genes, being CycA, Tbp and Rpl13A. These converging results stress the significance of including these genes in the normalization factor. In addition, both programs also agreed on ActB and 18S rRNA as the least stably expressed genes. Comparison of these data with those of recent studies revealed similarities and differences. For instance, Bonefeld *et al.* validated eight reference genes in rat hippocampal tissue and also identified CycA and Rpl13A as the most stably expressed genes and Act and 18S rRNA as the least stable genes [25]. Also Pernot *et al.* found that CycA and Tbp were stably expressed in hippocampus samples from a mouse model of TLE, obtained across different phases of the disease. However, in contrast to our study they also observed a stable ActB expression [147]. This discrepancy emphasizes the importance of validating reference genes in each experimental model.

Accurate normalization requires inclusion of multiple reference genes. Geometric averaging of the most stable reference genes is a validated method to obtain a reliable normalization factor [190]. Based on a cut-off value of 1.5, geNorm indicated that the normalization factor should be based on five reference genes. However, according to the geNorm manual, this cut-off value can be set differently. geNorm calculates the optimal number of reference genes by pairwise variation analysis. In that respect, the trend of changing V values after

adding additional genes can be used to obtain an estimate of the number of genes that should be included in the normalization factor. Determination of the optimal number of reference genes is always a trade-off between accuracy and practical considerations, but a minimum of three most stable reference genes is generally recommended [190]. As indicated in Figure 2.2B, a pairwise variation of 0.198 was observed after adding the third most stable gene. Inclusion of the fourth or fifth most stable gene influenced only slightly the pairwise variation. The high $V_{6/7}$ is caused by the high average M value of 18S rRNA, indicating that this gene is highly variably expressed under the present experimental conditions. The Acc.SD calculated by Normfinder suggested the use of six reference genes, though the additive value of genes four to six is minimal. Considering the pairwise variation values, the Acc.SD, and practical issues such as the available amount of RNA, we conclude that the geometric mean of *CycA*, *Rpl13* and *Tbp* should be used to obtain an accurate normalization factor in this experimental setup. If the RNA yield allows the inclusion of an extra reference gene, *GusB* and *Arbp* may be added to this panel. These data also show that 18S rRNA is unfit as reference gene in this model.

Inclusion of the Genorm/Normfinder selected reference genes in the normalization factor, revealed an increased *Cnr1* expression in HT animals that experienced FS. This finding is in agreement with quantitative western blot data from Chen *et al.* [41]. Upregulation of *Cnr1* could not be detected when expression levels were normalized to *ActB* and 18S rRNA, underscoring the suggestion that these 'classical' reference genes are not suitable for our experimental setup. In line with this observation, several studies have reported that including 18S rRNA or *ActB* in the normalization factor altered the estimated value of mRNA expression levels compared to normalization to geNorm proposed genes [25, 147]. As a possible explanation for erroneous normalization when 18S rRNA is used as reference gene, it has been suggested that this may relate to an imbalance between messenger RNA and ribosomal RNA [155].

In conclusion, the present study describes the expression stability of seven candidate reference genes in the hippocampal DG of rats, one week after FS. Our results also suggest that the geometric averaging of at least *CycA*, *Rpl13A* and *Tbp* allows a reliable interpretation of mRNA expression data in this experimental set-up. These data also show that *ActB* and 18S rRNA are unfit to serve as reference gene in this model.

3

Functional characterization of hippocampal dentate granule GABA_A receptors after experimental early-life febrile seizures

This chapter is based on:

Experimental early-life febrile seizures induce changes in GABA_AR-mediated inhibitory neurotransmission in the dentate gyrus

Ann Swijsen, Ariel Avila-Macaya, Bert Brône, Daniel Janssen, Govert Hoogland* and Jean-Michel Rigo*

* Both authors contributed equally to this work

Submitted

3.1 ABSTRACT

Febrile seizures (FS) are the most frequent type of seizures during childhood. Retrospective studies demonstrate that adult patients with hippocampal sclerosis-associated temporal lobe epilepsy (TLE) have a higher incidence of a FS history, suggesting a causal relationship. Experimental FS also cause persistent changes in hippocampal excitability resulting in enhanced seizure susceptibility. However, the mechanisms by which FS may lead to TLE are still largely unknown. Altered inhibitory neurotransmission in the dentate gyrus (DG) circuit, which is known as a critical checkpoint regulating excitability in the hippocampus, has been hypothesized to be involved in epileptogenesis. The aim of the present study is to analyze whether experimental FS change inhibitory synaptic input and postsynaptic GABA_AR function in dentate granule cells. Therefore, we made use of an established model, where FS are elicited in 10-day old rat pups by hyperthermia (HT; core temperature ~41-42.5°C). Normothermia (NT; core temperature ~35°C) littermates served as controls. GABA_AR-mediated inhibitory neurotransmission was studied using the whole-cell patch-clamp technique applied on dentate granule neurons in hippocampal slices within 6-9 days after HT-treatment. Our data show that frequencies of spontaneous inhibitory postsynaptic currents (sIPSCs) were reduced in HT rats that had experienced seizures whereas amplitudes of sIPSCs were enhanced. Whole-cell GABA responses revealed an increased GABA_AR sensitivity in dentate granule cells from HT-treated animals, compared to that of NT controls (EC₅₀: ~32 μM and ~65 μM; respectively). Analysis of spontaneous inhibitory events and whole-cell GABA responses showed similar kinetics in postsynaptic GABA_ARs of HT and NT rats. qPCR experiments indicated that these functional alterations were accompanied by changes in DG GABA_AR subunit expression, which was most pronounced for the α3 subunit. These data support the hypothesis that FS persistently alter neuronal excitability.

3.2 INTRODUCTION

Febrile seizures (FS) are the most common type of seizures during childhood, affecting 2-3% of the children between the age of 3 months and 5 years [191]. Retrospective studies have implicated early-life FS as a risk factor for hippocampal sclerosis-associated temporal lobe epilepsy (TLE) [2, 36, 66]. However, whether these early-life FS actually play a role in the process of epileptogenesis or are simply an indication of pre-existing lesions making the brain more susceptible to the development of seizures, still remains unclear [66, 121]. Since this issue cannot be clarified by correlative clinical studies, an appropriate-aged animal model of FS has been implemented to gain new insights in the potential epileptogenicity of FS [11].

Experimental prolonged FS can be elicited in young rat pups by exposing them to heated air at the age of 10-days when hippocampal development is comparable to that of human infants at the time where they are most susceptible to FS. These hyperthermic-induced behavioral seizures correlate with EEG recordings from the hippocampus [11], and lead to behavioral and electrographic spontaneous seizures later in life in 35% of FS rats and interictal epileptiform EEG abnormalities in 88% of FS rats [54]. Early and long-lasting enhancement in GABAergic inhibition has been found in CA1 pyramidal cells of rats that had experienced FS [39]. Importantly, the observed enhanced inhibition is associated with a persistent increase of limbic excitability [53]. The decrease in seizure threshold may be, at least partially, due to a depolarization shift of the hyperpolarization-activated cyclic nucleotide-gated (HCN) cation channel activation and a slowing of the kinetics of the hyperpolarization-activated (I_h) current in CA1 neurons [38]. The changes in HCN are associated with isoform-selective changes in HCN expression [28, 29]. Based on these findings, it has been hypothesized that FS also induce alterations in expression and/or function of other ion channels that are known to control hippocampal excitability. Pronounced changes have been already found in hippocampal excitatory [9, 22, 100, 126, 150, 202], as well as inhibitory ligand-gated ion channels (LGICs) [71, 112, 187] after seizures induced by chemovulsants or kindling. In this context, much attention has been dedicated to GABA_ARs (γ -aminobutyric acid type A receptor) in the dentate gyrus (DG). The DG normally

functions as a gate at the entrance to the hippocampal formation, filtering incoming excitation from the entorhinal cortex. It has been suggested that seizure-induced changes in GABA_AR-mediated neurotransmission may compromise this DG gatekeeper function and contribute to hippocampal hyperexcitability accompanying the process of epileptogenesis.

GABA_ARs that are known for their participation in mediating fast inhibitory transmission in the central nervous system and are members of the *cys-loop* family of ligand-gated ion channels, consist of pentameric assemblies of subunits belonging to different classes with multiple subunit subtypes (α 1-6, β 1-3, γ 1-3, δ). GABA_AR subunit subtype composition determines the physiological and pharmacological properties of the receptor. The rat hippocampus displays a heterogeneous distribution of GABA_AR subunits with α 1, α 2, α 4, β 2, β 3, γ 2 and δ being the predominant subunits in the DG and α 3 and γ 1 being present in smaller amounts in the DG [180]. Changes in the GABA_AR subunit expression pattern have been found in experimental and human epileptic DG tissue [170, 187]. These seizure-induced alterations in DG GABA_AR subunit expression are associated with prominent changes in GABA_AR-mediated synaptic inhibition. Whole-cell GABA_AR currents and spontaneous inhibitory postsynaptic currents (sIPSCs) were enhanced in dentate granule neurons from kindled and pilocarpine-treated rats, probably due to an increased number of postsynaptic GABA_ARs [42, 71, 112, 133, 134]. Some studies report relatively normal inhibitory synaptic input in dentate granule cells from animals treated with pilocarpine or kainate [42], but others found a considerable diminished frequency of IPSCs [99, 172, 183].

The aim of the present study was to analyze whether GABA_AR-mediated inhibitory neurotransmission in the DG changes after early-life FS. To this end, we made use of an appropriate-aged immature rat model in which FS are evoked in 10-day old rat pups by hyperthermia (HT). Six to nine days later, GABA_AR-mediated inhibitory neurotransmission was studied using whole-cell patch-clamp recordings from dentate granule neurons in hippocampal slices. Spontaneous inhibitory postsynaptic currents (sIPSCs) and whole-cell GABA-elicited responses were evaluated to analyze FS-associated alterations in postsynaptic GABA_AR function and inhibitory synaptic input.

3.3 MATERIALS AND METHODS

3.3.1 Induction of hyperthermic seizures

Litters of male Sprague-Dawley rat pups from Harlan (Horst, The Netherlands) were housed under standard conditions (12/12h dark-light cycle with water and food *ad libitum*). FS were induced in rat pups by exposure to heated air as described elsewhere [11, 110, 111]. Briefly, rat pups were injected subcutaneously on postnatal day 10 with 0.2 ml 0.9% NaCl to prevent dehydration, placed on the bottom of a Perspex cylinder and exposed to a regulated stream of heated air. Rectal temperatures were monitored at 2.5 min intervals. HT, defined as a core temperature of >39.5°C, was maintained for 30 min by adjusting the heated air stream aiming for a core temperature between 41-42.5°C. The occurrence of seizures was monitored by two observers independently using behavioral criteria [11]. Behaviorally, seizures were characterized by lying on side or back combined with clonic contractions of fore- and/or hindlimbs. Following HT treatment, rat pups were placed in a water bath at room temperature to decrease their body temperature to normal values and were then returned to their mother. Normothermia (NT) control rats underwent exactly the same procedure except that the stream of air was intended to maintain normal body temperature (~35°C). Three experimental groups were generated following the above described treatment: HT rats exhibiting behavioral seizures during HT treatment (HT+FS) (1), HT rats without behavioral seizures during HT treatment (HT-FS) (2), and NT control rats (3). All experiments were approved by the Hasselt University ethics committee for animals.

3.3.2 Preparation of hippocampal slices

6-9 days after FS induction, rats were sacrificed for brain slice preparation. Animals were decapitated, brains were quickly removed from the skull and placed in ice-cold oxygenated (95%O₂/5%CO₂) sucrose-based artificial cerebrospinal fluid (sucrose-aCSF) containing (in mM): 210 sucrose, 2.5 KCl, 26 NaHCO₃, 1.25 NaH₂PO₄, 25 glucose, 1 CaCl₂, and 7 MgSO₄ (pH 7.4, ~340 mOsm). Coronal 350-µm-thick brain slices were sectioned in ice-cold oxygenated sucrose-aCSF using a vibratome (Microm) and transferred for at

least 45 min to a heated (35°C) holding chamber with oxygenated normal aCSF containing (in mM): 124 NaCl, 3 KCl, 26 NaHCO₃, 1.25 NaH₂PO₄, 10 glucose, 2 CaCl₂, and 1 MgCl₂ (pH 7.4, ~310 mOsm). Afterwards, the brain slices were maintained at room temperature.

3.3.3 Whole-cell patch-clamp recordings

Individual slices were placed in a recording chamber and continuously superfused at room temperature with oxygenated normal aCSF. Granule cells in the dentate granule layer were visualized using an upright Nikon microscope (Eclipse FN1) equipped with a 40x water-immersion objective, infrared differential interference contrast (IR-DIC) optics and a CCD camera (Hitachi KP-M2RP). Recording patch pipettes (4-6 MΩ) were pulled from borosilicate glass on a P-97 Flaming-Brown horizontal puller (Sutter Instruments, Novato, CA, USA) and filled with an internal solution containing (in mM): 137 CsCl, 5 MgCl₂, 10 Hepes, 10 EGTA, 1 CaCl₂, 4 Na-ATP, 0.4 Na-GTP and 5 QX-314 (lidocaine N-ethyl bromide) (pH adjusted to 7.3 with CsOH; 290 mOsm). Small and medium sized neurons with typical oval-shaped cell bodies located in the dentate granule cell layer were identified as dentate granule neurons [6, 144] and were recorded in the whole-cell configuration of the patch-clamp technique at a holding potential of -60 mV. Signals were acquired and low-pass filtered at 1-5 kHz using an Axopatch 200B amplifier (Molecular Devices), collected using PClamp 10.0 (Molecular Devices) at a frequency of 20 kHz, stored on hard disk and analyzed off-line.

For the GABA concentration-response experiments, GABA (1-1000 μM) was applied topically via a multibarrel quartz glass pipet connected to a fast application perfusion system (SF-77B, Warner Instruments, Holliston, MA, USA), which allowed rapid movement of the solution interface generated between control aCSF and GABA-containing aCSF (solution exchange time ~50 msec). Fifty μM DL-2-amino-5-phosphonopentanoic acid (DL-APV) and 20 μM 6-cyano-7-nitroquinoxaline-2,3-dione (CNQX) were added to control and GABA-containing aCSF in order to block N-methyl-D-aspartate (NMDA) and α-amino-3-hydroxy-5-methyl-4-isoxazolepropionic acid (AMPA)/kainate receptor-mediated currents, respectively. GABA was applied for 10 sec and washed out with control

aCSF for 90 sec. For recording of GABA_AR-mediated sIPSCs, 50 μM DL-APV and 20 μM CNQX were also included in the aCSF.

3.3.4 Analysis of electrophysiological data

To detect sIPSCs, continuous recordings of 2 min were analyzed using MiniAnalysis software (Synaptosoft, Leonia, NJ, USA). The threshold for sIPSC detection was set at 5 times the root mean square noise. All events were individually validated and artefacts were excluded by visual inspection. Only events with an amplitude >10 pA and an area >50 pA/ms were included for further analysis. Peak amplitude and 10-90% rise time were determined for each verified sIPSC and averaged to obtain a mean value for each dentate granule neuron. The sIPSC charge transfer per second was determined by multiplying the mean number of events per second by the mean charge transfer per event. sIPSCs with an amplitude >20 pA and a decay phase that was not contaminated by other sIPSCs were selected for kinetic analysis. The time constant of the sIPSC current decay (τ) was obtained by fitting the decay phase with a single exponential equation of the form: $I(t) = I_0 \exp(-t/\tau)$ where $I(t)$ is the current amplitude at any given time and I_0 is the current amplitude at time 0. For each dentate granule cell, a mean decay time constant was obtained after individually fitting 50 random events.

GABA_AR current amplitudes at different GABA concentrations were measured using Clampfit 10.0 software (Molecular Devices) and normalized to the peak amplitude of the response at 1 mM GABA. Normalized GABA_AR currents at different GABA concentrations were fitted to a sigmoidal function using a four parameter logistic equation with a variable slope. The equation used to fit the dose-response relationship was: $I = I_{max} / (1 + 10^{((\log EC_{50} - \log [GABA]) * n_H)})$, with I being the GABA_AR peak current at a given GABA dose, I_{max} the maximal peak current, EC_{50} the concentration of GABA required for a half-maximal response and n_H the Hill slope. GABA concentration-response curves were obtained from pooled data from all recorded cells tested for GABA. GABA_AR current density was quantified on the basis of the peak amplitude of the response of a dentate granule cell to application of 1 mM GABA divided by the total capacitance for this given cell. GABA current desensitization was fitted by exponential functions, beginning shortly after the peak of the response using Axograph software

(Axograph Scientific, Sidney, Australia). Not all GABA responses could be fitted by a single exponential curve, hence curve fitting was performed with single or double exponential equations of the form $I(t) = I_f \exp(-t/\tau_f) + I_s \exp(-t/\tau_s)$, where I_f and I_s are the amplitudes of the fast and slow components, and τ_f and τ_s are their respective time constants. To compare desensitization times between different exponential conditions, we used a weighted time constant $\tau_{des} = [(I_f/(I_f + I_s)) \times \tau_f] + [(I_s/(I_f + I_s)) \times \tau_s]$.

3.3.5 Quantitative real time PCR

DG regions were microdissected from 350- μ m-thick coronal brain slices. Total RNA was isolated from DG tissue samples using a RNAqueous-Micro kit (Ambion), according to the manufacturer's protocol. Trace amounts of genomic DNA were removed by performing a treatment with DNase I provided with the kit. The concentration of total RNA was checked by measuring the optical density at 260 nm using the NanoDrop ND-1000 spectrophotometer (Thermo Fisher Scientific, Waltham, USA) and RNA purity was assessed by the 260/280 nm ratio. Total RNA (220 ng) was first incubated for 10 min at 70°C in order to prevent secondary structures and subsequently reverse transcribed using the Reverse Transcription System (Promega, Leiden, The Netherlands) in 20- μ l reaction volumes supplemented with 5 mM MgCl₂, 1x Reverse Transcription buffer, 1mM dNTP mixture, 0.25 μ g Oligo(dT)₁₅ primers, 0.25 μ g hexamer oligonucleotides, 20 U RNase inhibitor and 12.5 U AMV reverse transcriptase. The 20- μ l reactions were incubated in a BioRad Thermal Cycler (BioRad, Hercules, CA, USA) for 60 min at 42°C, for 5 min at 95°C and then held at 4°C. All cDNA samples were stored at -20°C.

Gene expression analysis of GABA_AR subunits was performed by quantitative real time PCR in optical 96-well plates with an ABI PRISM 7500 Fast sequence detection system (Applied Biosystems, Carlsbad, California) making use of pre-validated SYBR® Green-based RT² qPCR Primer assays (SABiosciences) (Table 3.1). qPCR was carried out in 10- μ l reaction volumes containing 5 μ l RT SYBR green qPCR master mix (SABiosciences), 0.4 μ M gene specific forward and reverse PCR primer and 11ng cDNA dissolved in nuclease-free water. A no-template control which contained nuclease-free water instead of cDNA was included to test for contamination of assay reagents. Reactions were run in

duplicates. Cycling conditions comprised of a 10-min preincubation at 95°C to activate the polymerase and 40 cycles at 95°C for 15s and 60°C for 60s. SYBR green fluorescence was detected and recorded from every well during the annealing step of each cycle. Each PCR program was followed by a general dissociation curve protocol to check PCR product specificity. Relative quantification of starting RNA copy numbers was performed by the comparative delta-delta Ct ($\Delta\Delta Ct$) method and normalization of data by geometric averaging of three internal reference genes [190]. A combination of Tbp, Rpl13A and CycA was used for normalization because these genes were indicated by GeNorm and Normfinder as most stable reference genes 6-9 days after HT-treatment (see chapter 2 for details).

3.3.6 Statistical analysis

Statistical significance of differences between cumulative probability distributions was assessed by the non-parametric Kolmogorov-Smirnov (KS) test using MiniAnalysis software. All other statistical analyses were performed using Graphpad Prism5 software. Significance of differences between means of different treatment groups were tested using one-way ANOVA and *post hoc* Bonferroni's multiple comparison tests for data with a normal distribution or a Kruskal-Wallis test and *post hoc* Dunn's comparison test when the data are not normally distributed. Significance of differences in best-fit values of EC₅₀ and n_H between the three treatment groups was assessed by an extra sum-of-squares F test following simultaneous curve fitting. A value of P<0.05 was considered as statistically significant. All data are presented as means ± standard error of the mean (SEM).

Table 3.1: SYBR® green-based qPCR primer assays used for quantitative real-time PCR

| Gene symbol | Gene of interest | SABiosciences qPCR assay ID^a or Primer sequence (5' → 3')^b | Amplicon length (bp) |
|--------------------|---------------------------------|---|-----------------------------|
| <i>Gabra1</i> | GABA _A R, α1 subunit | PPR55532A | 185 |
| <i>Gabra2</i> | GABA _A R, α2 subunit | PPR55173A | 103 |
| <i>Gabra3</i> | GABA _A R, α3 subunit | PPR44813B | 90 |
| <i>Gabra4</i> | GABA _A R, α4 subunit | PPR52284A | 191 |
| <i>Gabra5</i> | GABA _A R, α5 subunit | PPR44814A | 190 |
| <i>Gabrad</i> | GABA _A R, δ subunit | PPR45123A | 135 |
| <i>Gabrag2</i> | GABA _A R, γ2 subunit | PPR55300A | 176 |
| <i>Tbp</i> | TATA box binding protein | F: TGG GAT TGT ACC ACA GCT CCA R: CTC ATG ATG ACT GCA GCA AAC C | 131 |
| <i>Rpl13A</i> | Ribosomal protein L13A | F: GGA TCC CTC CAC CCT ATG ACA R: CTG GTA CTT CCA CCC GAC CTC | 132 |
| <i>CycA</i> | CyclophilinA | F: TAT CTG CAC TGC CAA GAC TGA GTG R: CTT CTT GCT GGT CTT GCC ATT CC | 126 |

^a qPCR primers used for gene expression analysis of GABA_AR subunits were commercially available prevalidated qPCR primer assays from SABiosciences

^b Sequences of qPCR primers used for gene expression analysis of *Tbp*, *Rpl13A* and *CycA* were based on literature [132]. *Tbp*, *Rpl13A* and *CycA* were found to be the optimal combination of reference genes according to geNorm and Normfinder (see chapter 2 for details).

3.4 RESULTS

Whole-cell recordings were obtained from dentate granule neurons in hippocampal slices from rats who received a HT treatment 6-9 days earlier, in order to investigate the influence of FS on GABA_AR-mediated inhibitory neurotransmission in the DG. These cells displayed no significant differences in passive membrane properties between NT, HT-FS and HT+FS animals (Table 3.2).

Table 3.2: Membrane properties of DG granule cells of normothermia (NT) animals and hyperthermia animals with (HT+FS) and without (HT-FS) seizures

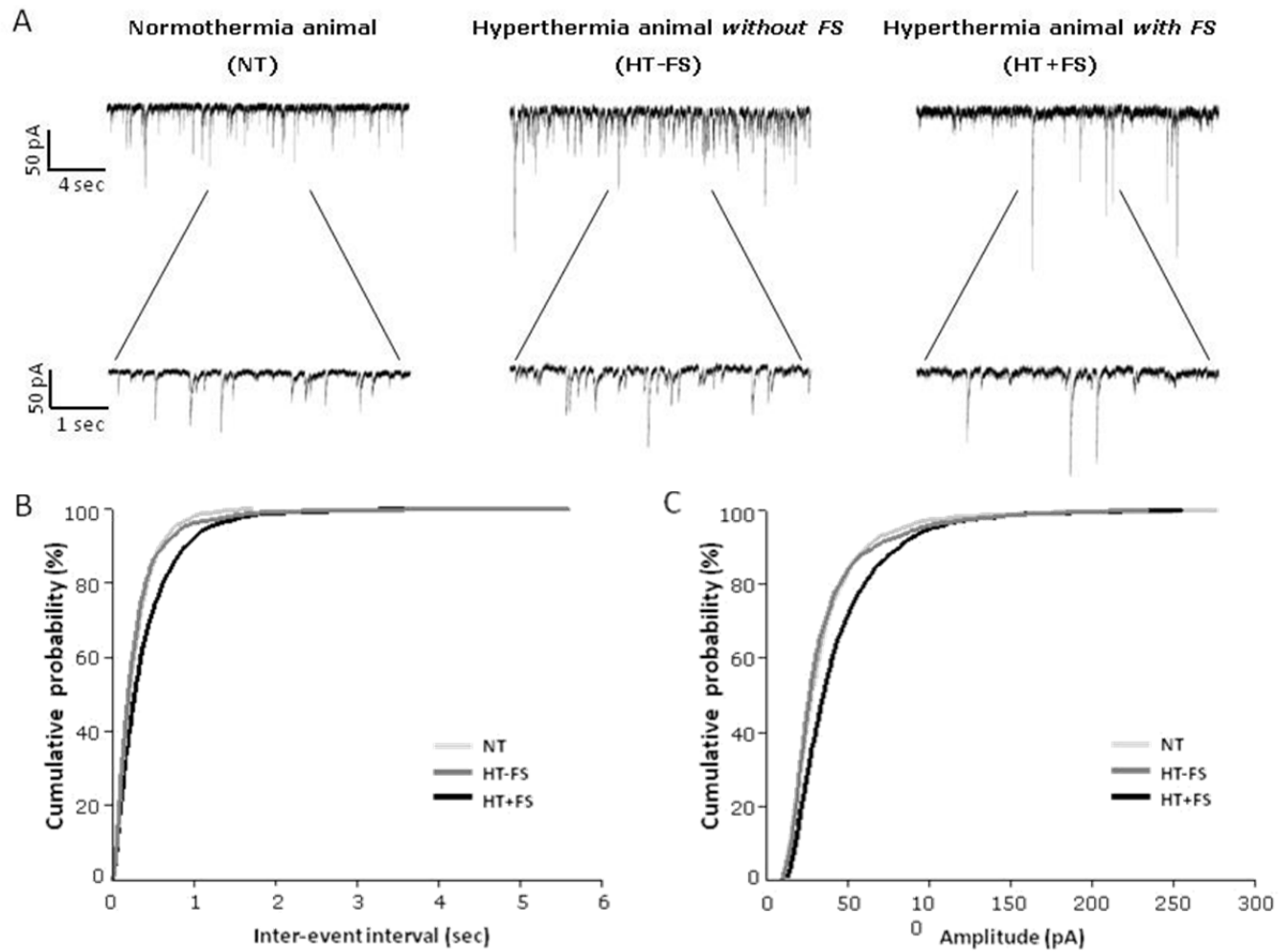
| Electrophysiological property | NT | HT-FS | HT+FS |
|---------------------------------|----------------|---------------|----------------|
| Resting membrane potential (mV) | -62.8±0.2 (17) | -62.4±0.3 (8) | -62.5±0.1 (15) |
| Input resistance (GΩ) | 1.0±0.2 (14) | 1.3±0.2 (23) | 1.4±0.2 (22) |
| Membrane capacitance (pF) | 25.1±2.5 (14) | 32.1±2.8 (23) | 30.3±3.2 (22) |

Experiments on dentate granule cells were carried out 6-9 days after normothermia/hyperthermia treatment. Data are presented as means ± SEM with n in parentheses. Membrane properties of dentate granule cells do not differ between NT, HT-FS and HT+FS animals (analyzed using one-way ANOVA and *post hoc* Bonferroni's multiple comparison test)

3.4.1 Properties of sIPSCs in dentate granule cells are changed after hyperthermic seizures

To examine the influence of HT-induced seizures on inhibitory spontaneous synaptic transmission, we recorded isolated spontaneous inward currents from dentate granule cells that were voltage clamped at -60 mV. sIPSCs were pharmacologically isolated by perfusing the slices with 50 μM DL-APV and 20 μM CNQX to inhibit glutamatergic spontaneous events. sIPSCs were less frequent in HT+FS (2.50 ± 0.29 Hz; n=8) rats in comparison with NT (3.61 ± 0.28 Hz; n=5) and HT-FS (3.34 ± 0.79 Hz; n=5) rats (Figure 3.1A). Although the mean frequency values were not significantly different, HT+FS rats showed a cumulative probability distribution of sIPSC inter-event intervals that was significantly different from NT (p<0.001) and HT-FS (p<0.001) rats (Figure

3.1B). This rightward shift of the cumulative probability distribution indicates larger inter-event intervals in cells from HT+FS rats, corresponding to the observed decrease in sIPSC frequency. The mean peak amplitude of sIPSCs from HT+FS (43.28 ± 3.48 pA; n=8) rats was also not significantly increased compared with NT (35.65 ± 6.28 pA; n=5) and HT-FS (34.03 ± 4.63 pA; n=5) rats. However, the cumulative probability distribution of sIPSC peak amplitudes of HT+FS rats displayed a rightward shift relative to NT and HT-FS rats, indicating significantly larger sIPSC peak amplitudes in HT+FS rats compared with NT ($p < 0.001$) and HT-FS ($p < 0.001$) rats (Figure 3.1C). In contrast to the changes in sIPSC frequency and peak amplitude, no changes were observed in sIPSC kinetics. The sIPSC 10-90% rise times of NT (2.21 ± 0.42 ms; n=5), HT-FS (2.88 ± 0.28 ms; n=5) and HT+FS (2.52 ± 0.16 ms; n=8) rats were comparable and sIPSC decay time constants from NT (25.99 ± 2.36 ms; n=5), HT-FS (23.71 ± 1.82 ms; n=5) and HT+FS (27.03 ± 1.58 ms; n=8) rats were also similar. In addition, the amount of charge transferred by sIPSCs recorded in dentate granule cells from NT (2.70 ± 0.51 pC/s; n=5), HT-FS (2.69 ± 0.88 pC/s; n=5) and HT+FS (2.57 ± 0.44 pC/s; n=8) was not different (Figure 3.1D).



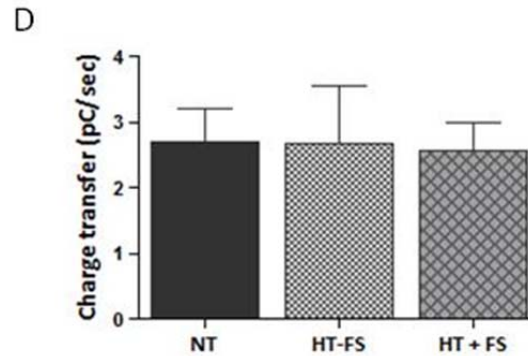
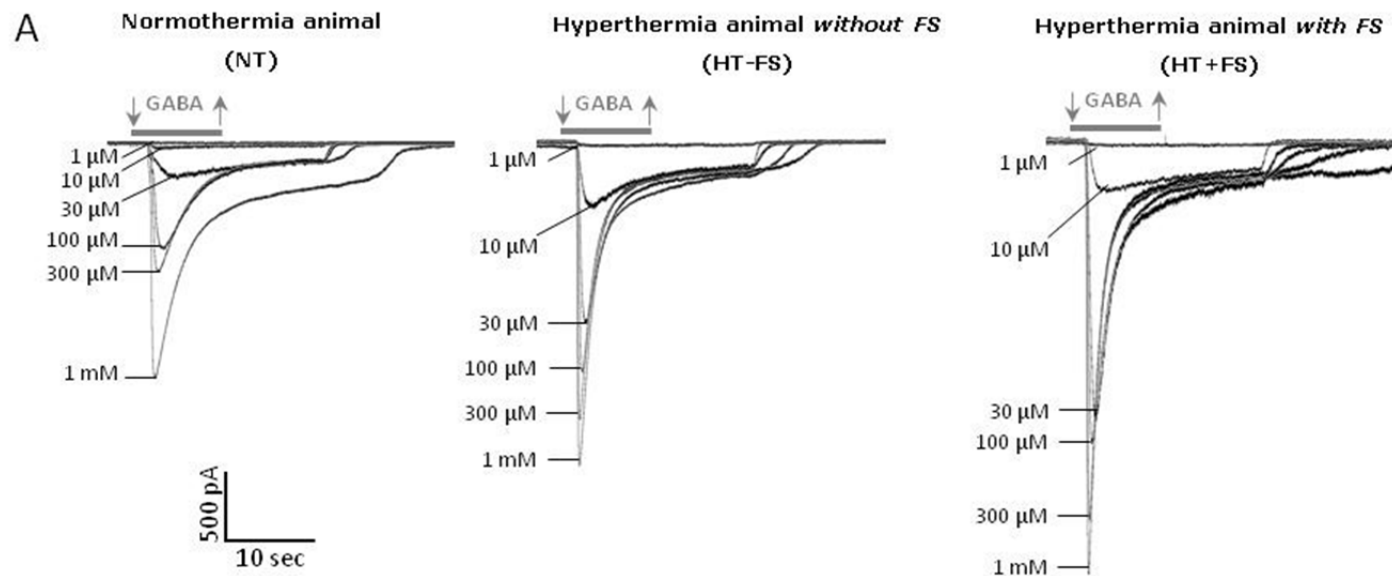


Figure 3.1: Comparison of sIPSCs in dentate granule cells of normothermia (NT) and hyperthermia rats with (HT+FS) and without (HT-FS) seizures. A: representative traces of sIPSCs displayed by dentate granule neurons from a NT, HT-FS and HT+FS animal. sIPSCs were measured as inward currents at -60 mV in the presence of 50 μ M DL-APV and 20 μ M CNQX. B: Cumulative probability distribution of sIPSC inter-event intervals reveals a shift to larger inter-event intervals, indicating a lower sIPSC frequency in HT+FS (n=8) rats compared with HT-FS (n=5) and NT (n=5) rats ($P < 0.001$; analyzed using KS test). C: Cumulative probability distribution of sIPSC amplitudes shows a rightward shift, indicating an enhanced sIPSC amplitude in HT+FS (n=8) rats compared with HT-FS (n=5) and NT (n=5) rats ($P < 0.001$; analyzed using KS test). D: Charge transfer of sIPSCs is similar in HT+FS (n=8), HT-FS (n=5) and NT (n=5) rats (analyzed using Kruskal Wallis test and *post hoc* Dunn's comparison test).

3.4.2 GABA-evoked currents in dentate granule neurons are altered after HT treatment

To evaluate the possible occurrence of HT-induced alterations in the sensitivity of GABA_ARs to GABA, GABA concentration-response curves were obtained from dentate granule cells of NT as well as HT animals. For that purpose GABA was applied to dentate granule neurons at concentrations ranging from 1 to 1000 μM for 10 s at a holding potential of -60 mV (Figure 3.2A). Normalized concentration-response curves demonstrated an EC₅₀ of $65.36 \pm 0.062 \mu\text{M}$ in NT dentate granule cells (n=5-6), whereas HT-FS (n=4-9) and HT+FS (n=6-12) dentate granule cells yielded an EC₅₀ of $36.94 \pm 0.062 \mu\text{M}$ and $31.56 \pm 0.060 \mu\text{M}$ respectively (Figure 3.2B). The EC₅₀ values of HT-FS and HT+FS dentate granule cells were significantly decreased compared with NT dentate granule cells ($p < 0.01$ and $p < 0.001$, respectively). The concentration-response relationships showed a Hill coefficient (n_H) of 1.24 ± 0.19 in NT dentate granule cells, 0.87 ± 0.11 in HT-FS dentate granule cells and 0.91 ± 0.11 in HT+FS dentate granule cells. These Hill coefficients were not significantly different. In addition to the HT-induced change in GABA potency, potential influences on GABA efficacy were also examined. GABA_AR current densities, quantified after application of 1 mM GABA, were $104 \pm 14 \text{ pA/pF}$, $97 \pm 2 \text{ pA/pF}$ and $124 \pm 21 \text{ pA/pF}$ in NT (n=12), HT-FS (n=9) and HT+FS (n=13) dentate granule cells respectively (Figure 3.2C). GABA_AR current densities between NT and HT-animals were not significantly different. GABA-elicited current kinetics was studied after applying GABA-concentrations ranging from 30 to 1000 μM . The rate of GABA current desensitization was determined by fitting the desensitizing phase by a single- or a two-exponential function (Figure 3.3A). There was no significant difference in the weighted desensitization constant (see Material and Methods) between NT (n=4-6), HT-FS (n=4-8) and HT+FS (n=8-12) dentate granule cells for none of the tested GABA concentrations (Figure 3.3B). These results from GABA-elicited whole-cell currents show that HT treatment induces changes in the functional properties of postsynaptic GABA_ARs.



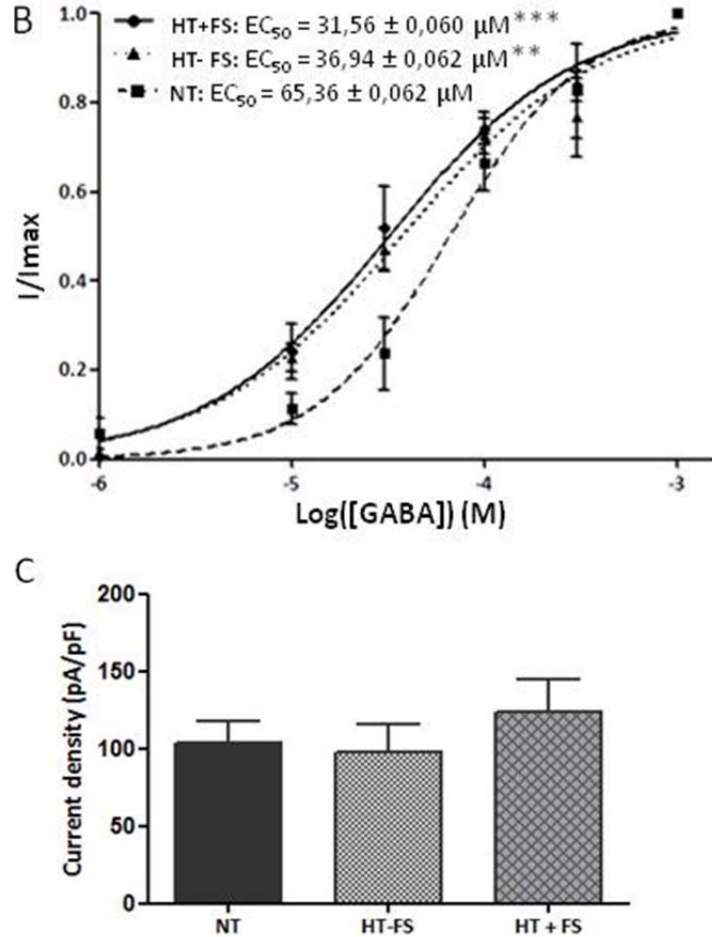


Figure 3.2: Physiological characterization of GABA-elicited currents in dentate granule cells from normothermia (NT) and hyperthermia rats with (HT+FS) and without (HT-FS) seizures.

A: representative traces of responses to GABA concentrations of 1-1000 μM in dentate granule neurons from a NT, HT-FS and HT+FS animal. GABA was applied via a drug pipette for a duration of 10 sec. B: GABA dose-response curves of NT (n=5-6), HT+FS (n=6-12) and HT-FS (n=4-9) dentate granule neurons. Currents were normalized to the peak amplitude of the response at 1 mM GABA. Each point represents the mean of normalized currents \pm SEM. Dose-response data were fit with the Hill equation. (**, $P < 0.01$; ***, $P < 0.001$; analyzed using F-test) C: GABA_AR current densities in NT (n=12), HT-FS (n=9) and HT+FS (n=13) dentate granule neurons, quantified after application of 1 mM GABA. Data are presented as mean current density \pm SEM. GABA_AR current densities in dentate granule cells do not differ significantly between NT, HT+FS and HT-FS animals (analyzed using one-way ANOVA and *post hoc* Bonferroni's multiple comparison test).

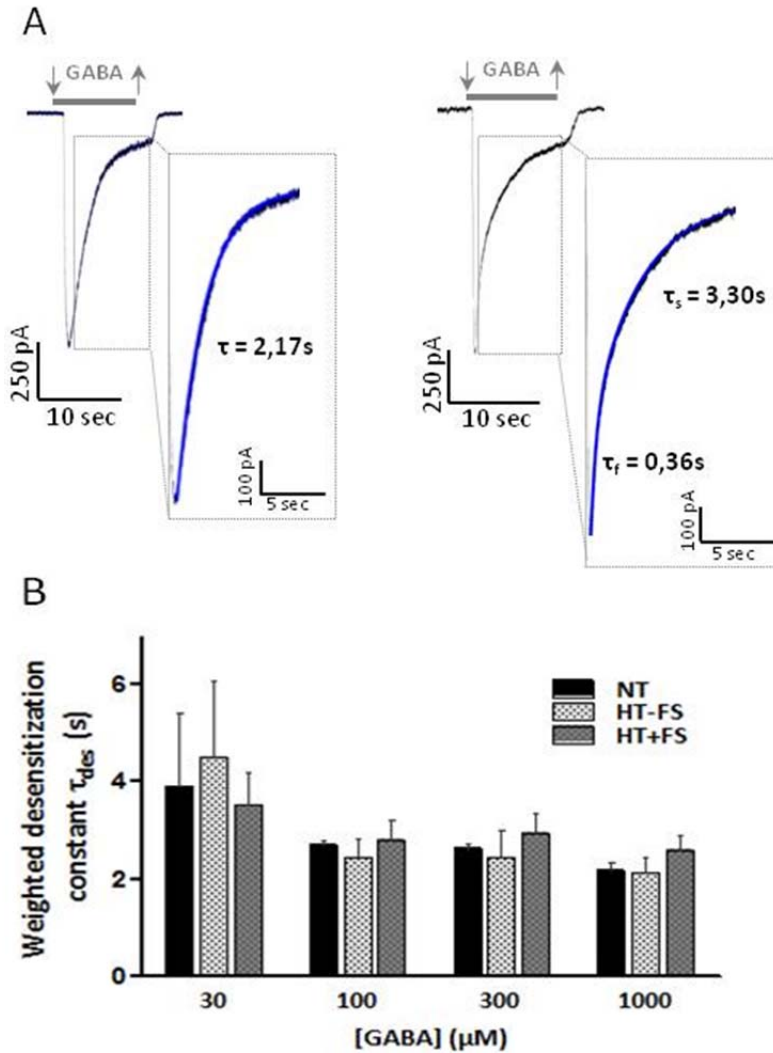
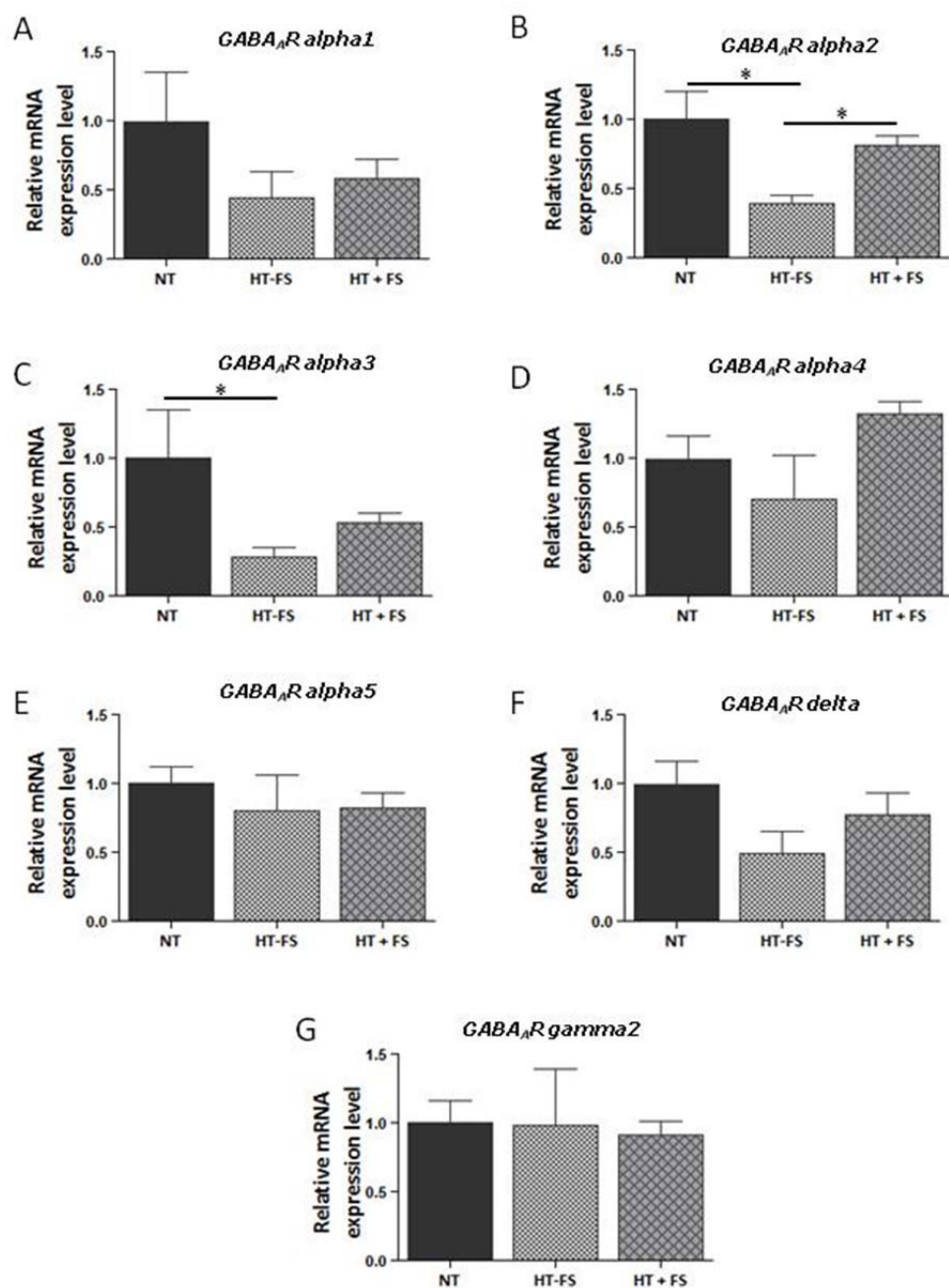


Figure 3.3: Desensitization kinetics of GABA-elicited currents in dentate granule cells from normothermia (NT) and hyperthermia rats with (HT+FS) and without (HT-FS) seizures. A: Examples of a single-exponential (*left*) and a two-exponential (*right*) fit of I_{GABA} desensitization in two dentate granule neurons of different animals during application of $100\mu\text{M}$ GABA. τ is the desensitization time constant of I_{GABA} , τ_f and τ_s are the fast and the slow desensitization time constants of I_{GABA} . A weighted desensitization time constant (τ_{des}) is used to compare desensitization times between different exponential conditions (see material and methods for details) B: Summary of the weighted τ_{des} of I_{GABA} in NT ($n=4-6$), HT+FS ($n=8-12$) and HT-FS ($n=4-8$) dentate granule neurons at the presence of different GABA concentrations ($30-1000\mu\text{M}$). Each column represents the mean $\tau_{des} \pm \text{SEM}$. τ_{des} of dentate granule cells do not differ between NT, HT+FS and HT-FS animals (analyzed using Kruskal Wallis test and *post hoc* Dunn's comparison test).

3.4.3 HT-associated alterations in GABA_AR subunit composition

To examine whether the alterations in GABA_AR function were accompanied by an altered GABA_AR subunit type expression at the mRNA level, quantitative real time PCR was performed on DG tissue isolated from HT animals and NT controls. The relative mRNA expressions of $\alpha 5$ and $\gamma 2$ subunits were unaltered after HT treatment (Figure 3.4 E/G). HT+FS as well as HT-FS animals showed a decrease in $\alpha 1$ subunit mRNA expression compared to the NT controls, however these differences were not significant (Figure 3.4A). The $\alpha 4$ subunit mRNA expressions were similar in NT and HT-FS animals whereas a slight increase was observed in the HT+FS animal group (Figure 3.4D). For the δ subunit, comparable mRNA expressions were seen in the NT and the HT+FS animals while a noticeable decrease was detected in the HT-FS animals (Figure 3.4F). No differences were seen in $\alpha 2$ subunit mRNA expression between NT and HT+FS animals. In contrast, HT-FS animals showed a significantly lower $\alpha 2$ subunit mRNA expression compared with the HT+FS group ($p < 0.05$) and the NT group ($p < 0.05$) (Figure 3.4B). Compared with the NT group, a significant decrease in $\alpha 3$ mRNA expression was observed in the HT-FS group ($p < 0.05$) and a trend in this direction was also observed in the HT+FS group (Figure 3.4C). These findings suggest that the enhanced GABA_AR sensitivity for GABA may be secondary to alterations in GABA_AR subunit composition.

Figure 3.4: Relative GABA_AR subunit mRNA expression in the dentate gyrus of normothermia and hyperthermia-rats. mRNA expression of different GABA_AR subunits in NT (n=6), HT-FS (n=4) and HT+FS (n=5-6) animals was analyzed using quantitative real time PCR. Expression levels of the different genes are expressed relative to the reference genes (Tbp, Rpl13A and CycA). Each column represents the mean relative expression level \pm SEM. (*, $P < 0.05$; analyzed using Kruskal Wallis test and *post hoc* Dunn's comparison test).



3.5 DISCUSSION

One of the main characteristics of epileptogenesis is an imbalance between excitation and inhibition, resulting in hippocampal hyperexcitability. In normal conditions, the DG circuit exhibits a low excitability level, allowing it to function as a filter at the entrance of the hippocampal formation thereby limiting the spread of synchronous excitatory activity from the entorhinal cortex to downstream hippocampal structures [46]. It has been hypothesized that seizure-induced changes in DG GABA_AR-mediated neurotransmission may compromise the DG filter function and contribute to hippocampal hyperexcitability. In this study, we examined, at 6-9 days after HT-induced seizures, whether FS change the inhibitory synaptic input to dentate granule cells and/or the properties of postsynaptic GABA_ARs in dentate granule cells. Our results demonstrate that FS induce: 1) a decrease in sIPSC frequency, 2) an enhancement in sIPSC amplitude, 3) no modifications in the kinetics of postsynaptic GABA_ARs, 4) an increased GABA potency and 5) changes in DG GABA_AR subunit mRNA expression.

Plasticity of GABA_AR-mediated neurotransmission after FS

sIPSC frequency, considered as a direct measure of granule cell inhibition, is reduced after HT-induced seizures. This finding is consistent with studies from other animal models of TLE that also report a diminished frequency of inhibitory synaptic events in dentate granule cells [99, 172, 183]. The frequency of inhibitory currents could be reduced by a lower spontaneous activity of presynaptic interneurons, by a diminished number of inhibitory synapses on dentate granule cells or by a combination of both factors. This remains to be determined in the hyperthermic seizure model. Other models of seizures induced by pilocarpine [99] or electrical stimulation [183] display profound interneuron loss in the dentate hilus, which has been reported to contribute to a reduction in sIPSC frequency. In contrast, hyperthermic seizures during the second postnatal week caused only transient injury of CA1 and CA3 pyramidal cells while neither acute nor long-term cell death of vulnerable hippocampal neuronal populations could be detected [19, 186]. However, one cannot completely rule out a transient injury of hilar interneurons that might influence inhibitory synaptic input to dentate granule cells one week after HT-induced seizures.

In contrast to a decrease in sIPSC frequency, an increase in sIPSC amplitude was detected in granule cells from HT+FS rats. An increase in the amplitude of spontaneous inhibitory events, which has also been observed in dentate granule cells from pilocarpine-treated [99, 112] and kindled rats [134], suggests the presence of more functionally active postsynaptic GABA_ARs [133, 134]. The enhancement in sIPSC amplitude is in accordance to our observed increase tendency of the amplitudes of GABA-induced whole-cell current densities in HT+FS DG neurons. Taken together, these results strongly suggest that postsynaptic GABA_ARs are upregulated after HT treatment. Interestingly, a recent autoradiographic binding study revealed a significant increased [³H] muscimol binding in the DG after hyperthermic seizures [73].

In addition to the upregulation of postsynaptic GABA_ARs, we also show that these receptors are more potently activated by GABA after HT treatment. Recent studies have shown that pre-exposure to HT-induced seizures or HT alone in immature rats reduces the incidence and increases the latency periods for subsequent seizures elicited by the chemical convulsant pentylenetetrazole (PTZ) that competitively antagonizes the GABA_AR [72, 86]. The authors of those studies already suggested an involvement of the GABA system to explain their results. Our own results indicating enhanced GABA potency and efficacy may, at least partly, explain the protective effect of HT-treatment against PTZ-induced seizures.

HT-induced increment in dentate granule GABA potency is accompanied by changed GABA_AR subunit expression levels in the DG. The most pronounced alterations concern $\alpha 2$ and $\alpha 3$ subunit expression, but a trend towards a change in expression levels has also been observed for the $\alpha 1$, $\alpha 4$ and δ subunit. Hyperthermic seizures were induced during the critical early postnatal period in which GABA_AR subunit expression undergoes marked reorganization, *i.e.* a developmental decrease of $\alpha 2/\alpha 3$ occurs concurrently with an increase of $\alpha 1$ [67, 70]. Kainate-induced seizures in 9-day old rat pups have been already shown to influence the normal developmental expression pattern of hippocampal $\alpha 1$, $\alpha 2$, $\alpha 3$ and $\gamma 2$ subunits during the first week following seizures [108]. An increase in $\alpha 1$ subunit expression without a change in $\alpha 4$ and δ was found in isolated dentate granule cells from rats treated with pilocarpine at the age of 10 days [201]. Conversely, pilocarpine- or kainate-elicited seizures in adult rats

induce marked changes in DG $\alpha 4$ as well as δ subunit expression associated with unaltered γ subunit expression and substantial changes in $\alpha 1$, $\alpha 2$, $\alpha 3$, and $\alpha 5$ subunit expression [187]. Taken together, these data indicate that seizures may change GABA_AR subunit expression levels, but the direction and magnitude of change is dependent on the moment and on the type of seizure induction. Seizure-induced alterations in GABA_AR subunit composition have been associated with changes in GABA_AR function and hence, may be of physiological relevance.

Possible mechanisms of enhanced GABA potency

Functional GABA binding sites are presumed to be situated at β - α subunit interfaces. Several amino acid residues lining the binding pocket have been identified to be relevant for agonist affinity of GABA_ARs and all amino acids identified until now are conserved among all β and α subunits [23, 24, 60, 82, 177, 178]. However, a combination of mutagenesis and electrophysiological studies has revealed that EC₅₀ values of GABA-induced chloride currents vary widely between recombinant GABA_ARs containing different α subunit isoforms, with $\alpha 3$ -containing isoforms displaying the lowest GABA sensitivity [23, 60]. Rat $\alpha x\beta 3\gamma 2$ receptors expressed in HEK 293 cells, showed varying GABA EC₅₀ values dependent on the incorporated α subunit in the range of $<1 \mu\text{M}$ to $>50 \mu\text{M}$ in the rank order $\alpha 6 > \alpha 1 > \alpha 2 > \alpha 4 > \alpha 5 > > > \alpha 3$. This suggests that structural determinants lying outside the putative GABA binding pocket may also influence GABA sensitivity. Indeed, a subunit-specific domain of four amino acids in the extracellular N-terminal region of α -subunits was identified as a determinant of GABA_AR GABA sensitivity. Replacement of this four amino acid motif in $\alpha 3$ by the corresponding motifs of $\alpha 1$ - $\alpha 5$ transfers the GABA sensitivity of the respective wildtype receptor to the mutant $\alpha 3\beta 3\gamma 2$ receptor [23]. These *in vitro* findings suggest that the enhanced GABA sensitivity of dentate granule GABA_ARs following HT treatment may be, at least partially, due to a reduced expression of the 'low GABA sensitive' $\alpha 3$ subunit in the DG.

The δ subunit has also been mentioned for its contribution to the GABA sensitivity of the GABA_AR. Expression of different rat GABA_AR subtypes in *Xenopus* oocytes revealed that incorporation of a δ subunit instead of a $\gamma 2$ subunit causes a shift in GABA EC₅₀ from 27.6 μM to 1.4 μM . Recently, a stretch

of amino acids in the δ subunit has been identified as an important determinant of conferring high GABA sensitivity to the $\alpha 4\beta 3\delta$ GABA_AR [200]. Because no significant FS-associated changes in δ subunit expression levels could be detected in whole DG tissue, our data do not support a contribution of the δ subunit to the enhanced GABA potency. However, it has to be mentioned that pilocarpine-induced seizures alter δ subunit expression levels differentially in dentate granule cells and interneurons [146]. This could suggest that the quantification of δ subunit expression levels in whole DG tissue and in single dentate granule cells may lead to different results.

Implications for FS-induced GABAergic alterations in epileptogenesis

The 'gatekeeper' function of the DG is a consequence of intrinsic dentate granule cell characteristics as well as of powerful feedforward and feedback GABAergic inhibition [46]. Monitoring the DG filter function by voltage-sensitive dye imaging techniques simultaneously with field potential and patch-clamp recordings of DG responses to perforant path activation in control aCSF, did not result in activation of the CA3 and hilar region. But perforant path activation during 25% GABAergic blockade by picrotoxin resulted in potent activation of the DG as well as the CA3 and of the hilar region, indicating that GABA_AR activation is essential for the DG to fulfill its filter function [8]. Consequently, FS-associated changes in GABA_AR-mediated neurotransmission may compromise the DG gatekeeper function, and thereby contribute to hippocampal hyperexcitability and facilitate seizure generation [53, 54]. In the present study, a moderate reduction of inhibitory synaptic input to dentate granule cells (*i.e.* decreased sIPSC frequency) was observed \sim 1 week after hyperthermic seizures. Concurrently, several mechanisms at the postsynaptic level (*i.e.* upregulation in GABA_AR density and enhanced GABA potency) seem to compensate for the diminished inhibitory synaptic input to dentate granule cells. This was evident from the equal average sIPSC charge transfer in NT and HT rats indicating that the decreased sIPSC frequency was offset by an increase in sIPSC amplitude. Observations from the current study are complementary to the study of Chen et al describing a depression of population spikes in the granule cell layer of the DG after stimulation of the perforant path in animals that experienced seizures one week before [39]. The absence of a net decrease in GABAergic inhibition might

seem inconsistent with the hypothesis that a compromised DG filter function may contribute to hippocampal hyperexcitability following FS. On the other hand, all observations were done at an age where the animals do not display spontaneous seizures or interictal epileptiform EEG abnormalities yet [54], suggesting that epileptogenesis requires the involvement of other mechanisms. Therefore, it is hypothesized that the observed alterations in GABA_AR-mediated inhibition (*i.e.* decreased sIPSC frequency, upregulation in GABA_AR density and enhanced GABA potency) may make the hippocampus more prone to seizures in combination with other changes accompanying the process of epileptogenesis.

Abnormal mossy fibre innervation of the granule cell and molecular layer was evident 3 months after experimental FS (but not after 10 days) [19], hence altering the excitatory synaptic input to dentate granule cells. In several animal models of TLE, mossy fibre sprouting contributes to abnormal recurrent excitation of dentate granule cells [118, 199]. The findings of the current study may imply that the decreased synaptic inhibitory input to dentate granule cells lead to an inadequate control of recurrent excitation. This would imply that the compensatory postsynaptic alterations do not suffice for an efficient inhibitory control of reorganized DG networks. Additionally to glutamate, mossy fibre terminals also contain high concentrations of zinc. Postsynaptic GABA_ARs in dentate granule cells from pilocarpine-treated animals become more sensitive to zinc, making the DG circuit susceptible to a zinc-induced failure of GABAergic inhibition [42, 71]. Sensitivity to zinc is largely dependent on the α subtype composition of the GABA_AR, whereby an upregulation of $\alpha 4$ is associated with an enhanced sensitivity to zinc [45]. Interestingly, our findings point to an altered GABA_AR subunit composition with a trend to an increase in $\alpha 4$ subunit expression in HT+FS rats.

Besides those seizure-induced network changes, intrinsic properties of the dentate granule cells may also counteract synaptic inhibition. Mature dentate granule neurons normally have a low intracellular Cl⁻ concentration, mediating a hyperpolarizing equilibrium potential for GABA (E_{GABA}). In contrast, immature dentate granule neurons show a more depolarized E_{GABA} due to a higher intracellular Cl⁻ concentration. Shifts in E_{GABA} during postnatal brain development are caused by an upregulation of the Cl⁻ extruding K⁺-Cl⁻ cotransporter (KCC2) synergistically with a down-regulation of the Cl⁻ importing Na⁺-K⁺-2Cl⁻

cotransporter (NKCC1) [15]. Positive shifts in E_{GABA} accompanied by changes in cation-Cl⁻ cotransporter expression levels, have been demonstrated in experimental [58, 143] and human [43, 129, 137] epileptic hippocampi. Although E_{GABA} was not sufficiently depolarizing to induce action potentials, it has been shown that excitatory postsynaptic potentials (EPSPs) are more likely to generate action potentials during depolarizing inhibitory postsynaptic potentials (IPSPs) in dentate granule neurons during the latent period following pilocarpine-induced seizures. Hence, a post-seizure shift in E_{GABA} facilitates action potential generation, alters synaptic integration, enhances dentate granule cell excitability and may in this way compromise the DG filter function [143].

In conclusion, we show that hyperthermic seizures induce presynaptic (*i.e.* reduced sIPSC frequency) and postsynaptic alterations (*i.e.* upregulation in GABA_AR density and enhanced GABA potency) in DG inhibitory synaptic transmission, which supports the hypothesis that FS persistently alter neuronal excitability in the hippocampus.

4

Phenotypical characterization of ligand-gated ion channels in dentate gyrus cells born after experimental early-life febrile seizures

This chapter is based on:

Long-lasting enhancement of GABA_A receptor expression in newborn dentate granule cells after early-life febrile seizures

Ann Swijssen, Bert Brône, Jean-Michel Rigo* and Govert Hoogland*

* Both authors contributed equally to this work

Submitted

4.1 ABSTRACT

Febrile seizures (FS) are the most common type of seizures in childhood and are suggested to play a role in the development of temporal lobe epilepsy (TLE). Preclinical evidence demonstrates that experimental FS induce a long-lasting change in hippocampal excitability, resulting in enhanced seizure susceptibility. Hippocampal neurogenesis and altered ion channel expression have both been proposed as mechanisms underlying this decreased seizure threshold. The aim of the present study was to analyze whether dentate gyrus (DG) cells that are born after FS and matured for 8 weeks, display an altered repertoire of ligand-gated ion channels (LGIC). To this end we applied an established model, where FS are elicited in 10-day old rat pups by hyperthermia (HT) and normothermia (NT) littermates serve as controls. From postnatal day 11 (P11) to P16, rats were injected with bromodeoxyuridine (BrdU) to label dividing cells immediately following FS. At P66, we evaluated BrdU-labeled DG cells for co-expression with GABA_A and NMDA receptors. In control animals, 40% of BrdU-labeled cells co-expressed GABA_AR whereas in rats that had experienced FS 60% of BrdU-labeled cells also expressed GABA_AR. The number of BrdU-NMDAR co-expressing cells was in both groups about 80% of BrdU-labeled cells. These results demonstrate that developmental seizures can cause a long-term increase in GABA_A receptor expression in DG cells. Whether this altered expression has consequences for hippocampal physiology remains to be demonstrated.

4.2 INTRODUCTION

Febrile seizures (FS) are the most common seizure type during childhood. 2-3% of the children between the age of 3 months and 5 years are suffering from FS [191]. Retrospective studies report that 40% of the adult patients with hippocampal sclerosis-associated temporal lobe epilepsy (TLE) have a history of FS [2], suggesting a causative role for FS in the pathogenesis of TLE [36, 66]. However, the mechanisms by which these early-life seizures contribute to the development of TLE have not been fully elucidated.

Using an appropriate-aged animal model of FS, previous research demonstrated a long-lasting enhancement of hippocampal excitability and an increased prevalence of limbic seizures at adulthood [53, 54]. This FS-induced decrease in seizure threshold is partially caused by a depolarization shift of the hyperpolarization-activated cyclic nucleotide gated (HCN) channel activation and a slowing of the kinetics of the hyperpolarization-activated (I_h) current [38]. These functional alterations are associated with a decreased expression of the fast-deactivating HCN1 isoform, an increased expression of the slow-deactivating HCN2 isoform and the formation of heteromeric HCN1/HCN2 channels in CA1 neurons [28, 29]. Based on these findings, it has been hypothesized that FS also change the expression of other ion channels that are known to control neuronal excitability in the hippocampus. In this context, ionotropic glutamate receptors for N-methyl-D-aspartate (NMDAR) and α -amino-3-hydroxy-5-methyl-isoxazole-4-propionic acid (AMPA), and members of the inhibitory cys-loop ligand-gated ion channel (LGIC) superfamily, such as the γ -aminobutyric acid type A receptor ($GABA_A$ R) and the glycine receptor (GlyR), are potential candidates. Interestingly, previous studies in chemo-convulsant models have already shown an altered hippocampal expression of these receptors [9, 26, 150, 157, 170, 201].

Seizure-induced hippocampal neurogenesis has been demonstrated in chemical and electrical seizure models [47, 91, 140, 151, 160, 171] and also occurs after experimental FS [110, 111]. These observations led to the hypothesis that newborn hippocampal neurons differentiate and/or migrate abnormally and thereby promote hippocampal hyperexcitability [104, 142, 165]. A pro-epileptogenic role for hippocampal cell proliferation was already suggested by

Jung *et al.* who reported that a suppression of seizure-induced neurogenesis attenuates the later development of spontaneous recurrent seizures [92].

Since seizure-induced changes in hippocampal neurogenesis occur concurrently with modifications in the expression of hippocampal excitatory and inhibitory LGICs, we aimed to explore if seizure-induced newborn dentate gyrus (DG) cells may themselves be a source of long-lasting alterations in LGIC expression [184]. To this end, we used an immature rat model in which FS are evoked by hyperthermia [11]. DG cells that divided immediately after FS were labeled with 5-bromo-2'-deoxyuridine (BrdU) and evaluated in adulthood for the expression of inhibitory (GABA_AR and GlyR) and excitatory (NMDAR and AMPAR) LGICs to look at possible candidates underlying the hippocampal hyperexcitability observed after FS.

4.3 MATERIAL AND METHODS

4.3.1 Induction of febrile seizures

Litters of male Sprague-Dawley rat pups plus a dam were obtained from Harlan (Horst, The Netherlands). Seizures were induced at postnatal day (P) 10 as described previously [11, 110, 111]. Briefly, pups were injected subcutaneously with 0.2 ml 0.9% NaCl to prevent dehydration and then placed in a Perspex cylinder (10 cm diameter; 1 pup/cylinder) and exposed to a regulated heated air stream placed 50 cm above them. Rectal temperature was measured every 2.5 min. The hyperthermia (HT) treatment lasted 30 min, starting from the moment that the core temperature reached 39.5°C. During HT, the heated air stream was adjusted in order to maintain a core temperature between 41-42.5°C. The occurrence of behavioral seizures, characterized by lying on side or back combined with clonic contractions of fore- and/or hindlimbs, was monitored by two observers [11]. Previous studies have shown that these seizures are associated with rhythmic epileptic discharges in the amygdala and hippocampus [11, 53]. After HT treatment, rat pups were placed in a water bath at room temperature (RT) to decrease body temperature to pretreatment values and then returned to the dam. The following three experimental groups were generated: (1) HT rats exhibiting behavioral seizures during HT treatment (HT+FS), (2) HT rats without behavioral seizures during HT treatment (HT-FS), and (3) normothermia (NT) littermates that underwent the same procedure with the exception that the stream of air was adjusted to maintain a pretreatment body temperature (~35°C). All experiments were approved by the Hasselt University ethics committee for animals.

4.3.2 BrdU labeling and tissue preparation

The thymidine-analog BrdU, integrating in newly synthesized DNA during the S-phase of mitosis, was used to identify cells that were born after FS. BrdU (Sigma-Aldrich) was dissolved in 0.9% NaCl (pH 7.6) to 2 mg/ml and sterilized by filtration (0.2 µm). From P11 to P16, all rats were injected intraperitoneally twice daily (minimum 6 hours apart) with 25 mg BrdU/kg body weight. At P66, rats were anesthetized with an overdose of Nembutal® and transcardially perfused with 100ml 0.9% NaCl followed by 100ml icecold 4%

paraformaldehyde (PFA) in phosphate buffered saline (PBS; pH 7.4). Brains were immediately removed from the skull, postfixed in 4% PFA in PBS (1hr; 4°C), cryoprotected in 20% sucrose in PBS (overnight; 4°C), and frozen using liquid nitrogen. Brains were coronally sectioned between bregma -2.8 and -4.5 mm on a cryostat (Leica Microsystems, Wetzlar, Germany) at 10 µm thickness. Sections were mounted serially on Superfrost-Plus slides (Menzel-Gläser).

4.3.3 Antibodies

NMDAR and AMPAR were visualized with polyclonal antibodies from rabbit. The NMDAR antibody (1:100; AB1548; Chemicon) equally recognizes both NR2A and NR2B subunits of the NMDAR. The AMPAR antibody (1:100; AB1506; Chemicon) is specific for GluR2 as well as GluR3 subunits. GlyRs were detected using a goat polyclonal antibody (1:50; N18 sc-17279; Santa Cruz Biotechnologies) which is specific for the $\alpha 2$ -subunit of the GlyR. GABA_ARs were stained with a mouse monoclonal antibody (1:100; clone 62-3G1; Chemicon) specific for the $\beta 2$ - and the $\beta 3$ - subunit of the GABA_AR. Primary antibodies from mouse and rabbit were detected with donkey anti-mouse (1:500; Molecular Probes) and donkey anti-rabbit (1:500; Molecular Probes) antibodies respectively. The GlyRa2 antibody, raised in goat, was visualized by making use of F(ab')₂ fragments of rabbit anti-goat antibodies (1:500; Molecular Probes). All secondary antibodies, visualizing LGICs, were conjugated to AlexaFluor488.

For BrdU detection, either a mouse monoclonal (1:200; 11170376001; Roche Diagnostics) or a sheep polyclonal (1:100; AB1893; Abcam) antibody was used. The sheep anti-BrdU was used in double labeling experiments with goat anti-GlyRa2 and mouse anti-GABA_AR $\beta 2/3$, whereas the mouse anti-BrdU was combined with rabbit anti-NMDAR 2A/B. Mouse and sheep anti-BrdU were both detected by a combination of biotinylated secondary antibodies raised in donkey (1:800; Jackson ImmunoResearch) and an AlexaFluor647-conjugated streptavidin (1:2000; Molecular Probes).

4.3.4 Immunofluorescent labeling

For BrdU detection, sections were first incubated in 2M HCl for 20 min at 37°C, immediately followed by a 10-min wash in 0.1M borate buffer (pH 8.5) at room temperature (RT). Blocking and permeabilization of the sections were performed

in PBS containing 20% normal donkey serum (NDS) and 0.1% Triton X-100 (60 min; RT). Mouse anti-BrdU was incubated overnight at 4°C and detected by a biotinylated donkey anti-mouse antibody (60 min; RT) and an AlexaFluor-conjugated streptavidin (90 min; RT). All antibodies were dissolved in PBS-1% NDS supplemented with 0.1% Triton X-100.

For double labeling experiments of anti-BrdU with either anti-NMDAR 2A/B or anti-GABA_AR β 2/3, sections were first pretreated with HCl and borate buffer as described above for BrdU detection. Sections were blocked and permeabilized in PBS containing 20% NDS and 0.1% Triton X-100 (60 min; RT). Both primary antibodies were incubated simultaneously (overnight; 4°C). Anti-BrdU was visualized by incubation of the appropriate biotin-linked secondary antibody (60 min; RT), followed by an AlexaFluor-conjugated streptavidin (90 min; RT). Finally, anti-NMDAR 2A/B or anti-GABA_AR β 2&3 were stained by their corresponding secondary antibody (60 min; RT). All antibodies were incubated in PBS-1% NDS supplemented with 0.1% Triton X-100.

Sequential incubation of the primary antibodies was required for BrdU-GlyRa2 double labeling experiments. Sections of the 4% PFA perfused brains were additionally fixed in 95% methanol-5% acetic acid (v/v) for 10 min at -20°C before blocking in PBS containing 20% normal rabbit serum (NRS) (60 min; RT). Overnight incubation (4°C) of anti-GlyRa2 in PBS-1% NRS was followed by staining with rabbit anti-goat F(ab')₂ fragments (60 min; RT). Next sections were postfixed with 4% PFA (10 min, RT) and subsequently treated with 2M HCl (10 min; 37°C) and 0.1M borate buffer (10 min; RT). Afterward, sections were blocked and permeabilized (30 min; RT) in PBS-20% NDS containing 0.1% Triton X-100. Anti-BrdU was incubated (overnight; 4°C) in PBS-1%NDS supplemented with 0.1% Triton X-100 and visualized by a biotinylated donkey anti-sheep antibody (60 min, RT) and an AlexaFluor-conjugated streptavidin (90 min, RT).

For AMPAR detection, sections of the 4% PFA perfused brains required first an additional fixation in 95% methanol-5% acetic acid (v/v) for 10 min at -20°C. Sections were blocked and permeabilized in PBS-20% NDS supplemented with 0.1% Triton X-100 and subsequently incubated with anti-GluR 2/3 (overnight; 4°C) and donkey anti-rabbit (60 min; RT), both dissolved in PBS-1%NDS with 0.1% Triton X-100.

During all immunofluorescent labeling experiments, sections were washed in PBS (3x 10 min) between the different incubation steps. At the end, coverslips were mounted in Vectashield medium containing propidium iodide (PI) (1.5 µg/ml) that stained the cell nuclei. The specificity of the immunostaining was verified in all experiments by controls in which one or two of the primary antibodies were omitted. No staining was observed in those conditions (data not shown).

4.3.5 Confocal microscopy and quantification

All sections, processed for immunolabeling, were visualized using a Zeiss LSM 510 META confocal microscope (Zeiss, Jena, Germany). AlexaFluor488 was excited with a 488-nm laser line, PI with a 543-nm laser line and AlexaFluor647 with a 633-nm laser line. Quantitative analysis was performed for 3 to 5 sections per animal using ImageJ software. The DG granule cell layer and hilar region were delineated in each section. Borders of the hilar region were defined as the virtual line connecting the proximal end of the CA3 pyramidal cell layer with the ends of both DG granule cell layer blades. All BrdU-immunoreactive (IR) cells in the delineated area were counted at 400x magnification and expressed as the number cells / 100,000 µm². Cell numbers of the HT groups were expressed as a percentage of the NT group that was set at 100%. For quantitative analysis of double IR cells, ~50 BrdU-IR DG cells were randomly chosen in each section. Every selected BrdU-IR cell was analyzed for double labeling with GABA_AR β2&3, NMDAR 2A/B or GlyRα2. The number of BrdU-IR cells that showed double labeling with GABA_AR β2&3 or NMDAR 2A/B was expressed as a percentage of the total number of BrdU-positive cells that was analyzed for double labeling.

4.3.6 Statistical analysis

Data are presented as mean ± standard error of the mean (SEM). Statistical analysis was performed using Graphpad Prism5 software. The data are tested for normality using a D'Agostino and Pearson test. Group differences were tested using one-way ANOVA and a *post hoc* Dunnett's multiple comparison test for data with a normal distribution or a Kruskal-Wallis test and *post hoc* Dunn's comparison test when the data were not normally distributed. Statistical significance was set at p<0.05.

4.4 RESULTS

4.4.1 Febrile seizures increase neurogenesis in the DG granule cell layer, but do not change the number newborn cells in the DG hilar region

Because seizure-induced newborn DG cells in the granule cell layer as well as ectopically expressed in the hilus may contribute to a hyperexcitable hippocampal network [139, 142], the influence of FS on newborn cells was examined in both regions. Numbers of newborn DG cells, labeled with BrdU immediately following HT treatment, were determined 7 weeks after the last BrdU injection *i.e.* at P66. At 8 weeks after HT-treatment, BrdU-IR cells were mostly found in the subgranular zone (Figures 4.1A-D) and occasionally in the hilus (Figures 4.1A and 4.1E-G). Quantification of the number of BrdU-IR cells in the DG revealed a no statistically significant effect in HT-FS rats ($120 \pm 6\%$) and a significant increase ($p < 0.05$) in HT+FS rats ($121 \pm 7\%$; Figure 4.1H). No group differences were found in the amount of BrdU-IR cells in the hilus (Figure 4.1H). To allow comparison with other studies, absolute numbers of BrdU-IR cells/ $100.000\mu\text{m}^2$ were also determined: in the granule cell layer NT = 77 ± 3 ($n=4$), HT-FS = 93 ± 5 ($n=4$), and HT+FS = 94 ± 5 ($n=6$), and in the hilus NT = 37 ± 5 ($n=4$), HT-FS = 30 ± 3 ($n=4$), and HT+FS = 33 ± 3 ($n=6$). Lemmens *et al* (2008) showed that nearly all newborn DG cells developed into mature neurons in HT-treated rats [111]. To determine whether these newborn DG neurons developed an inhibitory or an excitatory phenotype, we performed double immunolabelings using antibodies against the most important inhibitory or excitatory LGICs present in the DG on the one hand and against BrdU on the other.

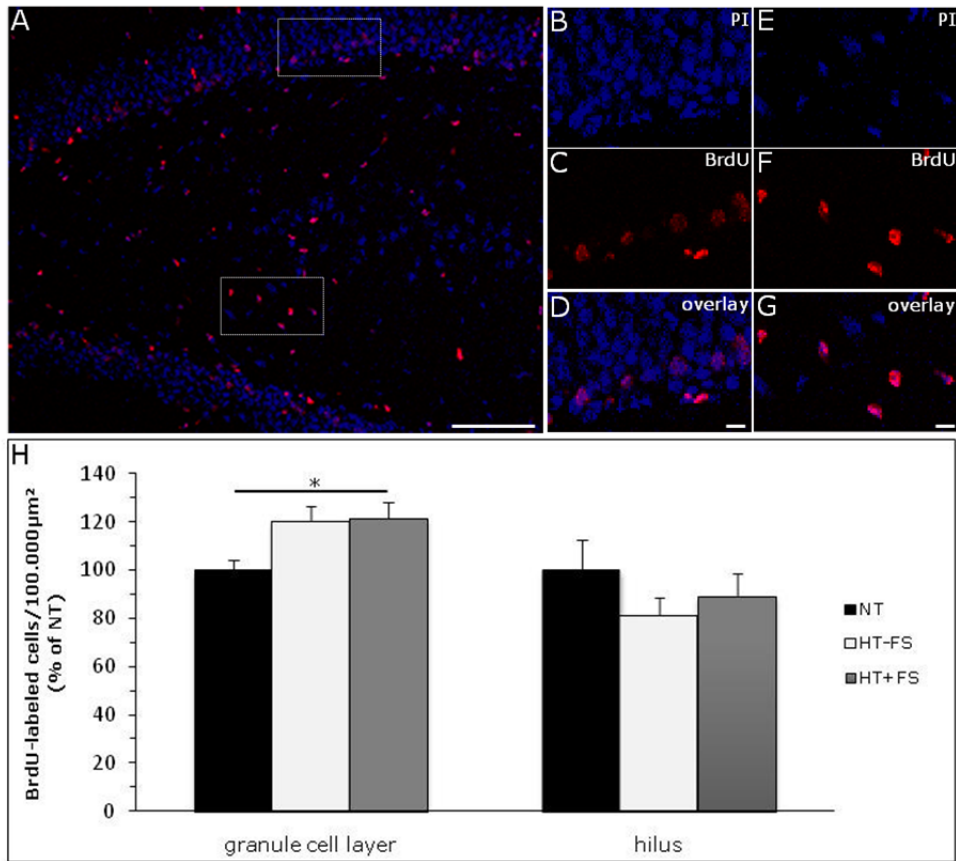


Figure 4.1: Hyperthermia-induced seizures increase the number of newborn DG granule cells. Representative pictures of a coronal hippocampal section of a NT rat stained for BrdU (red) and propidium iodide (PI, blue) (A-G). BrdU-immunoreactive cells were mainly located in the subgranular zone of the hippocampal DG (B-D), but some newly generated hippocampal cells were also found in the hilar region (E-G). Scale bars, 100 μm (A), 5 μm (B-G). Quantification of BrdU-immunoreactive nuclei (H) in the granule cell layer demonstrated about 21% more BrdU immunoreactive cells in HT+FS (n=6) rats than in NT rats. No significant differences were detected between HT-FS (n=4) and NT (n=4) rats. Quantitative analysis in the hilar region revealed no significant differences in the number of BrdU-immunoreactive cells between NT (n=4), HT-FS (n=4) and HT+FS (n=6) rats. Data are presented as mean ± SEM. (*P<0.05; analyzed using one-way ANOVA and *post hoc* Dunnett's multiple comparison test).

4.4.2 Cells born after FS express more often GABA_ARs and equally express GlyRs

Newborn DG cells were first analyzed for the expression of GABA_ARs by double labeling with antibodies directed against BrdU and with antibodies that recognize the $\beta 2$ and $\beta 3$ subunit of the GABA_AR. $\beta 2,3$ subunits are known as a major constituent of hippocampal GABA_ARs at every developmental age [67]. As expected, GABA_AR $\beta 2,3$ IR cells were ubiquitously present in the DG granule cell layer as well as in the hilar region (Figure 4.2A-C). This was in accordance to the $\beta 2,3$ staining pattern described by previous immunohistochemical reports studying $\beta 2,3$ distribution in rat hippocampal tissue [67, 149, 180]. None of the BrdU-IR hilar cells colocalized with GABA_AR (Figure 4.2C). In contrast, a significant proportion of the BrdU-IR DG granule cells showed GABA_AR $\beta 2,3$ expression (Figures 4.2C-F). Quantification of BrdU/GABA_AR $\beta 2,3$ double labeled DG granule cells revealed that $62 \pm 1\%$ of these BrdU-positive cells colocalized with GABA_AR $\beta 2,3$ in HT+FS rats (n=6). This is an increase of $\sim 21\%$ ($p < 0.01$) compared to NT control rats ($41 \pm 3\%$; n=4). The amount of BrdU/GABA_AR $\beta 2,3$ double labeled DG granule cells in HT-FS rats ($48 \pm 2\%$; n=4) did not differ significantly from NT nor from HT+FS rats (Figure 4.2G).

Although GABA_ARs are known as the principal mediators of inhibitory neurotransmission in rostral brain areas, GlyRs have also been implicated. Danglot *et al* (2004) reported a widespread distribution of the GlyR in the rat hippocampus and suggested that these GlyRs contain $\alpha 2$ but no $\alpha 1$ subunits [49]. Therefore, we identified GlyR-expressing newborn cells by an antibody that recognizes specifically the $\alpha 2$ subunit of the GlyR. $\alpha 2$ -containing GlyRs were clearly present on hilar cells, whereas only a faint GlyR $\alpha 2$ immunoreactivity was detected in the DG granule cell layer (Figures 4.3B and E). This pattern of GlyR expression is in agreement with immunohistochemical and electrophysiological studies [37, 49]. However, based on these studies we expected a stronger GlyR signal in the DG granule layer. Indeed, a much stronger GlyR signal was detected in the dentate granule cell layer when the HCl-step was omitted (data not shown). However, HCl pretreatment is necessary to unmask the BrdU antigen. It has been reported that HCl may be detrimental to other antigens of interest, particularly to cell surface antigens and receptors resulting in weaker or even absent immunolabeling [95]. Accurate quantification of the number of

BrdU/GlyRa2 double labeled DG granule cells was not possible because of a too faint GlyRa2 signal. Hence, cell counts were only performed for newborn hilar cells (Figures 4.3D-F). BrdU-IR hilar cells co-expressing GlyRa2 were observed in 3 out of 10 rats, and their number was $\sim 1\%$ of BrdU positive cells. No differences were seen between NT ($n=3$), HT-FS ($n=3$), and HT+FS ($n=4$) rats, suggesting that FS did not influence GlyR expression in newborn hilar cells.

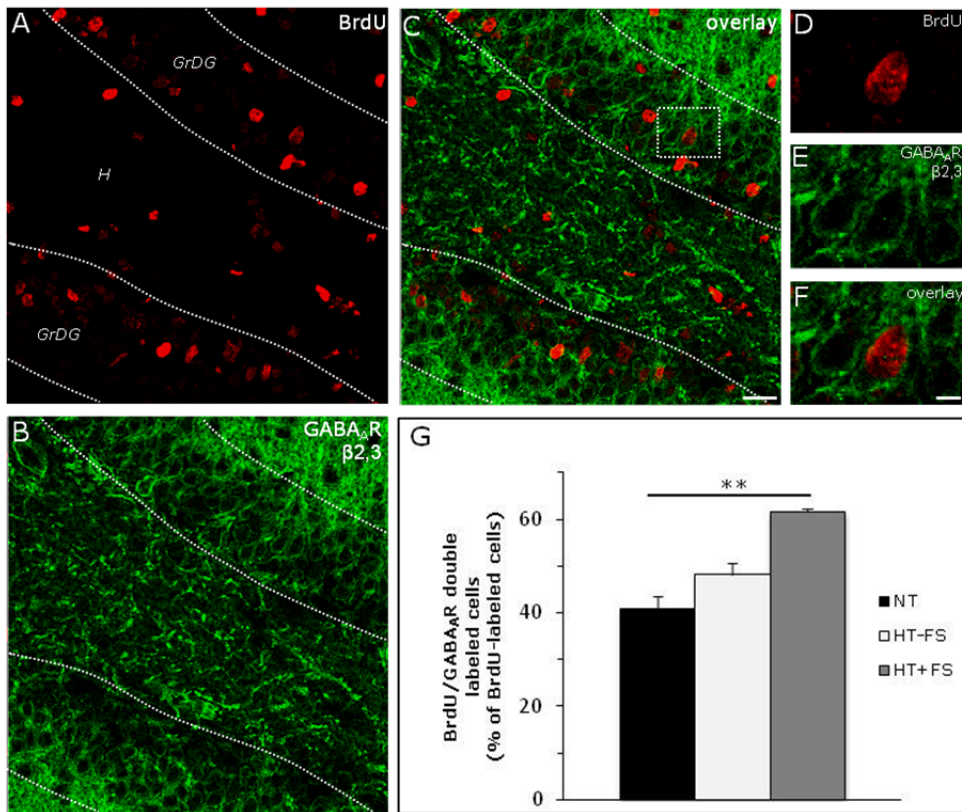


Figure 4.2: Hyperthermia-induced seizures significantly increased the number of BrdU/GABA_ARβ2,3 colocalizing DG granule cells. Representative pictures of a coronal hippocampal section of a HT+FS rat stained for BrdU (red) and GABA_ARβ2,3 (green) (A-C). No differences were observed in the staining pattern of BrdU-GABA_ARβ2,3 between NT, HT-FS and HT+FS animals. None of the BrdU-immunoreactive hilar cells expressed GABA_ARβ2,3, whereas several BrdU-immunoreactive dentate granule cells colocalized with GABA_ARβ2,3 (D-F). Scale bars, 20 μm (A-C), 5 μm (D-F); GrDG, granular dentate gyrus; H, hilus. Quantification of the BrdU/GABA_ARβ2,3 double labeled cells (G) showed a significant increase of $\sim 21\%$ in the number of double labeled cells in HT+FS ($n=6$) compared to NT control rats ($n=4$). HT-FS rats ($n=4$) did not differ significantly from the other experimental groups. Data are presented as mean \pm SEM. (** $P < 0.01$; analyzed using a Kruskal-Wallis test and *post hoc* Dunn's multiple comparison test).

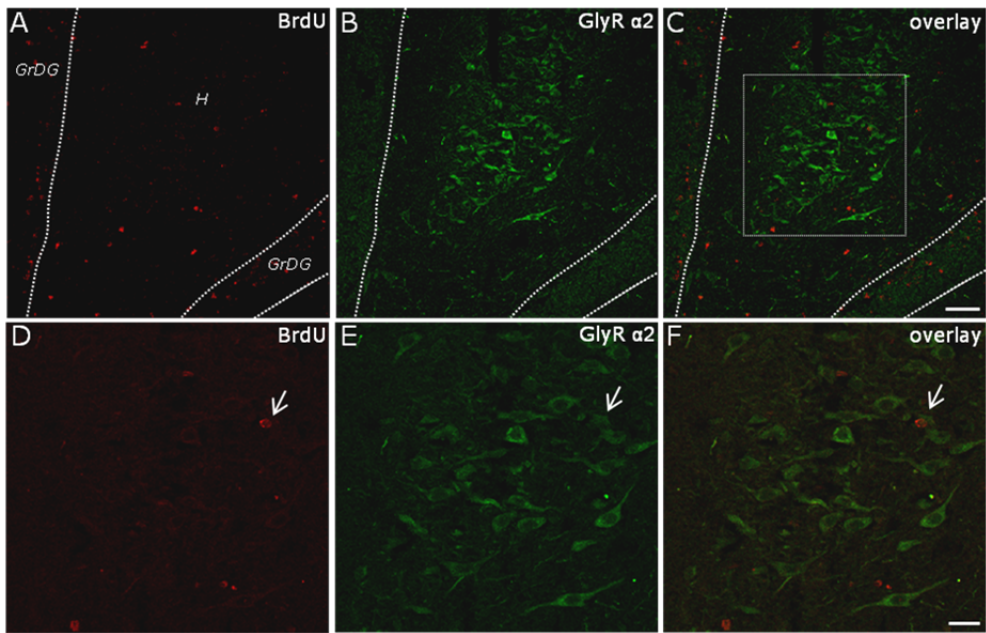
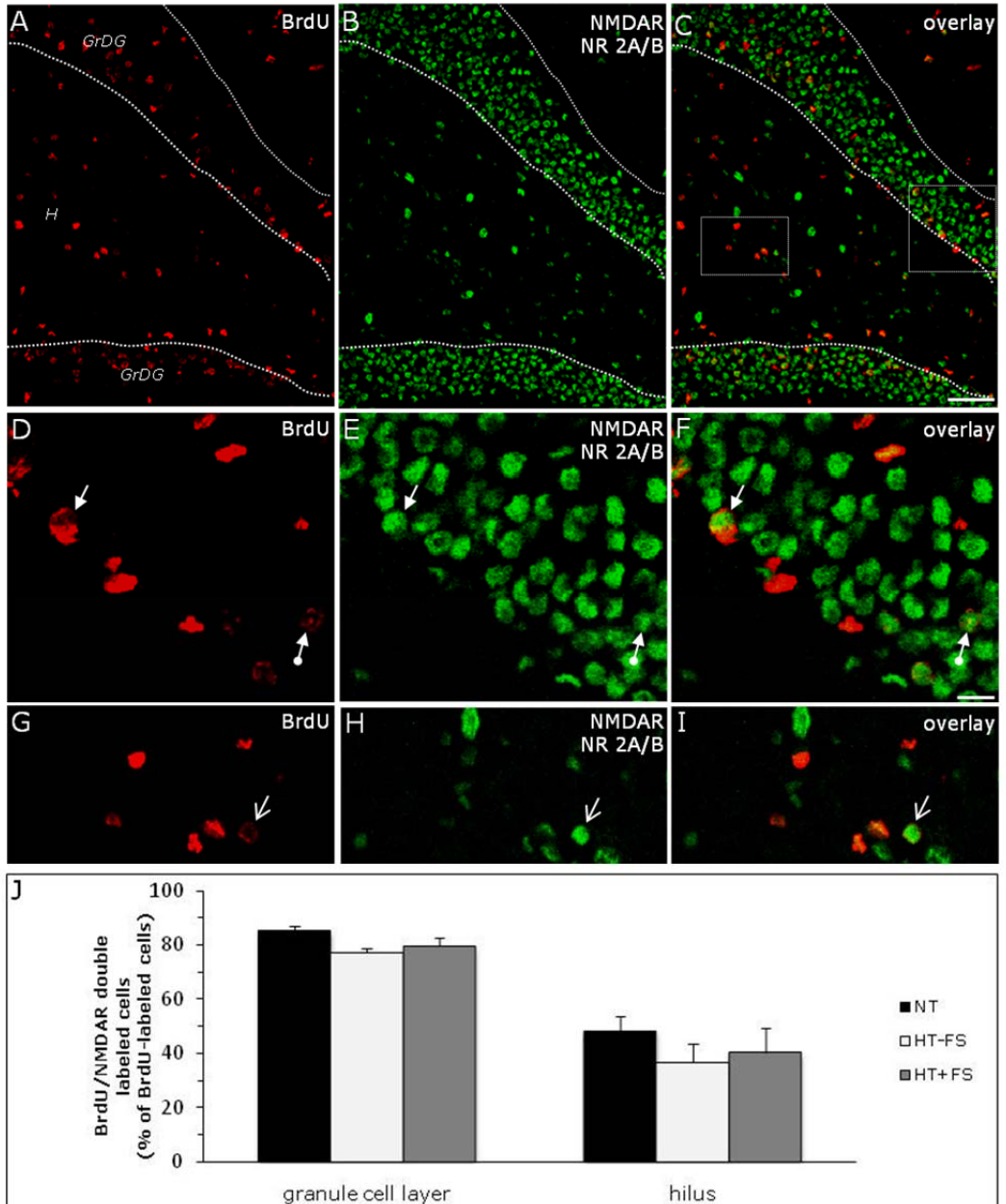


Figure 4.3: $\alpha 2$ -containing GlyRs were predominantly detected in the hilus and were hardly expressed by newborn cells. Representative pictures of a coronal hippocampal section of a NT rat stained for BrdU (red) and GlyRa2 (green) (A-F). Faint GlyRa2 immunoreactivity was detected in the granule cell layer (B), whereas clear GlyRa2 positive cells were present in the hilar region (B/E). No differences were observed in the staining pattern of GlyRa2 between NT, HT-FS and HT+FS animals. Only a few newborn hilar cells colocalized with GlyRa2 (see text for details). Scale bars, 50 μm (A-C), 20 μm (D-F); GrDG, granular dentate gyrus; H, hilus.

4.4.3 Febrile seizures do not alter the number of newborn DG cells expressing NMDARs

Newborn DG cells that express NMDARs were identified by an antibody that recognized the NR2A and NR2B subunit. NMDARs are heteromers, mostly composed of two NR1 and two NR2 subunits. NR2 subunits include four different types namely NR2A-D among which the NR2A and NR2B subunits are predominating in the adult forebrain [138]. In line with previous observations [38], we found abundant NMDARs expression in the granule cell layer and to some extent also in the hilus (Figures 4.4A-C). In the granule cell layer, about 80% of BrdU-IR cells were also NMDAR-IR (Figures 4.4D-F). This percentage did not differ between the different experimental groups (Figure 4.4J). Also in the hilus, where about 40% of BrdU-IR cells co-expressed NMDAR (Figures 4.4G-I), the percentage of BrdU/NMDAR-IR cells did not differ between the different

experimental groups (Figure 4.4J). These results indicated that FS did not change NMDAR expression in newborn DG cells.



Excitatory neurotransmission in the hippocampus is not only mediated by ionotropic NMDARs, but also by ionotropic non-NMDARs such as the AMPAR. Most hippocampal AMPARs are heteromers composed of GluR1/GluR2 or GluR2/GluR3 subunits [174]. To determine if FS affect AMPAR expression in the DG, we identified AMPARs by an antibody recognizing GluR2 as well as GluR3 subunits. As shown in Figure 4.5, AMPAR GluR2/3 subunits were predominantly expressed in the hilar region of the DG. After HCl treatment, required for BrdU visualization, AMPAR GluR2/3 staining was absent. Hence, it was not possible to draw conclusions concerning the relation between FS and AMPAR expression in newborn DG cells.

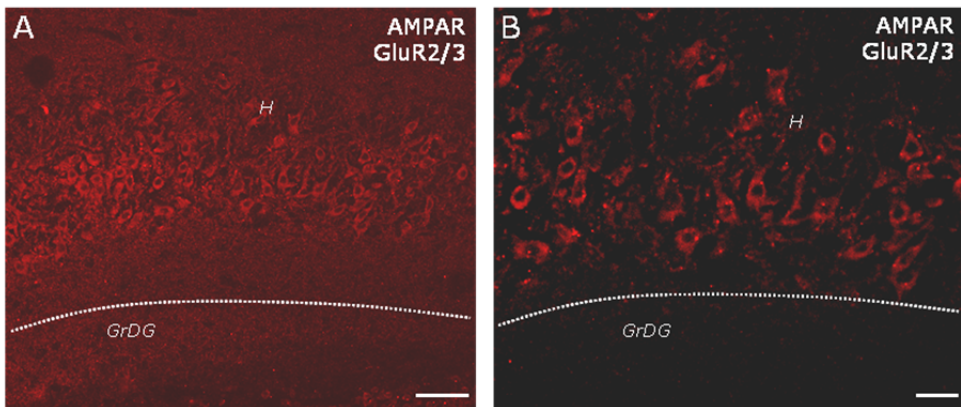


Figure 4.5: AMPAR GluR2/3 subunits were predominantly expressed in the hilar region. Representative pictures of a coronal hippocampal section of a NT rat stained for AMPAR GluR2/3 subunits (A-B). AMPARs were predominantly present in the hilar region of the DG (B). Scale bars, 50 μm (A), 20 μm (B) GrDG, granular dentate gyrus; H, hilus.



Figure 4.4: The number of BrdU/NMDAR NR2A/B colocalizing cells was similar in all experimental groups. Representative pictures of a coronal hippocampal section of a HT+FS rat stained for BrdU (red) and NMDAR (green) (A-C). No differences were observed in the staining pattern of BrdU-NMDAR between NT, HT-FS and HT+FS animals. Several BrdU immunoreactive dentate granule cells (D-F) as well as hilar newborn cells (G-I) colocalized with NMDAR (arrow). Scale bars, 50 μm (A-C), 10 μm (D-I); GrDG, granular dentate gyrus; H, hilus. No significant differences in the amount of BrdU-immunoreactive cells colocalizing with NMDAR were seen between NT (n=4), HT-FS (n=4) and HT+FS (n=6) rats, neither in the granule cell layer nor in the hilus (J) (analyzed using a Kruskal-Wallis test and *post hoc* Dunn's multiple comparison test). Data are presented as mean \pm SEM.

4.5 DISCUSSION

During the latent period following seizures, both an increase in hippocampal neurogenesis and alterations in inhibitory and excitatory LGIC expression have been observed in different animal models. In the present study we determined if seizure-induced newborn hippocampal cells themselves could be a source of long-lasting alterations in LGIC expression. Making use of an established model of early-life prolonged FS, DG cells born immediately following HT-induced seizures were labeled and their excitatory and inhibitory LGIC expression profile was characterized in adulthood. The major findings of this study are that experimental FS: 1) significantly increase the number of newborn cells in the DG granule layer but not in the hilar region, 2) significantly increase the number of newborn DG cells that express GABA_ARs, and 3) do not change the number of newborn GlyR or NMDAR expressing cells in the DG.

FS have already been associated with increased hippocampal cell proliferation. The 21% increase in newly born DG granule cells observed in FS animals of this study, is in line with a previously reported 25% increased number of BrdU-IR DG cells at 8 weeks after FS [110] and other studies in immature models [151, 160]. Additionally, in adult rodents, DG cell proliferation was also increased after pentylentetrazole- [91], pilocarpine- or kainate-induced seizures [47], amygdala kindling [140], and after an electroconvulsive shock [171]. The majority of newborn DG cells differentiate into neurons in the DG granule cell layer [111, 142, 151]. However, a fraction of newly generated DG cells may migrate aberrantly to the hilar region. BrdU labeling was significantly increased in the hilus at 14 and 35 days after pilocarpine-induced seizures compared with control animals [139]. Further morphological and immunohistochemical characterization revealed that these hilar BrdU-IR cells differentiate into DG granule cells although they resided outside their normal granule cell layer location. These ectopically migrated DG cells potentially contribute to hippocampal hyperexcitability [139, 142, 165]. Lemmens *et al.* already observed that following FS the majority of BrdU-IR cells developed into mature, NeuN-IR neurons in the granule cell layer, whereas a few BrdU-IR cells that were found in the hilus colabeled with GFAP [111]. However, until now hilar BrdU-IR cell numbers had not been quantified in this model. In contrast to pilocarpine-

treated animals, our results failed to demonstrate an effect of HT-induced seizures on the number of BrdU-IR hilar cells at 8 weeks after treatment. This suggests that prolonged experimental FS do not influence significantly the presence of newborn cells in the DG hilar region. Yet, minor changes in hilar BrdU-IR cell numbers cannot be excluded because we did not quantify cell numbers by stereological-based methods. Alternatively, newborn hilar cells may express an altered phenotype, even if the hilar BrdU-positive cell number is unaltered. In that respect, hilar newborn cells were also further characterized for the expression of different LGICs.

Although seizure-induced hippocampal cell proliferation is well documented, the function of this dynamic cell population in the existing hippocampal network following seizures is still largely unknown. In adult animals, seizures are often associated with neuronal cell loss in the CA1 and CA3 pyramidal cell layers and the DG hilus [14, 30]. Therefore, it was initially thought that newborn neurons may be beneficial by compensating for the neuronal cell loss [166]. However, young animals are less vulnerable to seizure-induced hippocampal cell loss than mature animals [161]. In this model of FS, HT-induced seizures caused only a transient injury of CA1 and CA3 pyramidal cells and no acute or long-term cell death [18, 186]. The absence of significant neuronal dropout after early-life FS suggests that seizure-induced newborn DG cells may display a more complicated role than just exerting a repair function. Blocking seizure-induced hippocampal neurogenesis during the latent period following pilocarpine treatment has been shown to attenuate the likelihood of developing spontaneous recurrent seizures, suggesting a pro-epileptogenic role for hippocampal cell proliferation [92]. In addition, it has been demonstrated that newborn DG cells migrated and incorporated aberrantly in the adult epileptic hippocampus, strongly suggesting the involvement of abnormal neurogenesis in the development of TLE [139, 142, 165]. Because the peak of DG neurogenesis occurs during the first weeks postnatally [136, 148], seizures in immature animals may induce even more effectively aberrant integration of new DG cells in the existing hippocampal circuitry [104]. Nearly all newborn cells generated after early-life FS display a mature neuronal phenotype in adulthood [111]. Further phenotypical characterization of these cells might give clues about their functional significance

in the hyperexcitable hippocampal network [39, 53]. Therefore, we examined if long-lasting alterations in inhibitory and/or excitatory LGIC expression in DG cells that are born immediately after early-life FS. This was performed by double labeling newborn DG cells with GABA_AR, GlyR, or NMDAR antibodies.

Of all BrdU-IR DG cells, 40% colocalized with GABA_AR in controls, whereas this percentage was increased to 60% in FS animals. A modified GABA_AR subunit expression profile has been detected in other neonatal [201] as well as adult [26, 157, 170] rodent models of seizures and human epileptic hippocampi [117]. In human TLE, DG cells show an upregulated GABA_AR α_1 , α_2 , $\beta_{2/3}$, and γ_2 -subunit expression [117]. Similar results are reported for the kainate model, in which expression of nearly all GABA_AR subunits (α_1 , α_2 , α_4 , α_5 , β_1 , β_2 , β_3 , and γ_2) is enhanced in the DG at 30 days after seizures. It has been suggested that this increased GABA_AR expression compensates, at least partially, the impaired GABA-mediated neurotransmission caused by a loss of GABA_AR-expressing cells in the CA1, CA3, and hilar region [170]. Yet in the current model, the functional consequences of an increased population of newborn DG cells expressing GABA_AR are unclear. Long-lasting enhancement of GABA_AR expression by newborn DG cells may be a compensatory, anticonvulsive response. However, next to their classical role in inhibitory neurotransmission, GABA_ARs may also have excitatory effects, especially in newborn cells and in pathological conditions. The polarity of GABA_AR-mediated neuronal currents is dependent on the transmembrane concentration gradient for Cl⁻, the most important ion to which GABA_ARs are permeable. The equilibrium potential for GABA (E_{GABA}) is depolarizing in the developing brain as a consequence of the higher intracellular Cl⁻ concentration in immature compared with mature neurons. E_{GABA} becomes hyperpolarizing during postnatal brain development, due to an upregulation of the Cl⁻ extruding K⁺-Cl⁻ cotransporter (KCC2) synergistically with a down-regulation of the Cl⁻ importing Na⁺-K⁺-2Cl⁻ cotransporter (NKCC1) [15]. Alterations in Cl⁻ homeostasis that cause a switch in GABA_AR-mediated neurotransmission from inhibitory to excitatory again, have been demonstrated in experimental [58, 143] and human [43, 129, 137] epileptic hippocampi. A depolarizing shift in dentate granule E_{GABA} was found during the latent period after pilocarpine-induced seizures, resulting in an altered synaptic integration

and increased DG excitability. Interestingly, this shift in E_{GABA} was accompanied by a decreased KCC2 expression [143]. Downregulation of KCC2 and upregulation of NKCC1 have been shown to persist up to 45 days after pilocarpine-treatment, demonstrating that seizures may have a long-lasting influence on cation-Cl⁻ cotransporter expression levels [114]. Taken together, the above mentioned studies point to an excitatory role for GABA after seizures implying that enhanced GABA_AR expression may have pro-epileptogenic rather than protective effects.

In contrast to GABA_AR expressing newborn cells, the number of BrdU-GlyR double labeled hilar cells did not differ between experimental groups. In the dentate granule layer the GlyR immunoreactivity was too low to allow an accurate estimation, most likely due to the BrdU labeling procedure. Studies addressing the role of the GlyRs in epilepsy are scarce compared to studies on GABA_ARs. This may be partly due to the fact that GABA was long considered as the main inhibitory neurotransmitter in the upper part of the neuroaxis, whereas glycine was thought to be confined to the lower part. It is now well established that GlyRs are expressed in the hippocampus [49], where they are involved in the regulation of neuronal excitability [37, 127]. Although GlyR activation may exert anticonvulsive effects by decreasing hippocampal hyperexcitability [37, 98, 179], recent studies suggest a pathophysiological role for GlyR mediated signaling [61] particularly in the context of TLE associated alterations in Cl⁻ homeostasis [50, 109]. In the light of these findings, further research exploring the possible involvement of GlyRs after early-life FS might be interesting. The use of alternative techniques to label newborn neurons (e.g. retroviral labeling [189]) may permit a stronger GlyR immunolabeling in the DG granule cell layer. Also in contrast to the observed changes in BrdU-GABA_AR colocalizing cell numbers, the number of newborn DG cells expressing NMDARs was equal in all experimental groups. This observation is in line with the study of Chen *et al.*, reporting that FS-induced functional alterations in the hippocampal network are highly specific to the principal inhibitory neurotransmitter system and do not involve the excitatory system [39].

In conclusion, the results presented in this study demonstrate that early-life FS have a persistent effect on the DG granule cell layer composition. FS-induced newborn DG granule cells are a source of long-lasting increased GABA_AR expression. Though the functional significance of this increase is not clear, it is a potential target for new anti-epileptogenic therapies.

5

Towards assessment of functional neurogenesis after experimental febrile seizures

5.1 ABSTRACT

Experimental febrile seizures (FS) induce neurogenesis in the hippocampal dentate gyrus (DG). Labeling of these newborn neurons by the thymidine analogue BrdU (5-bromo-2'deoxyuridine) has provided much information about their migration and differentiation. However, the BrdU method does not allow a functional characterization of newborn neurons. This may be overcome by a recently developed technique, in which green fluorescent protein (GFP)-expressing retroviral vectors are locally applied and have been shown to label newborn DG cells in the adult hippocampus.

In this study, we aimed at applying this viral technique in rats that had been exposed to FS at postnatal day 10. This warranted that the retroviral vector was stereotactically injected in the DG of 11-day old Sprague Dawley rats. Due to a lack of anatomical information, we first determined the stereotactic coordinates of the DG by injecting methylene blue. In this way, we found that injections at 3.0 mm anteriorly and 2.0 mm laterally from lambda, and 2.5 mm ventrally from the cortex were most successful at targeting the DG. *In vivo* injection of GFP-expressing retroviral vectors required testing for the absence of replication competent retrovirus. To this end, we developed a simple and fast method applying reverse transcriptase-polymerase chain reaction (RT-PCR) of glycoprotein G from vesicular stomatitis virus (VSVG), and demonstrated that the GFP-expressing retroviral vector was replication incompetent.

5.2 INTRODUCTION

Neurogenesis is not restricted to the prenatal period, but has been shown to persist in adulthood in at least two selected forebrain regions, namely (i) the subventricular zone which give rise to new interneurons in the olfactory bulb [5], and (ii) the subgranular zone of the hippocampal dentate gyrus (DG) [95]. The thymidine analogue BrdU (5-bromo-2'-deoxyuridine), which integrates into the newly synthesized DNA during the S-phase of mitosis, is a commonly used tool to label proliferating cells in the postnatal hippocampus [103]. Using the possibility to immunohistochemically detect BrdU, newly born cells have been studied extensively to assess the proliferative rate, migration, and differentiation. The BrdU method allows a sensitive and valid quantification of new neurons and, hence, has provided much information about the regulation of adult neurogenesis. In this way, generation of new neurons has been shown to be influenced by for instance stress [74], aging [103], environmental enrichment [96], exercise [188], stroke [115] and seizures [20, 47, 91, 140, 171]. A drawback of the BrdU method is that it requires tissue fixation, which makes this technique unfit to study the functioning of newborn cells. This can be overcome by using a retroviral vector expressing green fluorescent protein (GFP), because these viruses are taken up by dividing cells. This requires a complete cell cycle [113]. Gene products from the incorporated viruses can be detected long after a cell has been infected. Hence, transduction of proliferating cells with a GFP-expressing retroviral vector allows visualization of living cells by fluorescent microscopy enabling functional characterization. Van Praag and colleagues were the first who successfully applied this technique. Their study provided *ex vivo* evidence that new neurons can become functionally integrated granule cells [189].

Using the BrdU method, experimental febrile seizures (FS) have been found to persistently increase the number of newborn dentate granule cells [110, 111]. In this model, we recently demonstrated that an increased number of these newborn cells express the GABA_AR (γ -aminobutyric acid type A receptor; see chapter 4). Yet, it is unknown if these newborn cells are functionally altered and affect hippocampal physiology.

The purpose of this chapter was to adapt an appropriate-aged rat model of FS, used in all experiments of this thesis, to a model in which FS-induced

neurogenesis was visualized by GFP allowing *in situ* electrophysiological characterization. In order to label dividing cells immediately following FS, a GFP-expressing retroviral vector needed to be stereotactically injected in the DG the day after FS (*i.e.* postnatal day 11). However, a stereotactic atlas of the developing Sprague-Dawley rat brain does not exist. The first part of this chapter therefore discusses the determination of the DG stereotactic coordinates in 11-day old Sprague-Dawley rat pups by stereotactic injections of methylene blue. *In vivo* injection of GFP-expressing retroviral vectors require the absence of replication competent retroviruses (RCR). Therefore, the second part of this chapter focuses on a simple and fast technique which can be applied to test retroviruses for the presence of RCR.

5.3 MATERIAL AND METHODS

5.3.1 Stereotactic surgery

Litters of 5-10 male Sprague-Dawley rat pups (Harlan, Horst, The Netherlands) were housed with a dam under temperature controlled conditions and 12h dark-light cycle with water and food *ad libitum*. At postnatal day 11 (P11), rat pups were anaesthetized with isoflurane (induction: 5%; maintenance: 2%) and placed in a stereotactic frame with a neonatal rat adaptor (Stoelting, IL, USA) in which the head was immobilized with earbars containing rubber cuffs. 2% lidocaine was subcutaneously injected on the skull for local analgesia of the periost and skin incision. After midline incision of the skin, a bur hole was made in the skull at coordinates relative to lambda. Initial stereotactic coordinates of the DG were based on data from P5 Sprague Dawley rats [17]. Next, 1.5 μ l methylene blue (2% in PBS) was injected at a rate of 0.25 μ l/min using a 30-gauge needle connected to a 10 μ l Hamilton syringe. After the injection, the needle was left in place for an additional 5 min before it was slowly withdrawn from the brain. Pups were immediately decapitated after surgery, and brains were removed and snap frozen in liquid nitrogen. Cryosections (50 μ m) were cut using a cryostat (Leica Microsystems, Wetzlar, Germany) and immediately evaluated under a light microscope.

5.3.2 Production of eGFP-expressing retroviral vectors

A replication-deficient retroviral vector based on the Moloney murine leukemia virus was used to express enhanced GFP (eGFP) driven by a CAG promoter. Retroviral particles were assembled by a triple transient transfection of human embryonic kidney 293T cells with a packaging plasmid encoding viral proteins under control of a CMV promoter (CMV-gag/pol), an envelope plasmid encoding the glycoprotein G of vesicular stomatitis virus under control of a CMV promoter (CMV-VSVG), and a transfer plasmid encoding eGFP under control of a CAG promoter (CAG-eGFP) (kindly donated by prof. H. van Praag, Laboratory of Neurosciences, Biomedical Research Center NIA, Baltimore, USA). Transient transfection of 293T cells was carried out in 100-mm cell culture dishes containing 2.10^6 cells seeded the day prior transfection in Dulbecco's modified Eagle's medium (DMEM) high glucose (4500 mg/l) (Gibco BRL, Paisly, UK),

supplemented with L-glutamine and 10% (v/v) fetal calf serum (FCS). For every dish, a mixture of 50 μ L lipofectamine 2000 (Invitrogen, Merelbeke, Belgium) in 800 μ L Opti-MEM (Invitrogen) was prepared and incubated for 5 min at room temperature. Afterwards, the DNA mixture containing 7.5 μ g CAG-GFP, 5 μ g CMV-gag/pol and 2.5 μ g CMV-VSVG in 800 μ L Opti-MEM was added slowly to the lipofectamine mixture; incubated for 30 min at room temperature and then added dropwise to the 293T cells. After 5 h, the medium was replaced by fresh DMEM high glucose medium supplemented with 10% (v/v) FCS, L-glutamine, 100 U/ml penicillin and 100 μ g/ml streptomycin (Gibco BRL). Virus-containing supernatant was collected 72 h after transfection, filtered through a 0.22 μ m filter, concentrated by two rounds of ultracentrifugation (19,400 rpm; 4°C; 2 h), aliquoted and stored at -80°C. Final virus titers were determined by a QuickTiter™ Retrovirus Quantitation Kit according to the manufacturers' protocol (BioConnect, Huissen, The Netherlands).

5.3.3 Detection of replication competent retroviruses

Harvested supernatant was tested for the presence of replication-competent retroviral particles. To this end, $2 \cdot 10^5$ NIH 3T3 cells were seeded in 25 cm² cell culture flasks (Nunc, Waltham, MA, USA). NIH 3T3 cells were transduced with 3 ml retroviral supernatant containing 8 μ g/ml Polybrene (Chemicon, Temecula, CA, USA), incubated for 7 h during the first transduction (*i.e.* 24h after NIH 3T3 cell seeding) and for 4h during the second transduction (*i.e.* 48h after NIH 3T3 cell seeding). Retroviral cell infection was checked 4 days after the last transduction by confocal microscopy. Next, NIH 3T3 cell supernatant was collected and viral RNA was isolated using the QiaAmp MinElute Virus SpinKit (Qiagen, Venlo, The Netherlands). The concentration of total RNA was checked by measuring the optical density at 260 nm using the NanoDrop ND-1000 spectrophotometer (Thermo Fisher Scientific, Waltham, USA) and RNA purity was assessed by the 260/280 nm ratio. Viral RNA (10 μ L) was first incubated for 3 min at 85°C and then reverse transcribed using the Reverse Transcription System (Promega, Leiden, The Netherlands) in a 20- μ L reaction volume containing 5 mM MgCl₂, 1x Reverse Transcription buffer, 1mM dNTP mixture, 0.25 μ g Oligo(dT)₁₅ primers, 0.25 μ g hexamer oligonucleotides, 20 U RNase

inhibitor and 12.5 U AMV reverse for 90 min at 42°C, followed by 5 min at 95°C, and finally at 4°C. All cDNA samples were stored at -20°C until PCR analysis.

Reverse transcriptase (RT)-PCR was performed by adding 5 µL cDNA to an amplification mixture containing 2.5 µl 10x PCR buffer with MgCl₂, 0.75 µl Taq polymerase (1 U/µl), 0.25 µl dNTP mix (10 mM), 1 µl VSVG forward primer (10µM), 1 µl VSVG reverse primer (10µM) in a total volume of 25 µl. A denaturation step (3 min, 94°C) was followed by amplification over 40 cycles of denaturation (30 sec, 94°C), annealing (first 13 cycles 40 sec, 52°C; following 27 cycles 40 sec, 53°C), and elongation (10 min, 72°C). PCR reactions were performed using a BioRad Thermal Cycler (BioRad, Hercules, CA, USA). All PCR assay products were purchased from Roche Diagnostics (Vilvoorde, Belgium). Primer sequences were 5'-TCCGATCCTTCACTCCATCTG-3' and 5'-TAGCTGAGATCCACTGGAGAG-3' (Eurogentec, Seraing, Belgium). The PCR products were resolved by electrophoresis on a 1% agarose gel, stained with ethidium bromide and visualized by UV. Retroviral supernatant produced by 293T cells served as positive control.

5.4 RESULTS

5.4.1 Stereotactic coordinates of the dentate gyrus in P11 Sprague-Dawley rats

To determine the stereotactic coordinates of the DG in P11 Sprague-Dawley rats, methylene blue was injected at coordinates that were based on P5 Sprague-Dawley rats, *i.e.* relative to bregma: anteroposterior -1.2 mm; mediolateral 2.1 mm; dorsoventral -2.0 mm [131].

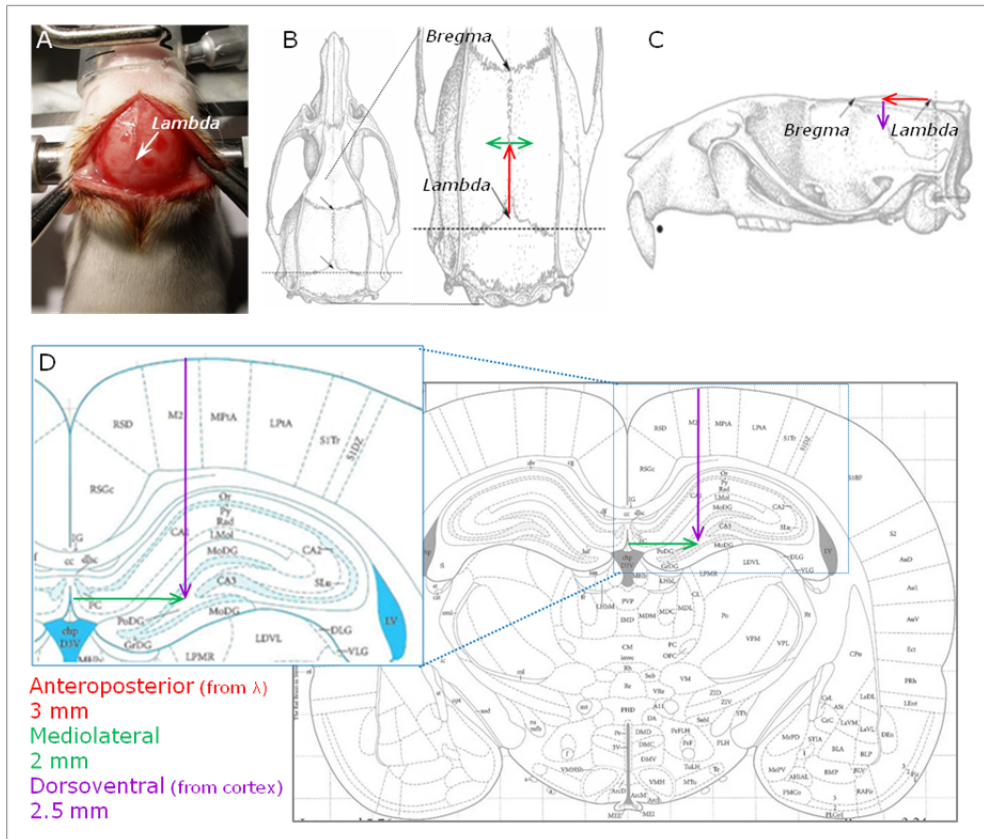


Figure 5.1: Stereotactic coordinates of the dentate gyrus in P11 Sprague-Dawley rats. P11 rat pups were placed in a stereotactic frame and coordinates for methylene blue injection were measured relative to lambda (A). Dorsal (B) and lateral (C) view of the skull with the positions of bregma and lambda, and anteroposterior (red), mediolateral (green), and dorsoventral (purple) directions for the injection site. Coronal section (D) adapted from Paxinos G. [145], locating the DG.

The site of injection was evaluated immediately after surgery. Based on the localization of the blue dot in coronal cryosections, coordinates for injection of the next animal were adjusted. This included a switch from bregma to lambda as reference point because unlike bregma, lambda was consistently visible. Ultimately, the injections 3.0 mm anteriorly, 2.0 mm laterally from lambda, and 2.5 mm ventrally from the cortical surface showed a blue dot in the DG in 4 out of 4 animals (Figure 5.1).

5.4.2 Detection of replication competent retroviral particles

NIH-3T3 cells were transduced with eGFP-expressing retroviral particles (virus titre 5.10^{11} viral particles/ml). These retroviruses are able to infect cells, as shown by eGFP fluorescence of transduced NIH 3T3 cells (Figure 5.2). Presence of the VSVG envelope protein in the supernatant of NIH 3T3 retroviral infected cells was used as indicative marker for RCR production. No RCRs were present as shown by the absence of VSVG expression in NIH 3T3 supernatant (Figure 5.3).

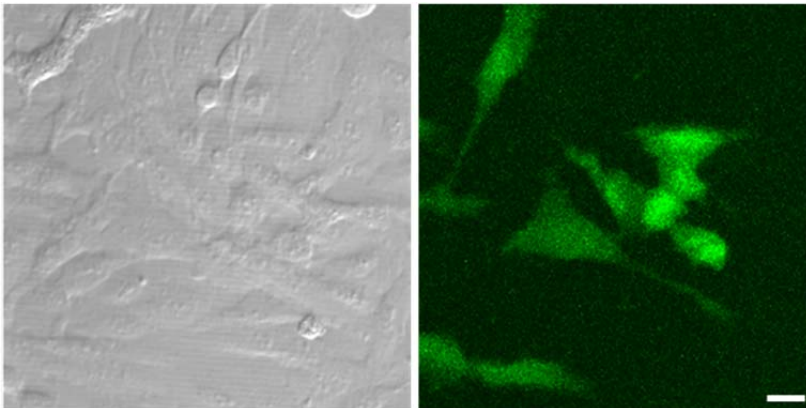


Figure 5.2: Fluorescent detection of eGFP positive NIH 3T3 cells. Bright field (left) and confocal microscope (right) images of NIH 3T3 cells 4 days after their second transduction with eGFP-expressing retroviruses, showing green, *i.e.* retroviral vector infected cells. Scale bar = 20 μ m.

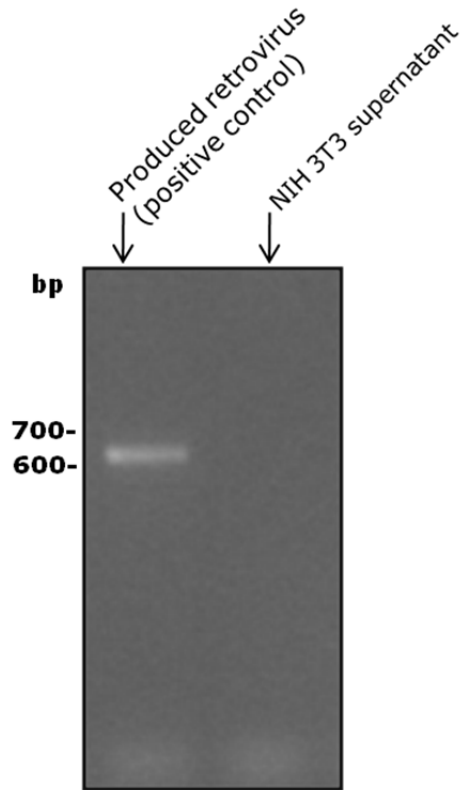


Figure 5.3: Analysis of VSVG expression in the supernatant of NIH 3T3 cells infected with eGFP-expressing retroviral vectors. RT-PCR analysis for VSVG expression in total RNA extracted from the supernatant of NIH 3T3 cell cultures (right lane). The produced eGFP-expressing retrovirus itself served as positive control (left lane). VSVG expression is absent in NIH 3T3 cell supernatant while a clear band of 667 bp was visible for the positive control.

5.5 DISCUSSION

In recent years, stereotactic injections of GFP-expressing retroviral vectors have become a popular tool in the study of newly born hippocampal cells [64, 107, 116]. The majority of these studies was performed in adult rodents using stereotactic coordinates that are not applicable in the quickly developing rat brain. Detailed stereotaxic atlases are available for the adult rodent brain, *e.g.* the stereotaxic atlas of Paxinos and Watson (2005) [145] for the rat brain is based on medium-sized (290 g) male Wistar rats. Additionally, the anatomical variation for female Wistar rats or rats from other strains has been estimated. Also variations for juvenile rats have been suggested, yet these apply to rats with a weight of about 180 g whereas an 11-day old rat pup weighs about 25 g. A stereotaxic atlas of the developing brain of Long-Evans female rats has been published [173]. However, it is known that brain development may vary considerably between different rat strains, which stress the necessity of verifying stereotactic coordinates of a brain region of interest in each specific rat strain at each specific developmental age. In this study, we determined the stereotactic coordinates of the DG in 11-days old Sprague-Dawley rats. This coordinate consistently targeted the DG in four out of four animals, and is therefore an interesting candidate for future injections with GFP-expressing retroviral vectors.

The Moloney murine leukemia virus based retroviral vectors used in the present study are designed to be replication defective. Intrinsic properties of the system, *e.g.* segregation of the viral protein coding sequences *gag-pol* and *env* onto separate plasmids and using coding sequences for envelope proteins of a heterologous virus (*i.e.* VSVG), minimize the probability of developing RCR. However, the occurrence of recombination events during retroviral vector production leading to RCR generation can never be completely excluded. Therefore, each batch of produced retroviral vector supernatant should be tested for the presence of RCR in order to guarantee safety for researchers and laboratory animals. Several biological as well as molecular assays have been proposed to test for RCR (for review see [162]). We checked retroviral vector supernatant for the presence of RCR by means of a RT-PCR for VSVG envelope. This method is based on the fact that replication deficient retroviral particles are capable of infecting host cells, *e.g.* NIH 3T3 cells, and integrate their viral

genome in the host cell genome. However they lack the genes necessary for the synthesis of viral particles. Hence, no VSVG envelope protein will be detected in the supernatant of NIH 3T3 cells that are transduced with replication deficient retroviruses.

In conclusion, we determined the stereotactic coordinates of the DG in P11 Sprague-Dawley rat pups, which can be used for future injections with GFP-expressing retroviral vectors. Also, we discussed a fast and simple technique, which provides information about the absence or presence of RCR and hence, the safety of the produced retroviral vectors for use in downstream applications.

6

Summary and general discussion

Retrospective studies report that adult patients with temporal lobe epilepsy (TLE) frequently had a history of early-life febrile seizures (FS), suggesting a causative role for FS in the process of epileptogenesis [56, 158, 163, 176]. Yet, the mechanisms by which FS may be linked to TLE are still largely unknown. TLE is characterized by a disturbed balance between excitation and inhibition in the hippocampal formation, thereby lowering the seizure threshold. Propagation of synchronous excitatory activity originating from the entorhinal cortex to downstream hippocampal structures, *i.e.* the hilus and CA3 area, is normally filtered by the dentate gyrus (DG). In other words the DG functions as a critical checkpoint regulating excitability in the limbic system [46]. It has been hypothesized that this 'gatekeeper' function of the DG is compromised in the process of epileptogenesis.

In this thesis, we aimed at elucidating some mechanisms by which early-life FS may lead to enhanced hippocampal excitability. We focused on the DG structure and investigated if FS-induced expressional and functional alterations of ligand-gated ion channels (LGICs) in the DG may contribute to a disturbed DG 'gate' function. To this end, we used an appropriate-aged animal model in which FS are evoked in 10-day old rat pups by exposing them to heated air [11]. In this model, FS are associated with long-term hippocampal hyperexcitability resulting in a decreased seizure threshold [39, 53]. 35% of rats with early-life FS develop TLE in adulthood, while 88% show interictal epileptiform EEG abnormalities [54].

This chapter discusses the most important results of the thesis. A schematic representation of the data is depicted in Figure 6.1.

Effects of early-life febrile seizures on DG granule GABA_ARs

Study of resected hippocampal tissue from TLE patients has already demonstrated an altered type A GABA receptor (GABA_AR) subunit expression profile. The most pronounced changes in surviving DG granule cells concerned the up-regulation of the $\alpha 1$, $\alpha 2$, $\beta 2/3$ and $\gamma 2$ subunits [117]. This reorganization of GABA_AR subtypes already stressed that GABA_AR-mediated neurotransmission may undergo plasticity during human epileptogenesis. Importantly, powerful GABAergic inhibition is necessary for maintenance of the DG filter function [46]. Hence, seizure-associated alterations in GABA_AR expression and/or function may

contribute to malfunctioning of the DG and may facilitate seizure generation. Therefore, we studied the influence of experimental early-life FS on GABA_AR-mediated neurotransmission by means of whole-cell patch-clamp recordings from DG granule cells in hippocampal slices (**chapter 3**). Our data reveal a reduced frequency of inhibitory synaptic currents ~1 week after experimental FS. Frequency alterations are known to be able to disturb the balance between inhibition and excitation in a neuronal network. However, concurrently with the presynaptic change, several alterations at the postsynaptic level (*i.e.* upregulation of GABA_AR density and enhanced GABA potency) seem to compensate for the decreased inhibitory synaptic input to dentate granule cells. At first sight, the lack of a net change in GABAergic inhibition contradicts the hypothesis that FS may compromise the DG filter function. However, it has to be stressed that the alterations in GABA_AR-mediated neurotransmission are detected during the latency period when no spontaneous seizures or interictal epileptiform EEG abnormalities are evident, implying that other mechanisms are required in the process of FS-associated epileptogenesis. Therefore, it is suggested that the observed changes in GABA_AR-mediated inhibition may contribute to a decreased seizure threshold, in combination with other changes occurring later in the process of epileptogenesis. Those other changes might include seizure-induced depolarizing GABAergic synaptic responses [50, 143] and alterations in excitatory synaptic input to granule cells by aberrant mossy fiber sprouting in the molecular layer [18, 89].

Quantitative real-time PCR (qPCR) analysis indicates that the alterations in the functional properties of GABA_ARs are associated with changes in DG GABA_AR subunit expression. The most pronounced change is a reduction in $\alpha 3$ subunit expression. This may explain, at least partly, the enhanced GABA potency of DG granule GABA_ARs following HT treatment. Indeed, *in vitro* mutagenesis and electrophysiological studies have indicated $\alpha 3$ as a subunit with low GABA sensitivity [23, 60]. Prior to the qPCR analysis of the different GABA_AR subunits, we determined the gene expression stability of seven frequently used reference genes (ActB, CycA, 18S rRNA, Rpl13A, Tbp, GusB and Arbp) in the hippocampal DG of rats that had experienced early-life FS one week before. The analysis of expression stability using two freely accessible software programs, geNorm and

Normfinder, demonstrated that normalization to CycA, Rpl13A and Tbp allowed a valid interpretation of mRNA expression data in our experimental set-up (**chapter 2**).

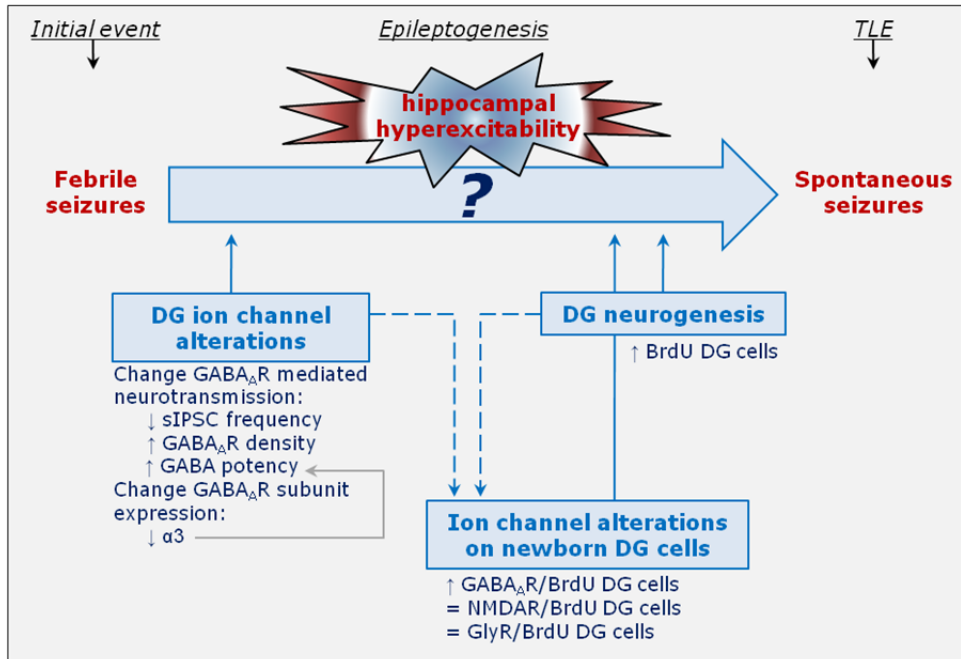


Figure 6.1: Schematic representation of febrile seizure-induced long-term changes in DG cells described in this thesis

Effects of early-life febrile seizures on LGIC expression by newborn DG cells

Seizure-induced hippocampal neurogenesis has been demonstrated in chemical and electrical seizure models [47, 91, 140, 151, 160, 171] and also after experimental FS [110, 111]. Moreover, some studies analyzing resected tissue from TLE patients point to the occurrence of increased neurogenesis after seizures [21]. Based on these results, enhanced hippocampal neurogenesis has been proposed as a mechanism by which seizures may modulate the hippocampal circuit. Seizure-induced newborn DG cells may differentiate and/or migrate abnormally and thereby promote hippocampal hyperexcitability. We already found functional and expressional changes in DG GABA_ARs (**chapter 3**). Additionally we explored whether long-term changes in LGICs can be attributed specifically to FS-induced newborn cells. Therefore, we investigated whether FS

may persistently alter the expression of LGICs in newborn DG cells (**chapter 4**). Dividing cells that were born immediately after FS were labeled with BrdU and evaluated in adulthood for the expression of excitatory and inhibitory LGICs by immunohistochemistry. Our results demonstrate that experimental early-life FS significantly increase the number of newborn DG granule cells that express GABA_ARs, while the number of newborn GlyR- or NMDAR-expressing cells in the DG granule layer and hilar region are not changed. Persistent enhancement of GABA_AR expression by newborn DG cells may be viewed as a compensatory anti-epileptogenic response supporting research from Raedt *et al.* [156] These authors found that suppression of hippocampal neurogenesis by brain radiation enhances excitability in the hippocampal network and slightly accelerates kindling epileptogenesis, which argues against a pro-epileptogenic role of neurogenesis. On the other hand, next to their classical role in inhibitory neurotransmission, GABA_ARs may also have excitatory effects, during development or in pathological conditions such as epilepsy [50]. This would imply that the detected increased GABA_AR expression on newborn DG cells may have a pro- rather than an anti-epileptogenic effect. Whether seizure-induced newborn hippocampal cells fulfill a beneficial role during the process of epileptogenesis or, to the opposite, contribute to hippocampal hyperexcitability, still remains unclear [101]. Five-week old DG granule cells born after electrically-induced seizures, receive less excitatory input due to a decreased overall release probability of glutamate while their inhibitory input is increased. This plasticity of both excitatory and inhibitory afferents would reduce the excitability of post-ictal born DG granule cells. Thus, once these new cells are fully integrated in the hippocampal network they would reduce the overall excitability of the DG, arguing for an anti-epileptogenic role for neurogenesis [88]. On the contrary, DG granule cells generated after rapid kindling exhibit an increased afferent excitatory synaptic drive, which would result in an enhanced excitability of these new cells and would point to a pro-epileptogenic role for neurogenesis [198]. Aforementioned data from two different animal models underscore the elusiveness concerning the functional role of neurogenesis in the process of epileptogenesis. So far, this issue is unexplored in the hyperthermic animal model applied in the current study. Our data which show an increased GABA_AR expression on newborn DG cells may suggest a contribution of this

particular cell population to the process of epileptogenesis. However, further research is needed to address the functional consequences of their changes in phenotype.

Febrile seizure-induced GABAergic alterations: future perspectives and general conclusion

The results of **chapter 3** revealed a decreased inhibitory input to DG granule cells one week after hyperthermic seizures. This finding points to FS-associated plasticity at the presynaptic level, though the underlying mechanism in the hyperthermic seizure model remains to be determined. In that context, dentate interneurons are interesting to study in the future. Indeed, inhibitory control of dentate granule cells is provided by dentate interneurons being a heterogeneous group of neurons that primarily use GABA as neurotransmitter. Different dentate interneuron types can be distinguished based on the laminar distribution of their axonal plexus, but also based on the expression of certain neurochemical markers such as neuropeptides and calcium-binding proteins [6]. Three hypothetical mechanisms may explain why the frequency of spontaneous inhibitory postsynaptic currents in DG granule cells was decreased in hyperthermic animals: (i) the spontaneous activity of presynaptic interneurons may be reduced, (ii) the number of inhibitory synapses on dentate granule cells may be diminished or (iii) the release probability of GABA may be decreased.

In models of TLE wherein seizures are induced in adult animals by pilocarpine [99] or electrical stimulation [183], diminished inhibitory input to dentate granule cells has been attributed to hilar interneuron loss. In contrast, immature animals, younger than two weeks of age, are known to be less vulnerable than mature animals to seizure-induced hippocampal cell loss [12]. This has been shown also for the animal model used in the current study. FS during the second postnatal week have been reported to cause transient injury of CA1 and CA3 pyramidal cells while neither acute nor long-term cell death of vulnerable neuronal populations could be detected [18, 186]. However, transient injury to hilar interneurons that might influence inhibitory synaptic input to dentate granule cells one week after HT-induced seizures cannot be ruled out based on current available data and needs further investigation. Besides death or injury of hilar interneurons, additional factors that determine interneuron function and, hence, modulate granule cell activity, may contribute to a reduced frequency of

sIPSCs in granule cells. Recent research in a rat model of TLE revealed functional abnormalities in the circuit of dentate basket cells [203]. These are inhibitory, often parvalbumin-positive interneurons with their cell bodies located at the border of the granule cell layer and hilus and their axon collaterals concentrated in the granule cell layer forming perisomatic synapses with dentate granule cells [6]. After pilocarpine-induced seizures, basket cells receive less excitatory synaptic input, the size of the readily releasable pool of synaptic vesicles is smaller and transmission at basket cell-to-granule cell synapses is more likely to fail [203]. Taken together, these data suggest seizure-induced impairment of the dentate basket cell circuit, which may contribute to a decreased inhibition of dentate granule cells. Hence, it might be interesting to explore the function of the dentate basket cell circuit in the light of its possible contribution to a decreased frequency of inhibitory synaptic events in DG granule cells one week after FS.

Yet, other dentate inhibitory interneuron types may be equally important. A contribution of cholecystokinin (CCK)-positive interneurons may be suggested based on previous research in the hyperthermic model. CCK-containing axon terminals of CA1 basket cells express cannabinoid type1 (CB1) receptors that are involved in endocannabinoid-mediated modulation of GABAergic transmission at basket cell-to-CA1 pyramidal cell synapses. This signaling cascade is triggered by a transient depolarization of the postsynaptic neuron and results in an endocannabinoid-mediated transient depression of GABA release from presynaptic interneurons, a process called depolarization-induced suppression of inhibition (DSI). CB1 receptor-mediated depression of GABA release is persistently enhanced in the CA1 pyramidal cell layer but also in the dentate granule cell layer one week FS. Also, dentate granule cells that normally do not display DSI, do show DSI one week after FS due to an upregulation of presynaptic CB1 receptors [41]. This enhanced CB1 receptor expression was detected at one week after FS by Western blotting whole hippocampal tissue by Chen *et al* [41] and by qPCR of DG tissue by us (**chapter 2**). In contrast to dentate CA1 cells, not dentate basket cells but Hilar Commissural-Associational Pathway related cells (HICAP cells) are CCK-immunoreactive interneurons with CB1 receptor expressing axon terminals. HICAP cells have their cell bodies located close to the granular cell layer or in the hilus and their axons branched

specifically in the inner one-third of the molecular layer where they form synapses with proximal portions of spiny granule cell dendrites [6]. Based on abovementioned findings, it might be interesting to examine synaptic efficacy from HICAP cells to dentate granule cells after FS.

In general, further study of dentate interneuron circuit function will help to unravel the mechanisms underlying the observed decreased inhibitory drive onto DG granule cells after hyperthermic seizures, which is important because different underlying mechanisms may require other different therapeutic strategies.

Taken together, the results from **chapter 3 and 4** demonstrate prominent GABA_AR changes in the DG after early-life FS, which may hold promises for the development of new anti-epileptic drugs. However, their functional significance in hippocampal excitability and epileptogenesis needs further research. Functional and expressional GABA_AR changes are evident in the general population of DG granule cells (**chapter 3**). Additionally, early-life FS cause a persistent increase in GABA_AR expression in specifically newborn DG granule cells (**chapter 4**). The netto effect of these observed GABA_AR alterations, and hence the influence on hippocampal excitability, will ultimately depend on the transmembrane concentration gradient for Cl⁻. E_{GABA} is depolarizing in the immature brain and becomes hyperpolarizing during development due to an upregulation of the Cl⁻ extruding KCC2 cotransporter and a down-regulation of the Cl⁻ importing NKCC1 cotransporter [15]. Alterations in Cl⁻ homeostasis leading to a switch in GABA action from hyperpolarizing to depolarizing again, has been found in experimental [58, 143] and human [43, 129, 137] epileptic hippocampi. This seizure-associated shift in E_{GABA} is accompanied by a decreased expression of KCC2 and an increased expression of NKCC1 [114]. Based on these results, it can be hypothesized that FS might also induce changes in Cl⁻ homeostasis. This needs to be determined in the hyperthermic seizure model by measuring cation-Cl⁻ cotransporter expression levels and by using gramicidin perforated patch-clamp techniques to evaluate the physiological effect of GABA on the membrane potential. In order to apply patch-clamp techniques on newborn DG cells, the hyperthermic seizure model needs adaptations. For the immunohistochemical characterization of newborn DG cells (**chapter 4**), we have

used a thymidine-analogue, BrdU, to label dividing cells. However, the BrdU method always requires tissue fixation and processing and, hence, does not allow a functional characterization of new neurons in living hippocampal slices. To help solving this issue, intrahippocampal injection of GFP-expressing retroviral vectors, which only labels dividing cells, has been introduced in neuroscience research [189]. GFP can be visualized under fluorescence microscopy, enabling electrophysiological characterization of newborn cells. Applied to the current hyperthermic seizure model, the GFP-expressing retroviral vector should be injected stereotactically in the DG the day after FS induction (*i.e.* postnatal day 11) in order to label dividing cells immediately after FS. Because of the lack of stereotactic atlases of the developing Sprague-Dawley rat brain, we determined the DG stereotactic coordinates in 11-day old Sprague-dawley rat pups by stereotactic injections of methylene blue (**Chapter 5**). In this way, we found the following coordinates: anteroposterior +3.0 mm from lambda, mediolateral, 2.0 mm and dorsoventral, -2.5 mm from the cortex, which can be used for future intrahippocampal injections with GFP-expressing retroviral vectors. This approach will allow a fine electrophysiological characterization of FS-induced newborn DG cells. More specifically, it will enable the determination of their intrinsic electrophysiological properties, the functional characterization of their ion channels, *e.g.* GABA_ARs, and the study of their afferent inhibitory and excitatory synaptic input. Taken together, such experiments will provide information about the behavior and functional integration of this dynamic cell population in the existing hippocampal circuitry and, hence, will help to find out if FS-induced neurogenesis has a positive or a negative impact on the excitability of the DG network.

In conclusion, the results presented in this thesis demonstrate that FS can cause persistent changes in GABA_AR-mediated neurotransmission in the DG, which supports the hypothesis that early-life FS lead to long-term alterations in hippocampal excitability. Our data also suggest that a particular population of GABA_AR-expressing newborn DG cells might contribute to the process of epileptogenesis. However, epileptogenesis is a multifactorial process. Taken together these results also propose the involvement of multiple mechanisms in the development of TLE, namely a role for ion channels, *i.e.* GABA_ARs, and for newborn DG cells. Yet further functional analysis is required to fully understand their contribution to the development of a hyperexcitable hippocampal network. The observed GABA_AR-associated alterations may be either pro- or anti-epileptogenic depending on the contribution of other seizure-associated changes (*e.g.* excitatory GABA effect or mossy fiber sprouting).

7

Nederlandse Samenvatting

Retrospectieve cohort studies hebben vastgesteld dat er een relatie bestaat tussen het optreden van febrile convulsies (FC) tijdens de kinderjaren en het ontwikkelen van temporaalkwab epilepsie tijdens de volwassenheid [56, 158, 163, 176], wat een causaal verband tussen FC en de pathogenese van temporaalkwab epilepsie suggereert. De mogelijk betrokken mechanismen zijn nog grotendeels onbekend en vormen een uitdaging binnen het actuele epilepsieonderzoek. Algemeen wordt epilepsie gekenmerkt door een verstoord evenwicht tussen excitatie en inhibitie in het hippocampale neuronale netwerk wat een verlaagde drempelwaarde voor het ontstaan van convulsies tot gevolg heeft. De excitabiliteit in de hippocampus wordt in normale fysiologische condities gereguleerd door de gyrus dentatus (DG). De DG maakt deel uit van de hippocampus en verhindert een ongecontroleerde voortgang van synchrone excitatorische activiteit afkomstig vanuit de enthorinale cortex naar downstream hippocampale structuren zoals de hilus en de CA3 regio [46]. Er wordt gepostuleerd dat deze zogenaamde 'filter' functie van de DG aangetast is in het proces van epileptogenese [46]. Daarom hebben we ons in deze thesis gericht op de DG structuur en bestudeerden we of veranderingen in ligand-geactiveerde ionenkanalen, zowel qua expressie als qua functionaliteit, zouden kunnen bijdragen tot een verstoorde DG 'filter' functie. Hiertoe werd gebruik gemaakt van een immatuur diermodel waarin FC uitgelokt worden in rat pups van 10 dagen oud door blootstelling aan warme lucht [11]. In dit model zijn FC geassocieerd met een verhoogde hippocampale excitabiliteit resulterend in een verlaagde drempelwaarde voor convulsies [39, 53, 54]. Tevens is de prevalentie voor het ontwikkelen van spontane convulsies en temporaalkwab epilepsie op latere leeftijd verhoogd in dit diermodel [54].

Studie van hippocampaal weefsel van temporaalkwab epilepsie patiënten heeft reeds duidelijke veranderingen in het type A GABA receptor ($GABA_{A,R}$) subeenheid expressie profiel aangetoond, hetgeen suggereert dat $GABA_{A,R}$ -gemedieerde neurotransmissie kan gewijzigd zijn tijdens humane epileptogenese [117]. Een efficiënte GABAerge inhibitie is nochtans noodzakelijk voor het behoud van de DG filter functie [46]. Bijgevolg kan verondersteld worden dat convulsie-gerelateerde veranderingen in $GABA_{A,R}$ expressie en/of functie kan bijdragen tot een verstoorde DG functie en zo ook een verlaging van de drempelwaarde voor het ontstaan van convulsies. We hebben daarom de invloed

van FC op GABA_AR-gemedieerde neurotransmissie bestudeerd door middel van whole-cell patch clamp metingen in DG granulaire cellen in hippocampale slices. In **hoofdstuk 3** werd aangetoond dat de frequentie van inhibitoire synaptische stromen verlaagd is één week na het optreden van FC. Deze veranderingen in frequentie zouden kunnen bijdragen tot een verstoord evenwicht tussen excitatie en inhibitie in het hippocampaal netwerk. Hoewel, tegelijkertijd vinden tevens verscheidene veranderingen plaats op het postsynaptische niveau (*i.e.* verhoging van de GABA_AR densiteit en stijging van de GABA potentie) die lijken te compenseren voor de gedaalde inhibitoire input naar de DG granulaire cellen. Op het eerste zicht schijnen deze resultaten tegenstrijdig met de hypothese dat FC de DG filter aantasten. Anderzijds moet benadrukt worden dat alle experimenten plaatsvonden tijdens de latente periode waarin noch spontane convulsies noch afwijkende interictale epileptoforme EEG activiteit kon waargenomen worden. Dit doet vermoeden dat de geobserveerde modificaties in GABA_AR-gemedieerde activiteit bijdragen aan de pathogenese van TLE, in combinatie met andere afwijkingen die optreden tijdens het proces van epileptogenese. Potentiële veranderingen zijn convulsie-geïnduceerde depolariserende GABAerge responsen [50, 143], alsook 'mossy fiber sprouting' in de moleculaire laag van de DG hetgeen de excitatorische input naar de DG granulaire cellen wijzigt [18, 89].

Kwantitatieve real time PCR (qPCR) experimenten (**hoofdstuk 3**) toonden aan dat de bovenbeschreven functionele GABA_AR veranderingen gepaard gaan met wijzigingen in DG GABA_AR subeenheid expressie. Meest uitgesproken is een verlaagde $\alpha 3$ subeenheid expressie. Dit kan, alleszins gedeeltelijk, de verhoogde GABA potentie van DG granulaire GABA_ARs verklaren. Inderdaad, *in vitro* mutagenese en electrofysiologische studies hebben de $\alpha 3$ aangewezen als een subeenheid met lage GABA sensitiviteit. Alvorens de qPCR analyse voor de verschillende GABA_AR subeenheden uit te voeren, bepaalden we de expressiestabiliteit van zeven frequent gebruikte referentiegenen (ActB, CycA, 18S rRNA, Rpl13A, Tbp, GusB and Arbp) in de hippocampale DG van ratten waarin een week eerder FC werden uitgelokt (**hoofdstuk 2**). De analyse van expressiestabiliteit, gebruik makende van twee publiek toegankelijke software programma's geNorm en Normfinder, toonde aan dat een combinatie van CycA,

Rpl13A en Tbp geschikt is voor normalisatie van qPCR data in de gegeven experimentele omstandigheden.

In verscheidene diermodellen is reeds aangetoond dat hippocampale neurogenese kan geïnduceerd worden door convulsies [47, 91, 140, 151, 160, 171], zo ook in het door ons gebruikte model van experimentele FC [110, 111]. Zelfs hippocampaal weefsel van epilepsiepatiënten wijst op een verhoogde neurogenese [21]. Gebaseerd op deze resultaten, is hippocampale neurogenese voorgesteld als een mechanisme waarbij convulsies het hippocampaal circuit kunnen reguleren. Nieuwgeboren DG cellen zouden afwijkend kunnen differentiëren en/of migreren en zodanig hippocampale hyperexcitabiliteit stimuleren. In **hoofdstuk 3** detecteerden we reeds veranderingen in DG GABA_ARs zowel op functioneel als op expressie niveau, in **hoofdstuk 4** wilden we nagaan of zulke veranderingen in ligand-geactiveerde ionenkanalen zich specifiek op FC-geïnduceerde nieuwgeboren cellen kunnen voordoen. Hiervoor werden delende cellen onmiddellijk na het optreden van FC gelabeld met BrdU en na acht weken geëvalueerd voor de expressie van excitatoire en inhibitoire ligand-geactiveerde ionenkanalen. Onze data tonen aan dat het aantal nieuwgeboren DG cellen dat GlyR of NMDAR tot expressie brengen ongewijzigd is na FC, terwijl er een stijging is van het aantal nieuwgeboren DG granulaire cellen dat GABA_AR tot expressie brengt. Deze stijging zou kunnen gezien worden als een compensatoir anticonvulsief mechanisme. Nochtans kunnen GABA_ARs, additioneel aan hun rol in inhibitoire neurotransmissie, ook excitatoire effecten uitoefenen, tijdens de ontwikkeling alsook in pathologische condities zoals epilepsie. Dit zou betekenen dat de verhoogde GABA_AR expressie eerder pro- dan anti-epileptogeen zou zijn.

De data beschreven in hoofdstuk 3 en 4 wijzen op prominente GABA_AR veranderingen in de DG na FC, wat veelbelovend zou kunnen zijn voor de ontwikkeling van nieuwe anti-epileptica. Echter is verder onderzoek vereist om hun functionele significantie in hippocampale excitabiliteit en epileptogenese na te gaan. Voor immunohistochemische karakterisatie van nieuwgeboren DG cellen (hoofdstuk 4) hebben we gebruik gemaakt van een thymidine-analoog, BrdU, om delende cellen te labelen. De BrdU-methode vereist altijd weefselfixatie en maakt bijgevolg functionele karakterisatie van neuronen in levende hippocampale slices onmogelijk. Intrahippocampale injectie van retrovirale

vectoren die GFP tot expressie brengen, biedt een oplossing [189]. Retrovirussen vertonen de eigenschap zich te integreren in prolifererende cellen. Voorts kan het GFP met behulp van fluorescentiemicroscopie gevisualiseerd worden wat electrofysiologische metingen van de desbetreffende cellen mogelijk maakt. Toegepast op het model van FC, betekent dit dat het GFP-retrovirus moet geïnjecteerd worden in Sprague-Dawley rat pups van 11 dagen oud zodanig dat de delende cellen onmiddellijk na het optreden van FC gelabeld worden. Aangezien stereotactische atlanten van het immature rat brein niet beschikbaar zijn, werden de stereotactische coördinaten van de DG bepaald in 11-dagen oude Sprague-Dawley rat pups door middel van stereotactische injecties met methyleen blauw (**hoofdstuk 5**). Op deze manier werden de volgende coördinaten bekomen: anteroposterior +3.0 mm ten opzichte van lambda, mediolateraal, 2.0 mm en dorsoventraal, -2.5 mm ten opzichte van de cortex. Deze coördinaten kunnen in de toekomst toegepast worden voor intrahippocampale injecties van GFP-retrovirussen, een benadering die electrofysiologische karakterisatie van FC-geïnduceerde nieuwgeboren DG cellen mogelijk maakt en bijgevolg inzichten kan verlenen betreffende de functionele rol van deze dynamische celpopulatie in hippocampale excitabiliteit.

Concluderend kunnen we stellen dat de resultaten voorgesteld in deze thesis, wijzen op persisterende veranderingen in GABA_AR-gemedieerde neurotransmissie in de DG. Deze bevinding ondersteunt de hypothese dat FC op lange termijn veranderingen teweeg brengen in de hippocampale excitabiliteit. Onze data suggereren eveneens dat een specifieke populatie van nieuwgeboren DG cellen, die ontstaan zijn na de FC, kunnen bijdragen aan het proces van epileptogenese. Afhankelijk van het optreden van andere convulsie-geassocieerde modificaties zoals 'mossy fiber sprouting' en excitatorische GABA effecten, zullen deze GABA_AR-geassocieerde veranderingen pro- dan wel anti-epileptogeen zijn.

Reference list

1. *Febrile seizures: long-term management of children with fever-associated seizures. Summary of an NIH consensus statement.* Br Med J, 1980. **281**(6235): p. 277-9.
2. Abou-Khalil, B., et al., *Temporal lobe epilepsy after prolonged febrile convulsions: excellent outcome after surgical treatment.* Epilepsia, 1993. **34**(5): p. 878-83.
3. Alheim, K. and T. Bartfai, *The interleukin-1 system: receptors, ligands, and ICE in the brain and their involvement in the fever response.* Ann N Y Acad Sci, 1998. **840**: p. 51-8.
4. Altman, J. and G.D. Das, *Autoradiographic and histological evidence of postnatal hippocampal neurogenesis in rats.* J Comp Neurol, 1965. **124**(3): p. 319-35.
5. Alvarez-Buylla, A. and J.M. Garcia-Verdugo, *Neurogenesis in adult subventricular zone.* J Neurosci, 2002. **22**(3): p. 629-34.
6. Amaral, D.G., H.E. Scharfman, and P. Lavenex, *The dentate gyrus: fundamental neuroanatomical organization (dentate gyrus for dummies).* Prog Brain Res, 2007. **163**: p. 3-22.
7. Andersen, C.L., J.L. Jensen, and T.F. Orntoft, *Normalization of real-time quantitative reverse transcription-PCR data: a model-based variance estimation approach to identify genes suited for normalization, applied to bladder and colon cancer data sets.* Cancer Res, 2004. **64**(15): p. 5245-50.
8. Ang, C.W., G.C. Carlson, and D.A. Coulter, *Massive and specific dysregulation of direct cortical input to the hippocampus in temporal lobe epilepsy.* J Neurosci, 2006. **26**(46): p. 11850-6.
9. Auzmendi, J., N. Gonzalez, and E. Girardi, *The NMDAR subunit NR2B expression is modified in hippocampus after repetitive seizures.* Neurochem Res, 2009. **34**(5): p. 819-26.
10. Avishai-Eliner, S., et al., *Stressed-out, or in (utero)?* Trends Neurosci, 2002. **25**(10): p. 518-24.
11. Baram, T.Z., A. Gerth, and L. Schultz, *Febrile seizures: an appropriate-aged model suitable for long-term studies.* Brain Res Dev Brain Res, 1997. **98**(2): p. 265-70.
12. Ben-Ari, Y., *Basic developmental rules and their implications for epilepsy in the immature brain.* Epileptic Disord, 2006. **8**(2): p. 91-102.
13. Ben-Ari, Y., et al., *Giant synaptic potentials in immature rat CA3 hippocampal neurones.* J Physiol, 1989. **416**: p. 303-25.
14. Ben-Ari, Y. and R. Cossart, *Kainate, a double agent that generates seizures: two decades of progress.* Trends Neurosci, 2000. **23**(11): p. 580-7.
15. Ben-Ari, Y., et al., *GABA: a pioneer transmitter that excites immature neurons and generates primitive oscillations.* Physiol Rev, 2007. **87**(4): p. 1215-84.
16. Ben-Ari, Y. and G.L. Holmes, *Effects of seizures on developmental processes in the immature brain.* Lancet Neurol, 2006. **5**(12): p. 1055-63.
17. Ben-Ari, Y., et al., *GABAA, NMDA and AMPA receptors: a developmentally regulated 'menage a trois'.* Trends Neurosci, 1997. **20**(11): p. 523-9.
18. Bender, R.A., et al., *Mossy fiber plasticity and enhanced hippocampal excitability, without hippocampal cell loss or altered neurogenesis, in an*

-
- animal model of prolonged febrile seizures*. Hippocampus, 2003. **13**(3): p. 399-412.
19. Bender, R.A., et al., *Enhanced expression of a specific hyperpolarization-activated cyclic nucleotide-gated cation channel (HCN) in surviving dentate gyrus granule cells of human and experimental epileptic hippocampus*. J Neurosci, 2003. **23**(17): p. 6826-36.
 20. Bengzon, J., et al., *Apoptosis and proliferation of dentate gyrus neurons after single and intermittent limbic seizures*. Proc Natl Acad Sci U S A, 1997. **94**(19): p. 10432-7.
 21. Blumcke, I., et al., *Increase of nestin-immunoreactive neural precursor cells in the dentate gyrus of pediatric patients with early-onset temporal lobe epilepsy*. Hippocampus, 2001. **11**(3): p. 311-21.
 22. Bo, T., et al., *Long-term effects of seizures in neonatal rats on spatial learning ability and N-methyl-D-aspartate receptor expression in the brain*. Brain Res Dev Brain Res, 2004. **152**(2): p. 137-42.
 23. Bohme, I., H. Rabe, and H. Luddens, *Four amino acids in the alpha subunits determine the gamma-aminobutyric acid sensitivities of GABAA receptor subtypes*. J Biol Chem, 2004. **279**(34): p. 35193-200.
 24. Boileau, A.J., et al., *Mapping the agonist binding site of the GABAA receptor: evidence for a beta-strand*. J Neurosci, 1999. **19**(12): p. 4847-54.
 25. Bonfeld, B.E., B. Elfving, and G. Wegener, *Reference genes for normalization: a study of rat brain tissue*. Synapse, 2008. **62**(4): p. 302-9.
 26. Bouilleret, V., et al., *Early loss of interneurons and delayed subunit-specific changes in GABA(A)-receptor expression in a mouse model of mesial temporal lobe epilepsy*. Hippocampus, 2000. **10**(3): p. 305-24.
 27. Bowser, D.N., et al., *Altered kinetics and benzodiazepine sensitivity of a GABAA receptor subunit mutation [gamma 2(R43Q)] found in human epilepsy*. Proc Natl Acad Sci U S A, 2002. **99**(23): p. 15170-5.
 28. Brewster, A., et al., *Developmental febrile seizures modulate hippocampal gene expression of hyperpolarization-activated channels in an isoform- and cell-specific manner*. J Neurosci, 2002. **22**(11): p. 4591-9.
 29. Brewster, A.L., et al., *Formation of heteromeric hyperpolarization-activated cyclic nucleotide-gated (HCN) channels in the hippocampus is regulated by developmental seizures*. Neurobiol Dis, 2005. **19**(1-2): p. 200-7.
 30. Buckmaster, P.S. and F.E. Dudek, *Neuron loss, granule cell axon reorganization, and functional changes in the dentate gyrus of epileptic kainate-treated rats*. J Comp Neurol, 1997. **385**(3): p. 385-404.
 31. Bustin, S.A., *Quantification of mRNA using real-time reverse transcription PCR (RT-PCR): trends and problems*. J Mol Endocrinol, 2002. **29**(1): p. 23-39.
 32. Bustin, S.A., et al., *The MIQE guidelines: minimum information for publication of quantitative real-time PCR experiments*. Clin Chem, 2009. **55**(4): p. 611-22.
 33. Cameron, H.A. and R.D. McKay, *Adult neurogenesis produces a large pool of new granule cells in the dentate gyrus*. J Comp Neurol, 2001. **435**(4): p. 406-17.
-

34. Carratala, F. and M. Moya, *Febrile convulsions induced by microwaves and the alteration in behavior of albino mouse OF1*. *Biol Neonate*, 1991. **60**(1): p. 62-8.
35. Cartmell, T., G.N. Luheshi, and N.J. Rothwell, *Brain sites of action of endogenous interleukin-1 in the febrile response to localized inflammation in the rat*. *J Physiol*, 1999. **518 (Pt 2)**: p. 585-94.
36. Cendes, F., *Febrile seizures and mesial temporal sclerosis*. *Curr Opin Neurol*, 2004. **17**(2): p. 161-4.
37. Chattipakorn, S.C. and L.L. McMahon, *Strychnine-sensitive glycine receptors depress hyperexcitability in rat dentate gyrus*. *J Neurophysiol*, 2003. **89**(3): p. 1339-42.
38. Chen, K., et al., *Persistently modified h-channels after complex febrile seizures convert the seizure-induced enhancement of inhibition to hyperexcitability*. *Nat Med*, 2001. **7**(3): p. 331-7.
39. Chen, K., T.Z. Baram, and I. Soltesz, *Febrile seizures in the developing brain result in persistent modification of neuronal excitability in limbic circuits*. *Nat Med*, 1999. **5**(8): p. 888-94.
40. Chen, K., et al., *Prevention of plasticity of endocannabinoid signaling inhibits persistent limbic hyperexcitability caused by developmental seizures*. *J Neurosci*, 2007. **27**(1): p. 46-58.
41. Chen, K., et al., *Long-term plasticity of endocannabinoid signaling induced by developmental febrile seizures*. *Neuron*, 2003. **39**(4): p. 599-611.
42. Cohen, A.S., et al., *Dentate granule cell GABA(A) receptors in epileptic hippocampus: enhanced synaptic efficacy and altered pharmacology*. *Eur J Neurosci*, 2003. **17**(8): p. 1607-16.
43. Cohen, I., et al., *On the origin of interictal activity in human temporal lobe epilepsy in vitro*. *Science*, 2002. **298**(5597): p. 1418-21.
44. Collingridge, G.L., et al., *A nomenclature for ligand-gated ion channels*. *Neuropharmacology*, 2009. **56**(1): p. 2-5.
45. Coulter, D.A., *Epilepsy-associated plasticity in gamma-aminobutyric acid receptor expression, function, and inhibitory synaptic properties*. *Int Rev Neurobiol*, 2001. **45**: p. 237-52.
46. Coulter, D.A. and G.C. Carlson, *Functional regulation of the dentate gyrus by GABA-mediated inhibition*. *Prog Brain Res*, 2007. **163**: p. 235-43.
47. Covolan, L., et al., *Cell damage and neurogenesis in the dentate granule cell layer of adult rats after pilocarpine- or kainate-induced status epilepticus*. *Hippocampus*, 2000. **10**(2): p. 169-80.
48. Crespel, A., et al., *Increased number of neural progenitors in human temporal lobe epilepsy*. *Neurobiol Dis*, 2005. **19**(3): p. 436-50.
49. Danglot, L., et al., *Morphologically identified glycinergic synapses in the hippocampus*. *Mol Cell Neurosci*, 2004. **27**(4): p. 394-403.
50. De Koninck, Y., *Altered chloride homeostasis in neurological disorders: a new target*. *Curr Opin Pharmacol*, 2007. **7**(1): p. 93-9.
51. Deindl, E., et al., *Differential expression of GAPDH and beta3-actin in growing collateral arteries*. *Mol Cell Biochem*, 2002. **236**(1-2): p. 139-46.
52. Derks, N.M., et al., *Housekeeping genes revisited: different expressions depending on gender, brain area and stressor*. *Neuroscience*, 2008. **156**(2): p. 305-9.

-
53. Dube, C., et al., *Prolonged febrile seizures in the immature rat model enhance hippocampal excitability long term*. *Ann Neurol*, 2000. **47**(3): p. 336-44.
 54. Dube, C., et al., *Temporal lobe epilepsy after experimental prolonged febrile seizures: prospective analysis*. *Brain*, 2006. **129**(Pt 4): p. 911-22.
 55. Dube, C., et al., *Interleukin-1beta contributes to the generation of experimental febrile seizures*. *Ann Neurol*, 2005. **57**(1): p. 152-5.
 56. Dube, C.M., A.L. Brewster, and T.Z. Baram, *Febrile seizures: mechanisms and relationship to epilepsy*. *Brain Dev*, 2009. **31**(5): p. 366-71.
 57. Dube, C.M., et al., *Fever, febrile seizures and epilepsy*. *Trends Neurosci*, 2007. **30**(10): p. 490-6.
 58. Dzhala, V.I., et al., *Progressive NKCC1-dependent neuronal chloride accumulation during neonatal seizures*. *J Neurosci*, 2010. **30**(35): p. 11745-61.
 59. Dzhala, V.I. and K.J. Staley, *Excitatory actions of endogenously released GABA contribute to initiation of ictal epileptiform activity in the developing hippocampus*. *J Neurosci*, 2003. **23**(5): p. 1840-6.
 60. Ebert, B., et al., *Differences in agonist/antagonist binding affinity and receptor transduction using recombinant human gamma-aminobutyric acid type A receptors*. *Mol Pharmacol*, 1997. **52**(6): p. 1150-6.
 61. Eichler, S.A., et al., *Glycinergic tonic inhibition of hippocampal neurons with depolarizing GABAergic transmission elicits histopathological signs of temporal lobe epilepsy*. *J Cell Mol Med*, 2008. **12**(6B): p. 2848-66.
 62. Eriksson, P.S., et al., *Neurogenesis in the adult human hippocampus*. *Nat Med*, 1998. **4**(11): p. 1313-7.
 63. Escayg, A., et al., *Mutations of SCN1A, encoding a neuronal sodium channel, in two families with GEFS+2*. *Nat Genet*, 2000. **24**(4): p. 343-5.
 64. Esposito, M.S., et al., *Neuronal differentiation in the adult hippocampus recapitulates embryonic development*. *J Neurosci*, 2005. **25**(44): p. 10074-86.
 65. Fisher, R.S., et al., *Epileptic seizures and epilepsy: definitions proposed by the International League Against Epilepsy (ILAE) and the International Bureau for Epilepsy (IBE)*. *Epilepsia*, 2005. **46**(4): p. 470-2.
 66. French, J.A., et al., *Characteristics of medial temporal lobe epilepsy: I. Results of history and physical examination*. *Ann Neurol*, 1993. **34**(6): p. 774-80.
 67. Fritschy, J.M., et al., *Switch in the expression of rat GABAA-receptor subtypes during postnatal development: an immunohistochemical study*. *J Neurosci*, 1994. **14**(9): p. 5302-24.
 68. Fukuda, M., et al., *Clinical study of epilepsy with severe febrile seizures and seizures induced by hot water bath*. *Brain Dev*, 1997. **19**(3): p. 212-6.
 69. Gaiarsa, J.L., V. Tseeb, and Y. Ben-Ari, *Postnatal development of pre- and postsynaptic GABAB-mediated inhibitions in the CA3 hippocampal region of the rat*. *J Neurophysiol*, 1995. **73**(1): p. 246-55.
 70. Galanopoulou, A.S., *GABA(A) receptors in normal development and seizures: friends or foes?* *Curr Neuropharmacol*, 2008. **6**(1): p. 1-20.
-

71. Gibbs, J.W., 3rd, M.D. Shumate, and D.A. Coulter, *Differential epilepsy-associated alterations in postsynaptic GABA(A) receptor function in dentate granule and CA1 neurons*. J Neurophysiol, 1997. **77**(4): p. 1924-38.
72. Gonzalez-Ramirez, M., et al., *Hyperthermic seizures and hyperthermia in immature rats modify the subsequent pentylenetetrazole-induced seizures*. Seizure, 2009. **18**(7): p. 533-6.
73. Gonzalez Ramirez, M., et al., *Hyperthermia-induced seizures modify the GABA(A) and benzodiazepine receptor binding in immature rat brain*. Cell Mol Neurobiol, 2007. **27**(2): p. 211-27.
74. Gould, E., et al., *Proliferation of granule cell precursors in the dentate gyrus of adult monkeys is diminished by stress*. Proc Natl Acad Sci U S A, 1998. **95**(6): p. 3168-71.
75. Harkin, L.A., et al., *Truncation of the GABA(A)-receptor gamma2 subunit in a family with generalized epilepsy with febrile seizures plus*. Am J Hum Genet, 2002. **70**(2): p. 530-6.
76. Harris, J.L., T.M. Reeves, and L.L. Phillips, *Injury modality, survival interval, and sample region are critical determinants of qRT-PCR reference gene selection during long-term recovery from brain trauma*. J Neurotrauma, 2009. **26**(10): p. 1669-81.
77. Haspolat, S., et al., *Interleukin-1beta, tumor necrosis factor-alpha, and nitrite levels in febrile seizures*. J Child Neurol, 2002. **17**(10): p. 749-51.
78. Hauser, W.A., *The prevalence and incidence of convulsive disorders in children*. Epilepsia, 1994. **35 Suppl 2**: p. S1-6.
79. Heid, C.A., et al., *Real time quantitative PCR*. Genome Res, 1996. **6**(10): p. 986-94.
80. Heida, J.G., L. Boisse, and Q.J. Pittman, *Lipopolysaccharide-induced febrile convulsions in the rat: short-term sequelae*. Epilepsia, 2004. **45**(11): p. 1317-29.
81. Helminen, M. and T. Vesikari, *Increased interleukin-1 (IL-1) production from LPS-stimulated peripheral blood monocytes in children with febrile convulsions*. Acta Paediatr Scand, 1990. **79**(8-9): p. 810-6.
82. Holden, J.H. and C. Czajkowski, *Different residues in the GABA(A) receptor alpha 1T60-alpha 1K70 region mediate GABA and SR-95531 actions*. J Biol Chem, 2002. **277**(21): p. 18785-92.
83. Holmes, G.L. and Y. Ben-Ari, *Seizures in the developing brain: perhaps not so benign after all*. Neuron, 1998. **21**(6): p. 1231-4.
84. Hsu, D., *The dentate gyrus as a filter or gate: a look back and a look ahead*. Prog Brain Res, 2007. **163**: p. 601-13.
85. Hu, S., et al., *Cytokine effects on glutamate uptake by human astrocytes*. Neuroimmunomodulation, 2000. **7**(3): p. 153-9.
86. Huang, R.Q., et al., *Pentylenetetrazole-induced inhibition of recombinant gamma-aminobutyric acid type A (GABA(A)) receptors: mechanism and site of action*. J Pharmacol Exp Ther, 2001. **298**(3): p. 986-95.
87. Huggett, J., et al., *Real-time RT-PCR normalisation; strategies and considerations*. Genes Immun, 2005. **6**(4): p. 279-84.
88. Jakubs, K., et al., *Environment matters: synaptic properties of neurons born in the epileptic adult brain develop to reduce excitability*. Neuron, 2006. **52**(6): p. 1047-59.
89. Jansen, J.F., et al., *Short- and long-term limbic abnormalities after experimental febrile seizures*. Neurobiol Dis, 2008. **32**(2): p. 293-301.

90. Jiang, W., T.M. Duong, and N.C. de Lanerolle, *The neuropathology of hyperthermic seizures in the rat*. *Epilepsia*, 1999. **40**(1): p. 5-19.
91. Jiang, W., et al., *Dentate granule cell neurogenesis after seizures induced by pentylentetrazol in rats*. *Brain Res*, 2003. **977**(2): p. 141-8.
92. Jung, K.H., et al., *Continuous cytosine-b-D-arabinofuranoside infusion reduces ectopic granule cells in adult rat hippocampus with attenuation of spontaneous recurrent seizures following pilocarpine-induced status epilepticus*. *Eur J Neurosci*, 2004. **19**(12): p. 3219-26.
93. Kamikawa, H., et al., *IL-1beta increases norepinephrine level in rat frontal cortex: involvement of prostanoids, NO, and glutamate*. *Am J Physiol*, 1998. **275**(3 Pt 2): p. R803-10.
94. Kang, J.Q., W. Shen, and R.L. Macdonald, *Why does fever trigger febrile seizures? GABAA receptor gamma2 subunit mutations associated with idiopathic generalized epilepsies have temperature-dependent trafficking deficiencies*. *J Neurosci*, 2006. **26**(9): p. 2590-7.
95. Kempermann, G., ed. *Adult Neurogenesis, stem cells and neuronal development in the adult brain.*, ed. O.U. Press. 2006: New York.
96. Kempermann, G., H.G. Kuhn, and F.H. Gage, *More hippocampal neurons in adult mice living in an enriched environment*. *Nature*, 1997. **386**(6624): p. 493-5.
97. Khazipov, R., et al., *Developmental changes in GABAergic actions and seizure susceptibility in the rat hippocampus*. *Eur J Neurosci*, 2004. **19**(3): p. 590-600.
98. Kirchner, A., et al., *Effects of taurine and glycine on epileptiform activity induced by removal of Mg²⁺ in combined rat entorhinal cortex-hippocampal slices*. *Epilepsia*, 2003. **44**(9): p. 1145-52.
99. Kobayashi, M. and P.S. Buckmaster, *Reduced inhibition of dentate granule cells in a model of temporal lobe epilepsy*. *J Neurosci*, 2003. **23**(6): p. 2440-52.
100. Kohr, G., Y. De Koninck, and I. Mody, *Properties of NMDA receptor channels in neurons acutely isolated from epileptic (kindled) rats*. *J Neurosci*, 1993. **13**(8): p. 3612-27.
101. Kokaia, M., *Seizure-induced neurogenesis in the adult brain*. *Eur J Neurosci*, 2011. **33**(6): p. 1133-8.
102. Kornack, D.R. and P. Rakic, *Continuation of neurogenesis in the hippocampus of the adult macaque monkey*. *Proc Natl Acad Sci U S A*, 1999. **96**(10): p. 5768-73.
103. Kuhn, H.G., H. Dickinson-Anson, and F.H. Gage, *Neurogenesis in the dentate gyrus of the adult rat: age-related decrease of neuronal progenitor proliferation*. *J Neurosci*, 1996. **16**(6): p. 2027-33.
104. Kwak, S.E., et al., *Hyperthermic seizure induces persistent alteration in excitability of the dentate gyrus in immature rats*. *Brain Res*, 2008. **1216**: p. 1-15.
105. Lahat, E., et al., *Interleukin-1beta levels in serum and cerebrospinal fluid of children with febrile seizures*. *Pediatr Neurol*, 1997. **17**(1): p. 34-6.
106. Langnaese, K., et al., *Selection of reference genes for quantitative real-time PCR in a rat asphyxial cardiac arrest model*. *BMC Mol Biol*, 2008. **9**: p. 53.
107. Laplagne, D.A., et al., *Functional convergence of neurons generated in the developing and adult hippocampus*. *PLoS Biol*, 2006. **4**(12): p. e409.

108. Lauren, H.B., et al., *Kainic acid-induced status epilepticus alters GABA receptor subunit mRNA and protein expression in the developing rat hippocampus*. J Neurochem, 2005. **94**(5): p. 1384-94.
109. Legendre, P., et al., *Glycine Receptors Caught between Genome and Proteome - Functional Implications of RNA Editing and Splicing*. Front Mol Neurosci, 2009. **2**: p. 23.
110. Lemmens, E.M., et al., *Gender differences in febrile seizure-induced proliferation and survival in the rat dentate gyrus*. Epilepsia, 2005. **46**(10): p. 1603-12.
111. Lemmens, E.M., et al., *Cytogenesis in the dentate gyrus after neonatal hyperthermia-induced seizures: what becomes of surviving cells?* Epilepsia, 2008. **49**(5): p. 853-60.
112. Leroy, C., et al., *Pharmacological plasticity of GABA(A) receptors at dentate gyrus synapses in a rat model of temporal lobe epilepsy*. J Physiol, 2004. **557**(Pt 2): p. 473-87.
113. Lewis, P.F. and M. Emerman, *Passage through mitosis is required for oncoretroviruses but not for the human immunodeficiency virus*. J Virol, 1994. **68**(1): p. 510-6.
114. Li, X., et al., *Long-term expressional changes of Na⁺ -K⁺ -Cl⁻ co-transporter 1 (NKCC1) and K⁺ -Cl⁻ co-transporter 2 (KCC2) in CA1 region of hippocampus following lithium-pilocarpine induced status epilepticus (PISE)*. Brain Res, 2008. **1221**: p. 141-6.
115. Liu, J., et al., *Increased neurogenesis in the dentate gyrus after transient global ischemia in gerbils*. J Neurosci, 1998. **18**(19): p. 7768-78.
116. Liu, S., et al., *Generation of functional inhibitory neurons in the adult rat hippocampus*. J Neurosci, 2003. **23**(3): p. 732-6.
117. Loup, F., et al., *Selective alterations in GABAA receptor subtypes in human temporal lobe epilepsy*. J Neurosci, 2000. **20**(14): p. 5401-19.
118. Lynch, M. and T. Sutula, *Recurrent excitatory connectivity in the dentate gyrus of kindled and kainic acid-treated rats*. J Neurophysiol, 2000. **83**(2): p. 693-704.
119. Markakis, E.A. and F.H. Gage, *Adult-generated neurons in the dentate gyrus send axonal projections to field CA3 and are surrounded by synaptic vesicles*. J Comp Neurol, 1999. **406**(4): p. 449-60.
120. Mathern, G.W., et al., *Seizures decrease postnatal neurogenesis and granule cell development in the human fascia dentata*. Epilepsia, 2002. **43 Suppl 5**: p. 68-73.
121. Mathern, G.W., J.K. Pretorius, and T.L. Babb, *Influence of the type of initial precipitating injury and at what age it occurs on course and outcome in patients with temporal lobe seizures*. J Neurosurg, 1995. **82**(2): p. 220-7.
122. Mathern, G.W., et al., *Human hippocampal AMPA and NMDA mRNA levels in temporal lobe epilepsy patients*. Brain, 1997. **120 (Pt 11)**: p. 1937-59.
123. Mathern, G.W., et al., *Increased hippocampal AMPA and NMDA receptor subunit immunoreactivity in temporal lobe epilepsy patients*. J Neuropathol Exp Neurol, 1998. **57**(6): p. 615-34.
124. Matsuo, M., et al., *Increased IL-1beta production from dsRNA-stimulated leukocytes in febrile seizures*. Pediatr Neurol, 2006. **35**(2): p. 102-6.

125. McCurley, A.T. and G.V. Callard, *Characterization of housekeeping genes in zebrafish: male-female differences and effects of tissue type, developmental stage and chemical treatment*. BMC Mol Biol, 2008. **9**: p. 102.
126. Mody, I. and U. Heinemann, *NMDA receptors of dentate gyrus granule cells participate in synaptic transmission following kindling*. Nature, 1987. **326**(6114): p. 701-4.
127. Mori, M., B.H. Gahwiler, and U. Gerber, *Beta-alanine and taurine as endogenous agonists at glycine receptors in rat hippocampus in vitro*. J Physiol, 2002. **539**(Pt 1): p. 191-200.
128. Moser, E., I. Mathiesen, and P. Andersen, *Association between brain temperature and dentate field potentials in exploring and swimming rats*. Science, 1993. **259**(5099): p. 1324-6.
129. Munoz, A., et al., *Cation-chloride cotransporters and GABA-ergic innervation in the human epileptic hippocampus*. Epilepsia, 2007. **48**(4): p. 663-73.
130. Nagaki, S., et al., *The role of vasopressin, somatostatin and GABA in febrile convulsion in rat pups*. Life Sci, 1996. **58**(24): p. 2233-42.
131. Namba, T., et al., *The fate of neural progenitor cells expressing astrocytic and radial glial markers in the postnatal rat dentate gyrus*. Eur J Neurosci, 2005. **22**(8): p. 1928-41.
132. Nelissen, K., et al., *Selection of reference genes for gene expression studies in rat oligodendrocytes using quantitative real time PCR*. J Neurosci Methods, 2010. **187**(1): p. 78-83.
133. Nusser, Z., et al., *Increased number of synaptic GABA(A) receptors underlies potentiation at hippocampal inhibitory synapses*. Nature, 1998. **395**(6698): p. 172-7.
134. Otis, T.S., Y. De Koninck, and I. Mody, *Lasting potentiation of inhibition is associated with an increased number of gamma-aminobutyric acid type A receptors activated during miniature inhibitory postsynaptic currents*. Proc Natl Acad Sci U S A, 1994. **91**(16): p. 7698-702.
135. Overstreet-Wadiche, L.S., et al., *Seizures accelerate functional integration of adult-generated granule cells*. J Neurosci, 2006. **26**(15): p. 4095-103.
136. Overstreet-Wadiche, L.S. and G.L. Westbrook, *Functional maturation of adult-generated granule cells*. Hippocampus, 2006. **16**(3): p. 208-15.
137. Palma, E., et al., *Anomalous levels of Cl⁻ transporters in the hippocampal subiculum from temporal lobe epilepsy patients make GABA excitatory*. Proc Natl Acad Sci U S A, 2006. **103**(22): p. 8465-8.
138. Pandis, C., et al., *Differential expression of NMDA and AMPA receptor subunits in rat dorsal and ventral hippocampus*. Neuroscience, 2006. **140**(1): p. 163-75.
139. Parent, J.M., et al., *Aberrant seizure-induced neurogenesis in experimental temporal lobe epilepsy*. Ann Neurol, 2006. **59**(1): p. 81-91.
140. Parent, J.M., et al., *Increased dentate granule cell neurogenesis following amygdala kindling in the adult rat*. Neurosci Lett, 1998. **247**(1): p. 9-12.
141. Parent, J.M., et al., *Inhibition of dentate granule cell neurogenesis with brain irradiation does not prevent seizure-induced mossy fiber synaptic reorganization in the rat*. J Neurosci, 1999. **19**(11): p. 4508-19.

142. Parent, J.M., et al., *Dentate granule cell neurogenesis is increased by seizures and contributes to aberrant network reorganization in the adult rat hippocampus*. J Neurosci, 1997. **17**(10): p. 3727-38.
143. Pathak, H.R., et al., *Disrupted dentate granule cell chloride regulation enhances synaptic excitability during development of temporal lobe epilepsy*. J Neurosci, 2007. **27**(51): p. 14012-22.
144. Paxinos, G., ed. *Hippocampal Formation*. In *The rat nervous system*. 2004, Elsevier Academic Press.
145. Paxinos, G. and C. Watson, eds. *The rat brain in stereotaxic coordinates*. ed. E.A. Press. 2005.
146. Peng, Z., et al., *Altered expression of the delta subunit of the GABAA receptor in a mouse model of temporal lobe epilepsy*. J Neurosci, 2004. **24**(39): p. 8629-39.
147. Pernot, F., et al., *Selection of reference genes for real-time quantitative reverse transcription-polymerase chain reaction in hippocampal structure in a murine model of temporal lobe epilepsy with focal seizures*. J Neurosci Res, 2010. **88**(5): p. 1000-8.
148. Piatti, V.C., M.S. Esposito, and A.F. Schinder, *The timing of neuronal development in adult hippocampal neurogenesis*. Neuroscientist, 2006. **12**(6): p. 463-8.
149. Pirker, S., et al., *GABA(A) receptors: immunocytochemical distribution of 13 subunits in the adult rat brain*. Neuroscience, 2000. **101**(4): p. 815-50.
150. Porter, B.E., X.N. Cui, and A.R. Brooks-Kayal, *Status epilepticus differentially alters AMPA and kainate receptor subunit expression in mature and immature dentate granule neurons*. Eur J Neurosci, 2006. **23**(11): p. 2857-63.
151. Porter, B.E., M. Maronski, and A.R. Brooks-Kayal, *Fate of newborn dentate granule cells after early life status epilepticus*. Epilepsia, 2004. **45**(1): p. 13-9.
152. Proper EA, H.G., van Veelen CWM and de Graan PNE, *Morphological changes in the human epileptogenic hippocampus*. Neuroscience Research Communications, 2001. **29**(3): p. 18.
153. Proper, E.A., et al., *A grading system for hippocampal sclerosis based on the degree of hippocampal mossy fiber sprouting*. Acta Neuropathol, 2001. **101**(4): p. 405-9.
154. Qu, L., et al., *Hyperthermia decreases GABAergic synaptic transmission in hippocampal neurons of immature rats*. Neurobiol Dis, 2007. **27**(3): p. 320-7.
155. Radonic, A., et al., *Guideline to reference gene selection for quantitative real-time PCR*. Biochem Biophys Res Commun, 2004. **313**(4): p. 856-62.
156. Raedt, R., et al., *Radiation of the rat brain suppresses seizure-induced neurogenesis and transiently enhances excitability during kindling acquisition*. Epilepsia, 2007. **48**(10): p. 1952-63.
157. Raol, Y.H., et al., *Increased GABA(A)-receptor alpha1-subunit expression in hippocampal dentate gyrus after early-life status epilepticus*. Epilepsia, 2006. **47**(10): p. 1665-73.
158. Reid, A.Y., et al., *Febrile seizures: current views and investigations*. Can J Neurol Sci, 2009. **36**(6): p. 679-86.

-
159. Rijkers, K., et al., *Polymorphisms in CACNA1E and Camk2d are associated with seizure susceptibility of Sprague-Dawley rats*. *Epilepsy Res*, 2010. **91**(1): p. 28-34.
 160. Sankar, R., et al., *Granule cell neurogenesis after status epilepticus in the immature rat brain*. *Epilepsia*, 2000. **41 Suppl 6**: p. S53-6.
 161. Sankar, R., et al., *Patterns of status epilepticus-induced neuronal injury during development and long-term consequences*. *J Neurosci*, 1998. **18**(20): p. 8382-93.
 162. Sastry, L. and K. Cornetta, *Methods in molecular biology, methods and protocols*. In: *Detection of replication competent retrovirus and lentivirus.*, C. Baum, Editor. 2009, Humana Press. p. 243-263.
 163. Scantlebury, M.H. and J.G. Heida, *Febrile seizures and temporal lobe epileptogenesis*. *Epilepsy Res*, 2010. **89**(1): p. 27-33.
 164. Scharfman, H.E., *Functional implications of seizure-induced neurogenesis*. *Adv Exp Med Biol*, 2004. **548**: p. 192-212.
 165. Scharfman, H.E., J.H. Goodman, and A.L. Sollas, *Granule-like neurons at the hilar/CA3 border after status epilepticus and their synchrony with area CA3 pyramidal cells: functional implications of seizure-induced neurogenesis*. *J Neurosci*, 2000. **20**(16): p. 6144-58.
 166. Scharfman, H.E. and W.P. Gray, *Relevance of seizure-induced neurogenesis in animal models of epilepsy to the etiology of temporal lobe epilepsy*. *Epilepsia*, 2007. **48 Suppl 2**: p. 33-41.
 167. Schinder, A.F. and F.H. Gage, *A hypothesis about the role of adult neurogenesis in hippocampal function*. *Physiology (Bethesda)*, 2004. **19**: p. 253-61.
 168. Schmittgen, T.D. and B.A. Zakrajsek, *Effect of experimental treatment on housekeeping gene expression: validation by real-time, quantitative RT-PCR*. *J Biochem Biophys Methods*, 2000. **46**(1-2): p. 69-81.
 169. Schuchmann, S., et al., *Experimental febrile seizures are precipitated by a hyperthermia-induced respiratory alkalosis*. *Nat Med*, 2006. **12**(7): p. 817-23.
 170. Schwarzer, C., et al., *GABA(A) receptor subunits in the rat hippocampus II: altered distribution in kainic acid-induced temporal lobe epilepsy*. *Neuroscience*, 1997. **80**(4): p. 1001-17.
 171. Scott, B.W., J.M. Wojtowicz, and W.M. Burnham, *Neurogenesis in the dentate gyrus of the rat following electroconvulsive shock seizures*. *Exp Neurol*, 2000. **165**(2): p. 231-6.
 172. Shao, L.R. and F.E. Dudek, *Changes in mIPSCs and sIPSCs after kainate treatment: evidence for loss of inhibitory input to dentate granule cells and possible compensatory responses*. *J Neurophysiol*, 2005. **94**(2): p. 952-60.
 173. Sherwood, N. and P. Timiras, eds. *A stereotaxic atlas of the developing rat brain*. ed. U.o.C. Press. 1970.
 174. Shi, S., et al., *Subunit-specific rules governing AMPA receptor trafficking to synapses in hippocampal pyramidal neurons*. *Cell*, 2001. **105**(3): p. 331-43.
 175. Shibasaki, K., et al., *Effects of body temperature on neural activity in the hippocampus: regulation of resting membrane potentials by transient receptor potential vanilloid 4*. *J Neurosci*, 2007. **27**(7): p. 1566-75.
-

176. Shinnar, S., *Febrile Seizures and Mesial Temporal Sclerosis*. *Epilepsy Curr*, 2003. **3**(4): p. 115-118.
177. Sigel, E., et al., *Point mutations affecting antagonist affinity and agonist dependent gating of GABAA receptor channels*. *EMBO J*, 1992. **11**(6): p. 2017-23.
178. Smith, G.B. and R.W. Olsen, *Identification of a [3H]muscimol photoaffinity substrate in the bovine gamma-aminobutyric acidA receptor alpha subunit*. *J Biol Chem*, 1994. **269**(32): p. 20380-7.
179. Song, W., S.C. Chattipakorn, and L.L. McMahon, *Glycine-gated chloride channels depress synaptic transmission in rat hippocampus*. *J Neurophysiol*, 2006. **95**(4): p. 2366-79.
180. Sperk, G., et al., *GABA(A) receptor subunits in the rat hippocampus I: immunocytochemical distribution of 13 subunits*. *Neuroscience*, 1997. **80**(4): p. 987-1000.
181. Spigelman, I., et al., *Dentate granule cells form novel basal dendrites in a rat model of temporal lobe epilepsy*. *Neuroscience*, 1998. **86**(1): p. 109-20.
182. Stahlberg, A., et al., *Properties of the reverse transcription reaction in mRNA quantification*. *Clin Chem*, 2004. **50**(3): p. 509-15.
183. Sun, C., et al., *Selective loss of dentate hilar interneurons contributes to reduced synaptic inhibition of granule cells in an electrical stimulation-based animal model of temporal lobe epilepsy*. *J Comp Neurol*, 2007. **500**(5): p. 876-93.
184. Swijssen, A., G. Hoogland, and J.M. Rigo, *Potential role for ligand-gated ion channels after seizure-induced neurogenesis*. *Biochem Soc Trans*, 2009. **37**(Pt 6): p. 1419-22.
185. Tapia, R., *Putting the heat on febrile seizures*. *Nat Med*, 2006. **12**(7): p. 729-30.
186. Toth, Z., et al., *Seizure-induced neuronal injury: vulnerability to febrile seizures in an immature rat model*. *J Neurosci*, 1998. **18**(11): p. 4285-94.
187. Tsunashima, K., et al., *GABA(A) receptor subunits in the rat hippocampus III: altered messenger RNA expression in kainic acid-induced epilepsy*. *Neuroscience*, 1997. **80**(4): p. 1019-32.
188. van Praag, H., G. Kempermann, and F.H. Gage, *Running increases cell proliferation and neurogenesis in the adult mouse dentate gyrus*. *Nat Neurosci*, 1999. **2**(3): p. 266-70.
189. van Praag, H., et al., *Functional neurogenesis in the adult hippocampus*. *Nature*, 2002. **415**(6875): p. 1030-4.
190. Vandesompele, J., et al., *Accurate normalization of real-time quantitative RT-PCR data by geometric averaging of multiple internal control genes*. *Genome Biol*, 2002. **3**(7): p. RESEARCH0034.
191. Verity, C.M., N.R. Butler, and J. Golding, *Febrile convulsions in a national cohort followed up from birth. I--Prevalence and recurrence in the first five years of life*. *Br Med J (Clin Res Ed)*, 1985. **290**(6478): p. 1307-10.
192. Vermeulen, J., et al., *Measurable impact of RNA quality on gene expression results from quantitative PCR*. *Nucleic Acids Res*, 2011.
193. Virta, M., M. Hurme, and M. Helminen, *Increased frequency of interleukin-1beta (-511) allele 2 in febrile seizures*. *Pediatr Neurol*, 2002. **26**(3): p. 192-5.

-
194. Viviani, B., et al., *Interleukin-1beta enhances NMDA receptor-mediated intracellular calcium increase through activation of the Src family of kinases*. J Neurosci, 2003. **23**(25): p. 8692-700.
 195. von Bohlen Und Halbach, O., *Immunohistological markers for staging neurogenesis in adult hippocampus*. Cell Tissue Res, 2007. **329**(3): p. 409-20.
 196. Wallace, R.H., et al., *Febrile seizures and generalized epilepsy associated with a mutation in the Na⁺-channel beta1 subunit gene SCN1B*. Nat Genet, 1998. **19**(4): p. 366-70.
 197. Wang, S., et al., *Interleukin-1beta inhibits gamma-aminobutyric acid type A (GABA(A)) receptor current in cultured hippocampal neurons*. J Pharmacol Exp Ther, 2000. **292**(2): p. 497-504.
 198. Wood, J.C., et al., *Functional integration of new hippocampal neurons following insults to the adult brain is determined by characteristics of pathological environment*. Exp Neurol, 2011. **229**(2): p. 484-93.
 199. Wuarin, J.P. and F.E. Dudek, *Excitatory synaptic input to granule cells increases with time after kainate treatment*. J Neurophysiol, 2001. **85**(3): p. 1067-77.
 200. You, H. and S.M. Dunn, *Identification of a domain in the delta subunit (S238-V264) of the alpha4beta3delta GABAA receptor that confers high agonist sensitivity*. J Neurochem, 2007. **103**(3): p. 1092-101.
 201. Zhang, G., et al., *Effects of status epilepticus on hippocampal GABAA receptors are age-dependent*. Neuroscience, 2004. **125**(2): p. 299-303.
 202. Zhang, G., et al., *Long-term alterations in glutamate receptor and transporter expression following early-life seizures are associated with increased seizure susceptibility*. J Neurochem, 2004. **88**(1): p. 91-101.
 203. Zhang, W. and P.S. Buckmaster, *Dysfunction of the dentate basket cell circuit in a rat model of temporal lobe epilepsy*. J Neurosci, 2009. **29**(24): p. 7846-56.
 204. Zhao, C., et al., *Distinct morphological stages of dentate granule neuron maturation in the adult mouse hippocampus*. J Neurosci, 2006. **26**(1): p. 3-11.

Curriculum Vitae

Ann Swijzen werd geboren op 22 juli 1980 te Herk-de-Stad. In 1998 behaalde ze haar diploma Algemeen Secundair Onderwijs (ASO) in de studierichting Latijn-Wiskunde aan het Ursula-Instituut te Herk-de-Stad. Vervolgens startte ze de opleiding Vroedkunde aan de Katholieke Hogeschool Limburg (KHLim) waar ze in 2002 haar diploma bachelor in de Vroedkunde behaalde. In hetzelfde jaar begon ze haar universitaire studies aan de Universiteit Hasselt/transnationale Universiteit Limburg (tUL) waar ze in 2006 met grote onderscheiding afstudeerde als master in de Biomedische Wetenschappen. In januari 2007 startte ze met haar doctoraatsonderzoek aan het Biomedisch Onderzoeksinstituut van de Universiteit Hasselt in het kader van een tUL beurs. Tijdens deze periode volgde ze de cursus proefdierleider FELASA C aan de KULeuven.

Bibliography

Publications

Potential role for ligand-gated ion channels after seizure-induced neurogenesis.

Swijzen A., Hoogland G. and Rigo JM.

Biochem Soc Trans. 2009 Dec;37(Pt 6):1419-22. Review

Validation of reference genes for quantitative RT-PCR studies in the dentate gyrus after experimental febrile seizures

Swijzen A., Nelissen K., Janssen D., Rigo JM.* and Hoogland G.*

(*equally contributed)

Submitted

Experimental early-life febrile seizures induce changes in GABA_AR-mediated inhibitory neurotransmission in the dentate gyrus

Swijzen A., Avila-Macaya A., Brône B., Janssen D., Hoogland G.* and Rigo JM.*

(*equally contributed)

Submitted

Long-lasting enhancement of GABA_A receptor expression in newborn dentate granule cells after early-life febrile seizures

Swijzen A., Brône B., Rigo JM.* and Hoogland G.*

(*equally contributed)

Submitted

Oral presentations

Synaptic and extra-synaptic ligand-gated ion channels in the hippocampus and their putative pathophysiological implication in excitability disorders.

Swijzen A., Hoogland G., Rigo JM.

Meeting Interuniversity Attraction Poles Program (IUAP – Belgian State – Belgian Science Policy) 2007 (December 1), UH Hasselt, Belgium

Phenotypical characterization of ligand-gated ion channels in newborn dentate gyrus cells in an animal model of TLE

Swijzen A., Hoogland G., Rigo JM.

13th Euron PhD student days 2009 (October 1-2), Nijmegen, the Netherlands

Characterization of ligand-gated ion channels in dentate gyrus cells after neonatal febrile seizures.

Swijzen A., Hoogland G., Janssen D., Rigo JM

9th Dutch Endo-Neuro-Psycho Meeting 2011 (May 30-June 1), Lunteren, the Netherlands

Poster presentations

Advanced electrophysiological and micro-fluorimetric study of ligand-gated ion channels.

Swijzen A., Smisdom N., Gielen E., vandeVen M., Ameloot M. and Rigo JM.

- Flanders Bio, "Knowledge for growth" June 2008, Gent, Belgium

Characterization of ligand-gated ion channels in newborn dentate gyrus cells after neonatal hyperthermia-induced seizures.

Swijzen A., Hoogland G., Schijns O.E.M.G., Lemmens E.M.P., Legendre P. and Rigo J.-M.

- 6thFENS Forum of European Neuroscience 2008 (July 12-16), Genève, Switzerland
- 12th Euron PhD student days 2008 (September 18-19), Aachen, Germany

Newborn dentate gyrus cells express glycine receptors and NMDA receptors in an animal model of TLE.

Swijzen A., Hoogland G., Schijns O.E.M.G., Lemmens E.M.P., Legendre P. and Rigo J.-M.

- Meeting Interuniversity Attraction Poles Program (IUAP – Belgian State – Belgian Science Policy) 2009 (January 7), KULeuven, Belgium

Characterization of excitatory ligand-gated ion channels in newborn dentate gyrus cells after neonatal hyperthermia-induced seizures. *Extended version 1*

Swijsen A., Carrea S., Brône B., Legendre P., Hoogland G. and Rigo J.-M.

- Meeting Belgian Society for Neuroscience 2009 (May 11), ULg Liège, Belgium

Characterization of ligand-gated ion channels in newborn dentate gyrus cells after neonatal hyperthermia-induced seizures. *Extended Version 2*

Swijsen A., Brône B., Legendre P. Hoogland G. and Rigo J.-M.

- Meeting Biochemical Society: Neuronal glutamate and GABA_A receptor function in health and disease 2009 (July 21 – July 24), University of Sint-Andrews, Great-Britain
- Meeting Interuniversity Attraction Poles Program (IUAP – Belgian State – Belgian Science Policy) 2009 (December 12), ULg Liège, Belgium

Characterization of ligand-gated ion channels in newborn dentate gyrus cells after neonatal hyperthermia-induced seizures.

Rigo J.-M., **Swijsen A.**, Brône B., Legendre P. and Hoogland G.

- Society for Neuroscience (SfN) meeting 2009 (October 17-21), Chicago, USA

Phenotypical characterization of ligand-gated ion channels in febrile seizure-induced newly generated dentate gyrus cells.

Swijsen A., Janssen D., Brône B., Legendre P. Hoogland G. and Rigo J.-M.

- 7thFENS Forum of European Neuroscience 2010 (July 3-7), Amsterdam, The Netherlands

Awards

BSN Poster prize – Meeting Belgian Society for Neuroscience 2009 (May 11), ULg Liège, Belgium

ASN Neuro Young Investigator Poster Prize (joint 2nd) – Meeting Biochemical Society: Neuronal glutamate and GABA_A receptor function in health and disease 2009 (July 21 – July 24), University of Sint-Andrews, Great-Britain

Dankwoord

Eindelijk! Het boekje is geschreven, helemaal klaar om naar de drukker te sturen! Ik moet eerlijk toegeven dat ik meermaals gedacht heb dat het nooit zou afraken... maar, het is gelukt! Dit boekje zou nochtans nooit tot stand zijn gekomen zonder hulp op de werkvloer of ondersteuning van het thuisfront. Ik wil dan ook graag van deze gelegenheid gebruik maken om iedereen te bedanken die zijn steentje heeft bijgedragen.

Allereerst zou ik een woordje van dank willen richten tot mijn promotor en co-promotor. Prof. Rigo, Jean-Michel, gedurende de afgelopen 4 jaar kon ik steeds bij u terecht. Ik dank je dan ook voor de bemoedigende woorden wanneer het onderzoek wat moeizamer verliep, voor het overbrengen van je electrofysiologische kennis en voor de tijd die je besteed hebt aan het bediscussiëren van de resultaten, aan het nalezen van dit werk en aan het doornemen van de posters en presentaties. Tevens ben ik dankbaar voor je vertrouwen en voor de kans die ik heb gekregen om nog een jaar als post-doc verder te werken binnen de fysiologiegroep. Merci beaucoup! Govert, deze thesis was niet hetzelfde geweest zonder jouw inzet. Je stond steeds paraat om naar Diepenbeek te komen om verder te helpen met de proefdierexperimenten, maar ook om de resultaten te bediscussiëren. Je enthousiasme voor het onderzoek werkt aanstekelijk. Zowel je wetenschappelijke input als je positieve feedback gedurende de voorbije 4 jaar zijn voor mij heel waardevol geweest. Dank je wel voor de aangename samenwerking!

Dear members of the jury, I would like to thank you for critically evaluating this work and for the constructive comments that have certainly given my thesis an additional value.

Verder wil ik natuurlijk al mijn BIOMED collega's bedanken die van dichtbij of iets verderaf betrokken zijn geweest bij mijn werk. Quirine, de 'aanvoerster' van ons zwemclubje, onze zwemuitstapjes zijn niet alleen goed voor de conditie, maar ook uiterst gezellig om bij te babbelen ☺. De overige zwemdames: Nina, Elke en Valérie. Mijn meest recente voorgangers: Inge en Katherine. De 'biofysica-jongens' in de kelder: Kristof, Rik en Ben. Nick, mijn 'lotgenoot' gedurende de laatste maanden, we hebben de deadline gehaald! Bedankt, jullie hebben allen gezorgd voor een leuke werksfeer gedurende de voorbije 4 jaar, ik

ben dan ook blij dat ik nog geen vaarwel moet zeggen. Bert, dank je voor je nuttige tips en suggesties bij tal van electrofysiologische problemen én frustraties ;). Ariel, it was nice to have a colleague at the 'slice patch clamp set-up'. I wish you, and also Ambily, success with your PhD! De meisjes van morfologie: Lies, Annelies, Sofie en Wendy die een extra dankwoordje verdient. Dank je voor je altijd luisterend oor als de zaken niet helemaal naar wens verliepen. Onze baklessen waren elke woensdag opnieuw een leuke afwisseling na al het schrijfwerk. Weet dat je ook steeds mag komen aankloppen bij mij nu jij aan de eindfase begint! Dan zal ik nu voor de cappuccino zorgen ;) Sheen, tot voor kort mijn bureau-collega. We hebben ergernissen gedeeld om mislukte experimenten, maar gelukkig ook vreugde om geslaagde experimenten. En kijk, uiteindelijk hebben we toch de finish bereikt! Ik kan me geen betere bureaugenoot voorstellen en met plezier zal ik terugdenken aan de tijd die we samen hebben doorgebracht tijdens de verschillende congressen, eurodisney, etc.!

Natuurlijk wil ik ook de 'oude garde fysiologen' zeker niet vergeten. Daniel, Sandy, Roeland, Jimmy en Koen, ik denk met plezier terug aan mijn beginperiode in gebouw D wanneer we de bureauruimte 'boven' deelden. Prof. Paul Steels, prof. Emmy van Kerkhove en Danny Jans die mij tijdens mijn opleiding en masterstage als eersten hebben laten kennis maken met de electrofysiologie. Ik denk ook aan Ellen, Ilse, Sara, Martin en waarschijnlijk nog een hele lijst... allen hebben ze bijgedragen tot een sfeer waarin het aangenaam werken was.

Rosette, Jo, Patrick, Paul, Wilfried en Regine, jullie hulp bij de qPCR experimenten, het maken van oplossingen, de celkweek, het verzorgen van onze proefdieren, de technische ondersteuning, het voorzien van zuiver glaswerk, het autoclaveren... was onmisbaar. Agnes, Ilse, Jean en Hilde, bedankt voor jullie administratieve ondersteuning. Magda, dank je voor de hulp wanneer er weer eens een poster moest gedrukt worden.

Daar het onmogelijk is alle collega's afzonderlijk op te sommen, een welgemeende dank je wel aan alle andere BIOMED collega's!

Tot slot wil ik natuurlijk ook mijn familie en vrienden bedanken: papa, mama en bomma, tante Irène en Walter, maar ook Annelies, Anneleen en Greet. Jullie vertrouwen in de goede afloop van mijn doctoraat was voor mij enorm motiverend! Jullie aanmoediging en interesse in mijn onderzoek waren een grote steun. De gezellige etentjes en leuke uitstapjes in het weekend hebben de nodige ontspanning opgeleverd gedurende de voorbije stressvolle maanden. Mama en papa, jullie hebben mij de kans gegeven te studeren wat ik wilde en zolang ik wilde. Jullie hulp, begrip, aanmoediging en vertrouwen in mijn kunnen gedurende de afgelopen jaren zijn van onschatbare waarde. Ik wil jullie dan ook bedanken voor alles wat jullie voor mij doen!

Hartelijk dank,

Ann, juni 2011